Contemporary Mathematics

Generalized polarization tensors, inverse conductivity problems, and dilute composite materials: a review

Habib Ammari and Hyeonbae Kang

Abstract. We provide a survey of some recent developments in inverse isotropic and anisotropic conductivity problems to detect diametrically small electric inclusions and review calculations of effective properties of dilute composite materials. The central concept in these developments is the generalized polarization tensors and our main approach is based on layer potential techniques.

Contents

1. Introduction

The present survey paper is concerned with recent developments in electrical impedance imaging of small conductivity inclusions and the theory of dilute composite materials. The unifying thread is the use of the generalized polarization tensors (GPT's) which depend only on the geometry and the conductivity of the inclusion.

Electrical impedance imaging uses measurements of boundary voltage potentials and associated boundary currents to infer information about the internal conductivity profile of an object. Complete information about all voltages and currents is known to uniquely characterize an isotropic conductivity distribution [**100, 129, 117, 36**]. In its most general form electrical impedance imaging is severely ill-posed and nonlinear [**1**]. These major and fundamental difficulties can be understood by means of a mean value type theorem in elliptic partial differential equations. The value of the voltage potential at each point inside the region can be expressed as a weighted average of its neighborhood potential where the weight is determined by the conductivity distribution. In this weighted averaging

2000 *Mathematics Subject Classification.* Primary 35R30; Secondary 35B30.

Key words and phrases. Inverse isotropic and anisotropic conductivity problems, polarization tensors, direct reconstruction algorithms, effective electrical properties.

way, the conductivity distribution is conveyed to the boundary potential. Therefore, the boundary data is entangled in the global structure of the conductivity distribution in a highly nonlinear way. This is the main obstacle to finding non-iterative reconstruction algorithms with limited data. If, however, in advance we have additional structural information about the conductivity profile, then we may be able to determine specific features about the conductivity distribution with a satisfactory resolution. One such type of knowledge could be that the body consists of a smooth background containing a number of unknown small inclusions with a significantly different conductivity. The inclusions might in a medical application represent potential tumors, in a material science application they might represent impurities in the material, and finally in a war or post-war situation they could represent anti-personnel mines.

Over the last 10 years or so a considerable amount of interesting work has been dedicated to the imaging of such low volume fraction inclusions [**71, 72, 73, 55, 52, 54, 45, 18**]. In this article we shall not attempt to give an exhaustive survey of all work of this nature, rather we shall focus attention on certain asymptotic representation formulae and their implications and applications. The method of asymptotic expansions of small volume inclusions provides a useful framework to accurately and efficiently reconstruct the location and geometric features of the inclusions in a stable way, even for moderately noisy data [**18**]. The higher-order terms are essential when the background voltage has some critical points inside the conductor [**15**]. The first-order perturbations due to the presence of the inclusions are of dipole-type. The dipole-type expansion is only valid when the potential within the inclusion is nearly constant. On decreasing the distance between the inclusion and the boundary of the background medium this assumption begins to fail because higher-order multi-poles become significant due to the interaction between the inclusion and the boundary of the background medium. A more complicated asymptotic formula should be used instead of dipole-type expansion when the inclusion is close to the boundary of the background medium.

The new concepts of GPT's associated with a bounded Lipschitz domain and an isotropic/or anisotropic conductivity are central in this asymptotic approach. The GPT's are the basic building blocks for the full asymptotic expansions of the boundary voltage perturbations due to the presence of a small conductivity inclusion inside a conductor. It is then important from an imaging point of view to precisely characterize these GPT's and derive some of their properties, such as symmetry, positivity, and optimal bounds on their elements, for developing efficient algorithms to reconstruct conductivity inclusions of small volume. The GPT's seem to contain significant information on the domain and its conductivity which are yet to be investigated. On the other hand, the use of these GPT's leads to stable and accurate algorithms for the numerical computations of the steady-state voltage in the presence of small conductivity inclusions. It is known that small size features cause difficulties in the numerical solution of the conductivity problem by the finite element or finite difference methods. This is because such features require refined meshes in their neighborhoods, with their attendant problems [**93**].

The analysis of the GPT's associated with anisotropic conductivities is parallel to that for the isotropic conductivity problems, apart from some technical difficulties due to the fact that we are dealing with a system, not a single equation, and the fundamentals solutions inside and outside the inclusion are different.

Let us straight away explain what makes the GPT's interesting in electrical impedance imaging. In all of the reconstruction algorithms based on dipole-type approximations (first-order boundary perturbations), the locations of the inclusions are found with an error of the common order of magnitude of their diameters, and little about their shapes can be reconstructed. Making use of the GPT's (higher-order boundary perturbations), we are able to reconstruct the small inclusions with

higher resolution [**33**]. Indeed, this allows us to identify quite general conductivity inclusions without restrictions on their sizes.

The concepts of higher-order polarization tensors generalize those of classical Pólya–Szegö polarization tensors which have been extensively studied in the literature by many authors for various purposes [**52, 29, 55, 66, 111, 110, 73, 98, 101, 120, 63**]. The notion of Pólya–Szegö polarization tensor appeared in problems of potential theory related to certain problems arising in hydrodynamics and in electrostatics. If the conductivity is zero, namely, if the inclusion is insulated, the polarization tensor of Pólya–Szegö is called the virtual mass.

We provide a survey of important symmetric properties and positivity of the GPT's and present certain inequalities satisfied by the tensor elements of the GPT's. These relations can be used to find bounds on the weighted volume.

The concept of polarization tensors also occurs in several other interesting contexts, in particular in asymptotic models of dilute composites [**116, 29, 65**]. The determination of the effective or macroscopic property of a two-phase medium consisting of inclusions of one material of known shape embedded homogeneously into a continuous matrix of another having physical properties different from its own has been one of the classical problems in physics. When the inclusions are well-separated d-dimensional spheres and their volume fraction is small, the effective electrical conductivity of the composite medium is given by the well-known Maxwell-Garnett formula.

Despite the importance of calculating the effective or macroscopic properties of composites there has been very little work addressing the influence of inclusion shape. Most theoretical treatments focus on generalizing the Maxwell-Garnett formula to finite concentrations. The methods include bounds on the effective properties of the mixtures and many effective medium type models have been proposed [**115**]. Indeed, there are effective medium calculations that attempt to extend the Maxwell-Garnett formula to higher powers of the volume fraction, but only for the case of d-dimensional spherical inclusions [**81, 126**].

Until recently, ellipsoids are the only family of inclusions that could be rigorously and accurately estimated [**136**]. Douglas and Garboczi [**66, 74, 111**] made an important advance in treating more complicated shape inclusions by formally finding that the leading order term in the expansion of the effective conductivity (and other effective properties) in terms of the volume fraction could be expressed by means of the polarization tensors of the inclusion shape. See also, in connection with this, the work of Sánchez-Palencia [**125**] and its extension to the Navier-Stokes equation by Lévy and Sánchez-Palencia [**105**].

We review a general unified layer potential technique for rigorously deriving very accurate asymptotic expansions of electrical effective properties of dilute media for non-spherical Lipschitz isotropic and anisotropic conductivity inclusions. The approach is valid for high contrast mixtures and inclusions with Lipschitz boundaries. We shall emphasize the fact that it gives us any higher-order term in the asymptotic expansion of the effective conductivity. Our results have important implications for imaging composites. They show that the volume fractions and the GPT's form the only information that can be reconstructed in a stable way from boundary measurements. The volume fraction is the simplest but most important piece of microstructural information. The GPT's involve microstructural information beyond that contained in the volume fractions (material contrast, inclusion shape and orientation).

The paper is organized as follows. In Section 2, we introduce the main tools for studying the isotropic and anisotropic conductivity problems and collect some notation and preliminary results regarding layer potentials. In Section 3, we introduce the GPT's associated with a bounded domain and an isotropic or anisotropic conductivity and provide a survey of their main properties. In Section 4, we present

non-iterative reconstruction algorithms based on asymptotic formulae of the boundary perturbations due to the presence of the conductivity inclusions. The methods presented in this section detect the locations and the GPT's from boundary measurements. It is the detected first-order polarization tensor which yields an information on the size and orientation of the inclusion. However, the information from the first-order polarization tensor is a mixture of the conductivity and the volume. Section 5 is devoted to the determination of the effective electrical conductivity of a two-phase composite material using boundary layer potentials.

Finally, we discuss the case where the conductivity inclusion is at a distance comparable to its diameter apart from the boundary of the background conductor. We provide in Section 6 some essential insight for understanding the interaction between the inclusion and the boundary of the background medium.

The paper is intended to be reasonably self-contained. No familiarity with layer potential techniques is required. The results discussed in this survey paper complete the material presented in our book [**18**].

2. Layer potentials and transmission problems

Our aim in this section is to collect together the various concepts, basic definitions and key theorems on layer potentials, with which the reader might not be familiar. We then provide an important decomposition formula due to Kang and Seo [**87**] of the steady-state voltage potential into a harmonic part and a refraction part.

Let us begin our study with the following boundary value problem:

$$\begin{cases} \Delta u = 0 \quad \text{in } \Omega, \\ \dfrac{\partial u}{\partial \nu}\Big|_{\partial\Omega} = g. \end{cases} \tag{2.1}$$

Here Ω is a bounded domain representing a conducting body, the function g represents the applied boundary current; it belongs to $L^2(\partial\Omega)$ and has mean value zero, and the solution u represents the voltage distribution in Ω generated by g. Here and throughout this paper $\partial u/\partial\nu = \nabla u \cdot \nu$ and ν is the outward normal to $\partial\Omega$.

We seek the solution to (2.1) in the form

$$u(x) = \int_{\partial\Omega} \Gamma(x-y)\phi(y)d\sigma(y), \quad x \in \Omega, \tag{2.2}$$

where Γ is a fundamental solution to the Laplacian and given by

$$\Gamma(x) := \begin{cases} \dfrac{1}{2\pi}\ln|x|, & d = 2, \\ \dfrac{1}{(2-d)\omega_d}|x|^{2-d}, & d \geq 3. \end{cases}$$

The function u defined by (2.2) is harmonic in Ω (also in $\mathbb{R}^d \setminus \overline{\Omega}$). Thus for u to be the solution to (2.1), it suffices to satisfy the boundary condition. For this purpose, we have to investigate the boundary behavior of

$$\frac{\partial}{\partial\nu}\int_{\partial\Omega}\Gamma(x-y)\phi(y)d\sigma(y),$$

as x approaches to $\partial\Omega$.

2.1. Layer potentials for Laplacian. Given a bounded Lipschitz domain D in $\mathbb{R}^d, d \geq 2$, we will denote the single and double layer potentials of a function

$\phi \in L^2(\partial D)$ as $\mathcal{S}_D\phi$ and $\mathcal{D}_D\phi$, respectively, where

$$\mathcal{S}_D\phi(x) := \int_{\partial D} \Gamma(x-y)\phi(y)\, d\sigma(y), \quad x \in \mathbb{R}^d,$$

$$\mathcal{D}_D\phi(x) := \int_{\partial D} \frac{\partial}{\partial \nu_y}\Gamma(x-y)\phi(y)\, d\sigma(y), \quad x \in \mathbb{R}^d \setminus \partial D.$$

Observe that both $\mathcal{S}_D\phi$ and $\mathcal{D}_D\phi$ are harmonic in D and $\mathbb{R}^d \setminus \overline{D}$. For a function u defined on $\mathbb{R}^d \setminus \partial D$, we denote

$$u\big|_{\pm}(x) := \lim_{t\to 0^+} u(x \pm t\nu_x), \quad x \in \partial D,$$

and

$$\frac{\partial}{\partial \nu_x} u\bigg|_{\pm}(x) := \lim_{t\to 0^+} \langle \nabla u(x \pm t\nu_x), \nu_x\rangle, \quad x \in \partial D,$$

if the limits exist. Here ν_x is the outward unit normal to ∂D at x, and $\langle , \rangle$ denotes the scalar product in $\mathbb{R}^d$.

We want to investigate $\frac{\partial}{\partial \nu}\mathcal{S}_D\phi\big|_{\pm}(x)$ and $\mathcal{D}_D\phi\big|_{\pm}(x)$ for $x \in \partial D$. Fix $z \in \partial D$. Since

$$\langle \nabla\Gamma(x-y), \nu_z\rangle = \frac{1}{\omega_d}\frac{\langle x-y, \nu_z\rangle}{|x-y|^d}, \quad x \in D,\ y \in \partial D,$$

we may expect that

$$\frac{\partial}{\partial \nu}\int_{\partial D} \Gamma(x-y)\phi(y)d\sigma(y) \to \frac{1}{\omega_d}\int_{\partial D} \frac{\langle z-y, \nu_z\rangle}{|z-y|^d}\phi(y)d\sigma(y) \quad \text{as } x \to z.$$

But this is not the case. The main difficulty is that since

$$\left|\frac{\langle z-y, \nu_z\rangle}{|z-y|^d}\right| \le C|z-y|^{1-d}$$

and ∂D is a manifold of dimension $d-1$, the righthand side of the above is not absolutely integrable. On the other hand, $(1/\omega_d)\langle x-y, \nu_z\rangle/|x-y|^d$ has a structure of the Poisson kernel. To see this, let us suppose that $d=2$, $z=0$, ∂D is the x-axis near 0, and D is a part below the x-axis. In this case, if $x = z - \epsilon\nu_z = (0, -\epsilon)$, then for $y = (y_1, 0) \in \partial D$, we have

$$\langle \nabla\Gamma(x-y), \nu_z\rangle = -\frac{1}{2\pi}\frac{\epsilon}{|y_1|^2 + \epsilon^2},$$

which is exactly $-1/2$ times the Poisson kernel. So we can expect that

$$\int_{\partial D} \langle \nabla\Gamma(x-y), \nu_z\rangle\phi(y)d\sigma(y)$$

will pick up $-(1/2)\phi(z)$ as $x \to z$ from inside D. The following theorem shows that it is indeed the case. Proofs of the theorem can be found in [**70**] for when D has a $\mathcal{C}^2$-boundary, and in [**132**] for D with a Lipschitz boundary.

THEOREM 2.1 (Jump formula). *Let D be a bounded Lipschitz domain in $\mathbb{R}^d$. For $\phi \in L^2(\partial D)$*

$$\mathcal{S}_D\phi\big|_{+}(x) = \mathcal{S}_D\phi\big|_{-}(x) \quad \text{a.e. } x \in \partial D,$$

$$\frac{\partial}{\partial \nu}\mathcal{S}_D\phi\bigg|_{\pm}(x) = \left(\pm\frac{1}{2}I + \mathcal{K}_D^*\right)\phi(x) \quad \text{a.e. } x \in \partial D, \tag{2.3}$$

$$(\mathcal{D}_D\phi)\big|_{\pm}(x) = \left(\mp\frac{1}{2}I + \mathcal{K}_D\right)\phi(x) \quad \text{a.e. } x \in \partial D, \tag{2.4}$$

where $\mathcal{K}_D$ is defined by

$$\mathcal{K}_D\phi(x) = \frac{1}{\omega_d}p.v.\int_{\partial D} \frac{\langle y-x, \nu_y\rangle}{|x-y|^d}\phi(y)\, d\sigma(y)$$

and $\mathcal{K}_D^*$ is the L^2-adjoint of $\mathcal{K}_D$, i.e.,

$$\mathcal{K}_D^*\phi(x) = \frac{1}{\omega_d} p.v. \int_{\partial D} \frac{\langle x-y, \nu_x\rangle}{|x-y|^d}\phi(y)\, d\sigma(y).$$

Here p.v. *denotes the Cauchy principal value.*

This theorem is based on the fact that the operators $\mathcal{K}_D$ is well-defined, which is guaranteed by the following celebrated theorem of Coifman-McIntosh-Meyer [**60**].

THEOREM 2.2. *The operators $\mathcal{K}_D$ and $\mathcal{K}_D^*$ are singular integral operators and bounded on $L^2(\partial D)$.*

We strongly recommend the readers to read [**60**] to have feeling of power and beauty of the classical harmonic analysis. If D has $\mathcal{C}^2$ boundary, or $\mathcal{C}^{1,\alpha}$ $(\alpha > 0)$ boundary for that matter, then there is an extra orthogonality, which is absent for the Lipschitz boundary, between $x-y$ $(x, y \in \partial D)$ and ν_x. Using this orthogonality, we can show that

$$\left|\frac{\langle x-y, \nu_x\rangle}{|x-y|^d}\right| \leq \frac{C}{|x-y|^{d-2}} \quad \left(\leq \frac{C}{|x-y|^{d-1-\alpha}} \text{ if } \partial D \text{ is } \mathcal{C}^{1,\alpha}\right),$$

and hence $\mathcal{K}_D^*$ becomes a compact operator on $L^2(\partial D)$. See [**70**] for this.

Let us state further mapping properties of layer potentials, whose proof can be found in [**132**]; see also [**18**].

THEOREM 2.3. *Let D be a bounded Lipschitz domain in $\mathbb{R}^d$. Then*

(i) $\mathcal{S}_D : L^2(\partial D) \to W_1^2(\partial D)$ *bounded.*
(ii) $\mathcal{K}_D : W_1^2(\partial D) \to W_1^2(\partial D)$ *bounded.*

Observe that if D is a two dimensional disk with radius r, then, as was observed in [**87**],

$$\frac{\langle x-y, \nu_x\rangle}{|x-y|^2} = \frac{1}{2r} \quad \forall\, x, y \in \partial D, x \neq y,$$

and therefore, for any $\phi \in L^2(\partial D)$,

$$\mathcal{K}_D^*\phi(x) = \mathcal{K}_D\phi(x) = \frac{1}{4\pi r}\int_{\partial D} \phi(y)\, d\sigma(y), \tag{2.5}$$

for all $x \in \partial D$. For $d \geq 3$, if D denotes a sphere with radius r, then, since

$$\frac{\langle x-y, \nu_x\rangle}{|x-y|^d} = \frac{1}{2r}\frac{1}{|x-y|^{d-2}} \quad \forall\, x, y \in \partial D, x \neq y,$$

we have, as shown by Lemma 2.3 of [**89**], that for any $\phi \in L^2(\partial D)$,

$$\mathcal{K}_D^*\phi(x) = \mathcal{K}_D\phi(x) = \frac{(2-d)}{2r}\mathcal{S}_D\phi(x)$$

for all $x \in \partial D$. In particular, if D is a ball in $\mathbb{R}^d$, $d \geq 2$, then $\mathcal{K}_D$ is a self-adjoint operator on $L^2(\partial D)$. The converse is also true: Let D be a Lipschitz domain. If $\mathcal{K}_D$ is self-adjoint, then D is a ball. This was proved by Lim in [**108**].

There is a conjecture that has not been resolved completely. Observe that $\mathcal{K}_D(1) = 1/2$, and hence $\mathcal{K}_D^*(1) = 1/2$ provided that D is a ball. The conjecture is that if $\mathcal{K}_D^*(1) = 1/2$ and D is a Lipschitz domain, then D is a ball. The conjecture has been proved to be true for some important classes of domains: Piecewise smooth domains in $\mathbb{R}^2$ by Martensen [**113**], star-shaped $\mathcal{C}^{2,\alpha}$-domains by Payne and Philippin [**119**] and Philippin [**121**], and $\mathcal{C}^{2,\alpha}$-domains by Reichel [**122, 123**]. Recently Mendez and Reichel proved the conjecture for bounded Lipschitz domains in $\mathbb{R}^2$ and bounded Lipschitz convex domains in $\mathbb{R}^d$ $(d \geq 3)$ [**114**].

Let us now go back to the problem (2.1). If the solution u takes the form $\mathcal{S}_\Omega\phi$ for some ϕ in Ω, then by the boundary condition we need to have

$$\frac{\partial}{\partial\nu}\mathcal{S}_\Omega\phi\Big|_- = g \quad \text{on } \partial\Omega.$$

It then follows from (2.3) that

$$(-\frac{1}{2}I + \mathcal{K}_D^*)\phi = g \quad \text{on } \partial\Omega.$$

In other words we need to invert the operator $(-(1/2)I + \mathcal{K}_D^*)$ on $L^2(\partial\Omega)$.

If D is a $\mathcal{C}^{1,\alpha}$ domain, then $\mathcal{K}_D^*$ is a compact operator, and hence $(-(1/2)I+\mathcal{K}_D^*)$ is a Fredholm operator of index zero. Therefore, by the Fredholm alternative, the question of invertibility is reduced to that of injectivity, and injectivity of $(-(1/2)I+\mathcal{K}_D^*)$ can be proved without much effort. See [**70**]. But if ∂D is merely Lipschitz, $\mathcal{K}_D^*$ is not a compact operator and invertibility of $(-(1/2)I + \mathcal{K}_D^*)$ is a serious matter. The following theorem is due to Verchota [**132**] for $|\lambda| = 1/2$ and Escauriaza *et al.* [**68**] for $|\lambda| > 1/2$.

THEOREM 2.4. *The operator $\lambda I - \mathcal{K}_D^*$ is invertible on $L_0^2(\partial D)$ if $|\lambda| \geq 1/2$, and for $\lambda \in]-\infty, -1/2]\cup]1/2, \infty[$, $\lambda I - \mathcal{K}_D^*$ is invertible on $L^2(\partial D)$.*

Here and throughout this paper, we define the space $L_0^2(\partial D)$ by

$$L_0^2(\partial D) := \left\{\phi \in L^2(\partial D) : \int_{\partial D} \phi\, d\sigma = 0\right\}.$$

The key fact in proving Theorem 2.4 is the following: For a function u the tangential derivative of u along ∂D is defined to be

$$\frac{\partial u}{\partial T} := \sum_{p=1}^{d-1} \frac{\partial u}{\partial T_p} T_p,$$

where $T_1, \ldots, T_{d-1}$ is an orthonormal basis for the tangent plane to ∂D at x.

LEMMA 2.5. *Let D be a bounded Lipschitz domain in $\mathbb{R}^d, d \geq 2$. Let u be a function such that either*

(i) *u is Lipschitz in $\overline{D}$ and $\Delta u = 0$ in D, or*
(ii) *u is Lipschitz in $\mathbb{R}^d \setminus D$, $\Delta u = 0$ in $\mathbb{R}^d \setminus \overline{D}$, and $|u(x)| = O(1/|x|^{d-2})$ when $d \geq 3$ and $|u(x)| = O(1/|x|)$ when $d = 2$ as $|x| \to +\infty$.*

Then there exists a positive constant C depending only on the Lipschitz character of D such that

$$\frac{1}{C}\left\|\frac{\partial u}{\partial T}\right\|_{L^2(\partial D)} \leq \left\|\frac{\partial u}{\partial \nu}\right\|_{L^2(\partial D)} \leq C\left\|\frac{\partial u}{\partial T}\right\|_{L^2(\partial D)}. \tag{2.6}$$

Lemma 2.5 says that the L^2 norms of the normal and tangential derivatives of a harmonic function are comparable, and can be proved using the Rellich identity [**132**]; see also [**18**]. Let us briefly see how Lemma 2.5 leads us to Theorem 2.4.

Let $u(x) = \mathcal{S}_D f(x)$, where $f \in L_0^2(\partial D)$. Because of the jump formula (2.3), we have

$$\frac{\partial u}{\partial \nu}\Big|_\pm = (\pm\frac{1}{2}I + \mathcal{K}_D^*)f,$$

and by (2.6)

$$\left\|\frac{\partial u}{\partial \nu}\Big|_-\right\|_{L^2(\partial D)} \simeq \left\|\frac{\partial u}{\partial \nu}\Big|_+\right\|_{L^2(\partial D)},$$

or equivalently

$$\frac{1}{C}\,||(\frac{1}{2}I + \mathcal{K}_D^*)f||_{L^2(\partial D)} \leq ||(\frac{1}{2}I - \mathcal{K}_D^*)f||_{L^2(\partial D)} \leq C\,||(\frac{1}{2}I + \mathcal{K}_D^*)f||_{L^2(\partial D)}. \tag{2.7}$$

Since $f = ((1/2)I + \mathcal{K}_D^*)f + ((1/2)I - \mathcal{K}_D^*)f$, (2.7) yields that

$$||(\frac{1}{2}I + \mathcal{K}_D^*)f||_{L^2(\partial D)} \geq C||f||_{L^2(\partial D)}.$$

We also have the following estimate from [**16**].

LEMMA 2.6. *There exists a constant C depending only on the Lipschitz character of D such that for any $|\lambda| \geq 1/2$*

$$\|\phi\|_{L^2(\partial D)} \leq C\frac{1}{|\lambda|}\,\|(\lambda I - \mathcal{K}_D^*)\,\phi\|_{L^2(\partial D)}$$

for all $\phi \in L_0^2(\partial D)$.

2.2. Neumann and Dirichlet functions. Let Ω be a bounded Lipschitz domain in $\mathbb{R}^d, d \geq 2$. Let $N(x,z)$ be the Neumann function for Δ in Ω corresponding to a Dirac mass at z. That is, N is the solution to

$$\begin{cases} \Delta_x N(x,z) = -\delta_z \quad \text{in } \Omega, \\ \dfrac{\partial N}{\partial \nu_x}\Big|_{\partial\Omega} = -\dfrac{1}{|\partial\Omega|}, \displaystyle\int_{\partial\Omega} N(x,z)\,d\sigma(x) = 0 \quad \text{for } z \in \Omega. \end{cases} \tag{2.8}$$

Note that the Neumann function $N(x,z)$ is defined as a function of $x \in \overline{\Omega}$ for each fixed $z \in \Omega$. The operator defined by $N(x,z)$ is the solution operator for the Neumann problem

$$\begin{cases} \Delta U = 0 \quad \text{in } \Omega, \\ \dfrac{\partial U}{\partial \nu}\Big|_{\partial\Omega} = g, \end{cases} \tag{2.9}$$

namely, the function U defined by

$$U(x) := \int_{\partial\Omega} N(x,z)g(z)d\sigma(z)$$

is the solution to (2.9) satisfying $\int_{\partial\Omega} U\,d\sigma = 0$.

For D, a subset of Ω, let

$$\mathcal{N}_D f(x) := \int_{\partial D} N(x,y)f(y)\,d\sigma(y).$$

The following lemma from [**15**] relates the fundamental solution with the Neumann function.

LEMMA 2.7. *For $z \in \Omega$ and $x \in \partial\Omega$, let $\Gamma_z(x) := \Gamma(x-z)$ and $N_z(x) := N(x,z)$. Then*

$$\left(-\frac{1}{2}I + \mathcal{K}_\Omega\right)(N_z)(x) = \Gamma_z(x) \quad \textit{modulo constants}, \quad x \in \partial\Omega, \tag{2.10}$$

or, to be more precise, for any simply connected Lipschitz domain D compactly contained in Ω and for any $g \in L_0^2(\partial D)$, we have for any $x \in \partial\Omega$

$$\int_{\partial D}\left(-\frac{1}{2}I + \mathcal{K}_\Omega\right)(N_z)(x)g(z)\,d\sigma(z) = \int_{\partial D}\Gamma_z(x)g(z)\,d\sigma(z).$$

Observe that we can express (2.10) in the following form: for any $g \in L_0^2(\partial D)$

$$\mathcal{N}_D g(x) = \left(-\frac{1}{2}I + \mathcal{K}_\Omega\right)^{-1}\left((\mathcal{S}_D g)|_{\partial\Omega}\right)(x), \quad x \in \partial\Omega. \tag{2.11}$$

We have a similar formula for the Dirichlet function. Let $G(x,z)$ be the Green's function for the Dirichlet problem in Ω, that is, the unique solution to

$$\begin{cases} \Delta_x G(x,z) = -\delta_z \quad \text{in } \Omega, \\ G(x,z) = 0 \quad \text{on } \partial\Omega, \end{cases}$$

and let $G_z(x) = G(x,z)$. Then for any $x \in \partial\Omega$, and $z \in \Omega$ we can prove that

$$\left(\frac{1}{2}I + \mathcal{K}_\Omega^*\right)^{-1}\left(\frac{\partial \Gamma_z(y)}{\partial \nu_y}\right)(x) = -\frac{\partial G_z}{\partial \nu_x}(x).$$

2.3. Transmission problems. Let Ω be a bounded domain in $\mathbb{R}^d$ with a connected Lipschitz boundary and conductivity equal to 1. Consider a bounded domain $D \subset\subset \Omega$ with a connected Lipschitz boundary and conductivity $0 < k \neq 1 < +\infty$. Let $g \in L_0^2(\partial\Omega)$, and consider the following transmission problem:

$$\begin{cases} \nabla \cdot \Big(1 + (k-1)\chi(D)\Big)\nabla u = 0 \quad \text{in } \Omega, \\ \dfrac{\partial u}{\partial \nu}\Big|_{\partial\Omega} = g, \\ \displaystyle\int_{\partial\Omega} u(x)\, d\sigma(x) = 0, \end{cases} \tag{2.12}$$

where $\chi(D)$ is the characteristic function of D. By integrating the equation against functions with compact supports, we can easily see that the problem (2.12) can be rephrased as

$$\begin{cases} \Delta u = 0 & \text{in } \Omega \setminus \partial D, \\ u\big|_- - u\big|_+ = 0 & \text{on } \partial D, \\ k\dfrac{\partial u}{\partial \nu}\Big|_- - \dfrac{\partial u}{\partial \nu}\Big|_+ = 0 & \text{on } \partial D, \\ \dfrac{\partial u}{\partial \nu}\Big|_{\partial\Omega} = g, \\ \displaystyle\int_{\partial\Omega} u(x)\, d\sigma(x) = 0. \end{cases}$$

At this point we have all the necessary ingredients to state a decomposition formula of the steady-state voltage potential u into a harmonic part and a refraction part which will be the main tool for deriving the asymptotic expansion, for designing efficient reconstruction algorithms, and for calculating effective properties of composite materials in later sections. This decomposition formula is unique and inherits geometric properties of the inclusion D.

The following theorem was proved in [**87, 88, 90**]. The original formula in [**87**] is rather complicated even if it contains all the idea. The following formula has appeared in [**90**] with a simpler proof.

THEOREM 2.8. *Suppose that D is a domain compactly contained in Ω with a connected Lipschitz boundary and conductivity $0 < k \neq 1 < +\infty$. Then the solution u of the Neumann problem* (2.12) *is represented as*

$$u(x) = H(x) + \mathcal{S}_D\phi(x), \quad x \in \Omega, \tag{2.13}$$

where the harmonic function H is given by

$$H(x) = -\mathcal{S}_\Omega(g)(x) + \mathcal{D}_\Omega(f)(x), \quad x \in \Omega, \quad f := u|_{\partial\Omega}, \tag{2.14}$$

and $\phi \in L_0^2(\partial D)$ satisfies the integral equation

$$\left(\lambda I - \mathcal{K}_D^*\right)\phi = \frac{\partial H}{\partial \nu}\Big|_{\partial D} \quad \text{on } \partial D, \tag{2.15}$$

$$\lambda = \frac{k+1}{2(k-1)}. \tag{2.16}$$

The decomposition (2.13) *into a harmonic part and a refraction part is unique. Moreover,* $\forall\, n \in \mathbb{N}$*, there exists a constant* $C_n = C(n, \Omega, dist(D, \partial\Omega))$ *independent of* $|D|$ *and the conductivity* k *such that*

$$\|H\|_{\mathcal{C}^n(\overline{D})} \leq C_n \|g\|_{L^2(\partial\Omega)}.$$

Furthermore, the following holds

$$H(x) + \mathcal{S}_D\phi(x) = 0, \quad \forall\, x \in \mathbb{R}^d \setminus \overline{\Omega}.$$

Similar formulae can be derived when there are several inclusions. Consider the following problem in the presence of multiple inclusions $D_1, \ldots, D_m$:

$$\begin{cases} \nabla \cdot \left(\chi(\Omega \setminus \bigcup_{s=1}^m \overline{D_s}) + \sum_{s=1}^m k_s \chi(D_s)\right)\nabla u = 0 \quad \text{in } \Omega, \\ \left.\dfrac{\partial u}{\partial \nu}\right|_{\partial\Omega} = g, \\ \displaystyle\int_{\partial\Omega} u(x)\, d\sigma(x) = 0. \end{cases} \tag{2.17}$$

The following theorem was first proved in [**102**].

THEOREM 2.9. *Let* H *be a harmonic function in* Ω *as defined in (2.14). There are unique functions* $\phi^{(l)} \in L_0^2(\partial D_l)$*,* $l = 1, \ldots, m$*, such that the solution* u *to (2.17) can be represented as*

$$u(x) = H(x) + \sum_{l=1}^m \mathcal{S}_{D_l}\phi^{(l)}(x). \tag{2.18}$$

The potentials $\phi^{(l)}$*,* $l = 1, \ldots, m$*, are the unique solution to the system of integral equations*

$$(\lambda_l I - \mathcal{K}_{D_l}^*)\phi^{(l)} - \sum_{s \neq l} \frac{\partial(\mathcal{S}_{D_s}\phi^{(s)})}{\partial\nu^{(l)}}\Big|_{\partial D_l} = \frac{\partial H}{\partial\nu^{(l)}}\Big|_{\partial D_l} \quad \text{on } \partial D_l, \tag{2.19}$$

where $\nu^{(l)}$ *denotes the outward unit normal to* ∂D_l *and*

$$\lambda_l = \frac{k_l + 1}{2(k_l - 1)}.$$

Let $\delta := \min\{\text{dist}(D_l, D_{l'}) : l \neq l'\}$. Then since $\phi^{(l)} \in L_0^2(\partial D_l)$, we have

$$\frac{\partial(\mathcal{S}_{D_s}\phi^{(s)})}{\partial\nu^{(l)}}(x) = \int_{\partial D_s} \left[\frac{\partial}{\partial\nu^{(l)}(x)}\Gamma(x-y) - \frac{\partial}{\partial\nu^{(l)}(x)}\Gamma(x-y_0)\right]\phi^{(s)}(y)d\sigma(y),$$

for some $y_0 \in \partial D_s$, and hence if $l \neq s$, then

$$\frac{\partial(\mathcal{S}_{D_s}\phi^{(s)})}{\partial\nu^{(l)}}(x) = O(\delta^{-d}).$$

It then follows from (2.19) that

$$\phi^{(l)} = (\lambda_l I - \mathcal{K}_{D_l}^*)^{-1}\left(\frac{\partial H}{\partial\nu^{(l)}}\Big|_{\partial D_l}\right) + O(\delta^{-d}) \quad \text{on } \partial D_l. \tag{2.20}$$

Thus if the inclusions are far apart, in other words, if δ is large, then

$$\phi^{(l)} \approx (\lambda_l I - \mathcal{K}_{D_l}^*)^{-1}\left(\frac{\partial H}{\partial\nu^{(l)}}\Big|_{\partial D_l}\right).$$

We note that the formulae (2.15) and (2.19) are valid even for extreme conductivities $k = 0, \infty$ [**88**]. If $k_l = 0$, then from (2.3) and (2.18) we obtain

$$\left.\frac{\partial u}{\partial\nu^{(l)}}\right|_+ = \frac{\partial H}{\partial\nu^{(l)}} + (\frac{1}{2}I + \mathcal{K}_{D_l}^*)\phi^{(l)} + \sum_{s \neq l} \frac{\partial(\mathcal{S}_{D_s}\phi^{(s)})}{\partial\nu^{(l)}}\Big|_{\partial D_l} \quad \text{on } \partial D_l.$$

Since $\lambda_l = -1/2$, we have

$$\left.\frac{\partial u}{\partial \nu^{(l)}}\right|_+ = 0 \quad \text{on } \partial D_l,$$

which means that ∂D_l is insulated. On the other hand, if $k_l = \infty$, then by the same argument, we can see that

$$\left.\frac{\partial u}{\partial \nu^{(l)}}\right|_- = 0 \quad \text{on } \partial D_l,$$

and hence $u =$ constant in D_l, which means that D_l is a perfect conductor.

Observe that the harmonic function H depends on f and hence on the inclusion D. We now present another decomposition of the solution where the harmonic part is independent of D, which was derived in [**15**]. Let U be the solution without the inclusion D, *i.e.*, the solution to

$$\begin{cases} \Delta U = 0 \quad \text{in } \Omega, \\ \left.\dfrac{\partial U}{\partial \nu}\right|_{\partial\Omega} = g, \\ \displaystyle\int_{\partial\Omega} U(x)\, d\sigma(x) = 0. \end{cases} \tag{2.21}$$

Then U can be written as

$$U(y) = \mathcal{N}_\Omega g(y) = \int_{\partial\Omega} N(x,y) g(x)\, d\sigma(x).$$

THEOREM 2.10. *The solution u of* (2.17) *can be represented as*

$$u(x) = U(x) - \sum_{l=1}^{m} \mathcal{N}_{D_l} \phi^{(l)}(x), \quad x \in \partial\Omega, \tag{2.22}$$

where $\phi^{(l)}$ is defined in (2.19).

Recall that the Neumann-to-Dirichlet (NtD) map $\Lambda_D : L^2_0(\partial\Omega) \to W^2_{\frac{1}{2}}(\partial\Omega)$ corresponding to the conductivity distribution $\chi(\Omega \setminus \bigcup_{s=1}^m \overline{D_s}) + \sum_{s=1}^m k_s \chi(D_s)$ is defined, for $g \in L^2_0(\partial\Omega)$, by

$$\Lambda_D(g) := u|_{\partial\Omega},$$

where u is the unique weak solution to (2.17). The space $W^2_{\frac{1}{2}}(\partial\Omega)$ is defined by $f \in W^2_{\frac{1}{2}}(\partial\Omega)$ if and only if $f \in L^2(\partial\Omega)$ and

$$\int_{\partial\Omega}\int_{\partial\Omega} \frac{|f(x) - f(y)|^2}{|x-y|^d}\, d\sigma(x)\, d\sigma(y) < +\infty.$$

See for instance [**75**] .

It then follows from (2.14) and (2.18) that

$$-u + \mathcal{D}_\Omega(u|_{\partial\Omega}) = \mathcal{S}_\Omega(g)|_{\partial\Omega} - \sum_{j=1}^{m} \mathcal{S}_{D_j}\phi^{(j)}|_{\partial\Omega} \quad \text{in } \Omega,$$

and hence, by (2.4), we get

$$(-\frac{1}{2}I + \mathcal{K}_\Omega)(u|_{\partial\Omega}) = \mathcal{S}_\Omega(g)|_{\partial\Omega} - \sum_{j=1}^{m} \mathcal{S}_{D_j}\phi^{(j)}|_{\partial\Omega} \quad \text{on } \partial\Omega.$$

We then have from (2.11) that

$$\Lambda_D(g) = (-\frac{1}{2}I + \mathcal{K}_\Omega)^{-1}\left(\mathcal{S}_\Omega(g)|_{\partial\Omega} - \sum_{j=1}^{m} \mathcal{S}_{D_j}\phi^{(j)}|_{\partial\Omega}\right) = \Lambda_0(g) - \sum_{l=1}^{m} \mathcal{N}_{D_l}\phi^{(l)},$$

which is exactly the formula (2.22).

We have a similar representation for solutions of the Dirichlet problem. Let $f \in W^{2}_{\frac{1}{2}}(\partial\Omega)$, and let v and V be the (variational) solutions of the Dirichlet problems:

$$\begin{cases} \nabla \cdot \Big(1 + (k-1)\chi(D)\Big)\nabla v = 0 \quad \text{in } \Omega, \\ v = f \quad \text{on } \partial\Omega, \end{cases} \tag{2.23}$$

and

$$\begin{cases} \Delta V = 0 \quad \text{in } \Omega, \\ V = f \quad \text{on } \partial\Omega. \end{cases} \tag{2.24}$$

The following representation theorem holds.

THEOREM 2.11. *Let v and V be the solution of the Dirichlet problems (2.23) and (2.24). Then $\partial v/\partial\nu$ on ∂D can be represented as*

$$\frac{\partial v}{\partial \nu}(x) = \frac{\partial V}{\partial \nu}(x) - \frac{\partial}{\partial \nu} G_D \phi(x), \quad x \in \partial\Omega,$$

where ϕ is defined in (2.15) with H given by (2.14) and $g = \partial v/\partial\nu$ on $\partial\Omega$, and

$$G_D \phi(x) := \int_{\partial D} G(x,y)\phi(y)\, d\sigma(y).$$

2.4. Periodic transmission problem. We now consider the following periodic transmission problem used in calculating effective properties of dilute composite materials. Let $Y =]-1/2, 1/2[^d$ denote the unit cell and $\overline{D} \subset Y$. Consider the periodic transmission problem:

$$\begin{cases} \nabla \cdot \Big(1 + (k-1)\chi(D)\Big)\nabla u_i = 0 \quad \text{in } Y, \\ \\ u_i - y_i \text{ periodic with period 1 (in each direction)}, \\ \int_Y u_i(y)dy = 0, \end{cases} \tag{2.25}$$

for $i = 1, \ldots, d$.

In order to derive a representation formula for the solution to (2.25), we need a periodic Green's function. Let

$$G(x) = -\sum_{n \in \mathbb{Z}^d \setminus \{0\}} \frac{e^{i2\pi n \cdot x}}{4\pi^2 |n|^2}.$$

Then we get, in the sense of distributions,

$$\Delta G(x) = \sum_{n \in \mathbb{Z}^d \setminus \{0\}} e^{i2\pi n \cdot x} = \sum_{n \in \mathbb{Z}^d} e^{i2\pi n \cdot x} - 1.$$

It then follows from the Poisson summation formula

$$\sum_{n \in \mathbb{Z}^d} e^{i2\pi n \cdot x} = \sum_{n \in \mathbb{Z}^d} \delta(x+n),$$

that

$$\Delta G(x) = \sum_{n \in \mathbb{Z}^d} \delta(x+n) - 1. \tag{2.26}$$

Appearance of the constant 1 in (2.26) may be a little peculiar. It is the volume of Y and an integration by parts shows that it should be there. In fact,

$$\int_Y \Delta G(x) dx = \int_{\partial Y} \frac{\partial G}{\partial \nu} d\sigma,$$

and the righthand side is zero because of the periodicity.

For simplicity we only detail the two-dimensional case. The following results were obtained in [**29**].

LEMMA 2.12. *Suppose that $d = 2$. There exists a harmonic function $R(x)$ in the unit cell Y such that*

$$G(x) = \frac{1}{2\pi} \ln |x| + R(x). \tag{2.27}$$

Moreover, the Taylor expansion of $R(x)$ at 0 is given by

$$R(x) = R(0) - \frac{1}{4}(x_1^2 + x_2^2) + O(|x|^4). \tag{2.28}$$

The periodic single layer potential of the density function $\phi \in L_0^2(\partial D)$ is defined by

$$\mathcal{G}_D\phi(x) := \int_{\partial D} G(x-y)\phi(y)\, d\sigma(y), \quad x \in \mathbb{R}^2.$$

Lemma 2.12 shows that

$$\mathcal{G}_D\phi(x) = \mathcal{S}_D\phi(x) + \mathcal{R}_D\phi(x), \tag{2.29}$$

where $\mathcal{R}_D$ is a smoothing operator defined by

$$\mathcal{R}_D\phi(x) := \int_{\partial D} R(x-y)\phi(y)\, d\sigma(y).$$

Thanks to (2.29), we have

$$\frac{\partial}{\partial \nu}\mathcal{G}_D\phi\Big|_{\pm}(x) = \frac{\partial}{\partial \nu}\mathcal{S}_D\phi\Big|_{\pm}(x) + \frac{\partial}{\partial \nu}\mathcal{R}_D\phi(x), \quad x \in \partial D.$$

Thus we can understand $\frac{\partial}{\partial \nu}\mathcal{G}_D\phi|_{\pm}$ as a compact perturbation of $\frac{\partial}{\partial \nu}\mathcal{S}_D\phi|_{\pm}$. Based on this natural idea, we obtain the following results from [**29**].

LEMMA 2.13. (i) *Let $\phi \in L_0^2(\partial D)$. The following trace formula holds:*

$$\frac{\partial}{\partial \nu}\mathcal{G}_D\phi\Big|_{\pm}(x) = (\pm\frac{1}{2}I + \mathcal{B}_D^*)\phi(x) \text{ on } \partial D,$$

where $\mathcal{B}_D^* : L_0^2(\partial D) \to L_0^2(\partial D)$ is given by

$$\mathcal{B}_D^*\phi(x) = p.v. \int_{\partial D} \frac{\partial}{\partial \nu_x} G(x-y)\phi(y)\, d\sigma(y).$$

(ii) *If $\phi \in L_0^2(\partial D)$, then $\mathcal{G}_D\phi$ is harmonic in D and $Y \setminus \overline{D}$.*
(iii) *If $|\lambda| \geq \frac{1}{2}$, then the operator $\lambda I - \mathcal{B}_D^*$ is invertible on $L_0^2(\partial D)$.*

Analogously to Theorem 2.9 the following result holds.

THEOREM 2.14. *Let u_i be the unique solution to the transmission problem (2.25). Then u_i can be expressed as follows*

$$u_i(x) = x_i + C_i + \mathcal{G}_D(\lambda I - \mathcal{B}_D^*)^{-1}(\nu_i)(x) \quad \text{in } Y, \quad i = 1, 2,$$

where λ is given by (2.16), C_i is a constant and ν_i is the i-component of the outward unit normal ν to ∂D.

2.5. Anisotropic transmission problem. Let D be a bounded Lipschitz domain in $\mathbb{R}^d$, $d = 2, 3$. Let A be a positive-definite symmetric matrix and A_* be the positive-definite symmetric matrix such that $A^{-1} = A_*^2$. Let $\Gamma^A(x)$ be the fundamental solution of the operator $\nabla \cdot A\nabla$:

$$\Gamma^A(x) := \begin{cases} \dfrac{1}{2\pi\sqrt{|A|}} \ln ||A_* x||, & d = 2, \\ -\dfrac{1}{4\pi\sqrt{|A|}||A_* x||}, & d = 3, \end{cases}$$

where $|A|$ is the determinant of A, and $||\cdot||$ is the usual norm of the vector in $\mathbb{R}^d$. The single and double layer potentials associated with A of the density function ϕ on ∂D are defined by

$$\mathcal{S}_D^A \phi(x) := \int_{\partial D} \Gamma^A(x-y)\phi(y) d\sigma(y), \quad x \in \mathbb{R}^d,$$

and

$$\mathcal{D}_D^A \phi(x) := \int_{\partial D} \nu_y \cdot A\nabla\Gamma^A(x-y)\phi(y) d\sigma(y), \quad x \in \mathbb{R}^d \setminus \partial D.$$

The following jump formulae are well-known:

$$\nu_x \cdot A\nabla \mathcal{S}_D^A \phi(x)|_+ - \nu_x \cdot A\nabla \mathcal{S}_D^A \phi(x)|_- = \phi(x) \quad \text{a.e. } x \in \partial D, \tag{2.30}$$

$$\mathcal{D}_D^A \phi(x)|_+ - \mathcal{D}_D^A \phi(x)|_- = -\phi(x) \quad \text{a.e. } x \in \partial D.$$

Let $\widetilde{A}$ be a constant $d \times d$ positive-definite symmetric matrix with $\widetilde{A} \neq A$. We always suppose that $\widetilde{A} - A$ is either positive-definite or negative-definite. We will use $\mathcal{S}_D^{\widetilde{A}}$ as a notation for the single layer potential associated with the the domain D and the matrix $\widetilde{A}$.

The following result of Escauriaza and Seo [**69**] is of importance to us.

THEOREM 2.15. *For each $(F, G) \in W_1^2(\partial D) \times L^2(\partial D)$, there exists a unique solution $(f, g) \in L^2(\partial D) \times L^2(\partial D)$ of the integral equation*

$$\begin{cases} \mathcal{S}_D^{\widetilde{A}} f - \mathcal{S}_D^A g = F \\ \nu \cdot \widetilde{A}\nabla \mathcal{S}_D^{\widetilde{A}} f|_- - \nu \cdot A\nabla \mathcal{S}_D^A g|_+ = G \end{cases} \quad \text{on } \partial D. \tag{2.31}$$

Moreover, there exists a constant C depending only on the largest and smallest eigenvalues of $\widetilde{A}$, A, and $\widetilde{A} - A$, and the Lipschitz character of D such that

$$\|f\|_{L^2(\partial D)} + \|g\|_{L^2(\partial D)} \leq C(\|F\|_{W_1^2(\partial D)} + \|G\|_{L^2(\partial D)}).$$

We can easily see that if $G \in L_0^2(\partial D)$, then the solution g of (2.31) lies in $L_0^2(\partial D)$. Moreover, if $G = 0$ and $F =$ constant, then $g = 0$. We summarize these facts in the following lemma.

LEMMA 2.16. *Let (f, g) be the solution to (2.31). If $G \in L_0^2(\partial D)$, then $g \in L_0^2(\partial D)$. Moreover, if F is constant and $G = 0$, then $g = 0$.*

Let Ω be a bounded Lipschitz domain in $\mathbb{R}^d$, $d = 2, 3$. Suppose that Ω contains an inclusion D. Suppose that the conductivity of the background $\Omega \setminus D$ is A and that of D is $\widetilde{A}$. The conductivity profile of the body Ω is given by

$$\gamma_\Omega := \chi_{\Omega \setminus \overline{D}} A + \chi_D \widetilde{A},$$

where χ_D is the characteristic function corresponding to D.

For a given $g \in L^2_0(\partial\Omega)$, let u denote the steady-state voltage in the presence of the conductivity anisotropic inclusion D, *i.e.*, the solution to

$$\begin{cases} \nabla \cdot \gamma_\Omega(x)\nabla u = 0 \quad \text{in } \Omega, \\ \nu \cdot A\nabla u\Big|_{\partial\Omega} = g, \\ \displaystyle\int_{\partial\Omega} u(x)\, d\sigma(x) = 0. \end{cases} \tag{2.32}$$

Let

$$H^A(x) := -\mathcal{S}^A_\Omega(g)(x) + \mathcal{D}^A_\Omega(f)(x), x \in \Omega, \quad f := u|_{\partial\Omega}. \tag{2.33}$$

The following representation formula from [**84**] holds.

THEOREM 2.17. *Let H^A be defined by (2.33). Then the solution u to (2.32) can be represented as*

$$u(x) = \begin{cases} H^A(x) + \mathcal{S}^A_D\phi(x), \quad x \in \Omega \setminus \overline{D}, \\ \mathcal{S}^{\widetilde{A}}_D\psi, \quad x \in D, \end{cases}$$

where the pair (ϕ, ψ) is the unique solution in $L^2(\partial D) \times L^2(\partial D)$ to the system of integral equations

$$\begin{cases} \mathcal{S}^{\widetilde{A}}_D\psi - \mathcal{S}^A_D\phi = H^A \\ \nu \cdot \widetilde{A}\nabla\mathcal{S}^{\widetilde{A}}_D\psi|_- - \nu \cdot A\nabla\mathcal{S}^A_D\phi|_+ = \nu \cdot A\nabla H^A \end{cases} \quad \text{on } \partial D.$$

3. Generalized polarization tensors

In this section we introduce the notion of generalized polarization tensors (GPT's) associated with a bounded Lipschitz domain and an isotropic or an anisotropic conductivity and study their basic properties. The GPT's generalize the concepts of classical Pólya–Szegö polarization tensors which have been extensively studied by many authors for various purposes. As it will be shown later, the GPT's are the basic building blocks for the full asymptotic expansions of the boundary voltage perturbations due to the presence of a small conductivity inclusion inside a conductor. The GPT's contain higher-order information on the inclusion shape and conductivity than the first-order polarization tensor. Our main purpose in studying the GPT's is to understand what kind of information can be extracted from them and how.

We first consider the polarization tensors associated with multiple inclusions. We state their symmetry and positivity. We then estimate their eigenvalues in terms of the total volume of the inclusions. We also give explicit formulae for the GPT's in the multi-disk case. We conclude the section by establishing similar results for the (generalized) anisotropic polarization tensors (APT's). These tensors are defined in the same way as the GPT's. However, they occur due to not only the presence of discontinuity, but also the difference of the anisotropy.

The properties of the GPT's and APT's provided here will be used to obtain accurate reconstructions of small conductivity inclusions from a small number of boundary measurements. They also play an essential role in deriving the effective properties of dilute electrical composites.

3.1. Generalized polarization tensors. For this section we suppose that $B = \cup_{l=1}^m B_l \subset \mathbb{R}^d$ where $\overline{B}_l$'s are mutually disjoint, and the conductivity of B_l is k_l. We first define the overall conductivity $\bar{k}$ and the center $\bar{z}$ of B as follows:

$$\frac{\bar{k}-1}{\bar{k}+1}\sum_{s=1}^m |B_s| := \sum_{s=1}^m \frac{k_s-1}{k_s+1}|B_s|, \tag{3.1}$$

and

$$\frac{\bar{k}-1}{\bar{k}+1}\bar{z}\sum_{s=1}^{m}|B_s| = \sum_{s=1}^{m}\frac{k_s-1}{k_s+1}\int_{B_s} x\,dx. \tag{3.2}$$

Note that if k_s is the same for all s then $\bar{k}=k_s$ and $\bar{z}$ is the center of mass of B.

To motivate the definition of the generalized polarization tensors, we begin with deriving the far-field expansion of the solution to the transmission problem in free space. Suppose that $\bar{z}=0$ for the sake of simplicity and consider the following transmission problem on $\mathbb{R}^d$:

$$\begin{cases} \nabla\cdot\Big(\chi(\mathbb{R}^d\setminus\bigcup_{l=1}^{m}\overline{B_l})+\sum_{l=1}^{m}k_l\chi(B_l)\Big)\nabla u=0 \quad \text{in } \mathbb{R}^d,\\ u(x)-H(x)=O(|x|^{1-d}) \quad \text{as } |x|\to\infty, \end{cases} \tag{3.3}$$

where H is a harmonic function in $\mathbb{R}^d$. The solution u to (3.3) is the electric charge distribution caused by the dipole moment ∇H at infinity in the presence of the set of inclusions $\cup_{l=1}^{m}B_l$. As a direct consequence of Theorem 2.9, the solution u to (3.3) is represented as

$$u(x)=H(x)+\sum_{l=1}^{m}\mathcal{S}_{B_l}\phi^{(l)}(x), \quad x\in\mathbb{R}^d, \tag{3.4}$$

where $\phi^{(l)}\in L^2_0(\partial B_l)$, $l=1,\dots,m$, is the solution of the system of integral equations (2.19).

For a multi-index $\alpha=(\alpha_1,\dots,\alpha_d)\in\mathbb{N}^d$, let $\partial^\alpha f=\partial_1^{\alpha_1}\cdots\partial_d^{\alpha_d}f$ and $x^\alpha:=x_1^{\alpha_1}\cdots x_d^{\alpha_d}$. Let $\alpha=(\alpha_1,\dots,\alpha_d),\beta=(\beta_1,\dots,\beta_d)\in\mathbb{N}^d$ be multi-indices. For $l=1,\dots,m$, let $\phi_\alpha^{(l)}$ be the solution of

$$(\lambda_l I-\mathcal{K}_{B_l}^*)\phi_\alpha^{(l)}-\sum_{k\neq l}\frac{\partial(\mathcal{S}_{B_k}\phi_\alpha^{(k)})}{\partial\nu^{(l)}}\Big|_{\partial B_l}=\frac{\partial x^\alpha}{\partial\nu^{(l)}}\Big|_{\partial B_l} \quad \text{on } \partial B_l. \tag{3.5}$$

Since $H(x)=\sum_{|\alpha|=0}^{+\infty}\frac{1}{\alpha!}\partial^\alpha H(0)x^\alpha$ where the series converges uniformly and absolutely on any compact set, we get

$$\phi^{(l)}=\sum_{|\alpha|=1}^{+\infty}\frac{1}{\alpha!}\partial^\alpha H(0)\phi_\alpha^{(l)}, \quad l=1,\dots,m. \tag{3.6}$$

By Taylor expansion, we have

$$\Gamma(x-y)=\sum_{|\beta|=0}^{+\infty}\frac{(-1)^{|\beta|}}{\beta!}\partial^\beta\Gamma(x)y^\beta, \quad y \text{ in a compact set}, \quad |x|\to\infty. \tag{3.7}$$

It then follows from (3.4), (3.6), and (3.7) that

$$u(x)=H(x)+\sum_{|\alpha|=1}^{+\infty}\sum_{|\beta|=0}^{+\infty}\frac{(-1)^{|\beta|}}{\alpha!\beta!}\partial^\alpha H(0)\partial^\beta\Gamma(x)\sum_{l=1}^{m}\int_{\partial B_l}y^\beta\phi_\alpha^{(l)}(y)d\sigma(y), \quad |x| \text{ large}. \tag{3.8}$$

Observe that

$$\sum_{|\alpha|=1}^{+\infty}\frac{1}{\alpha!}\partial^\alpha H(0)\sum_{l=1}^{m}\int_{\partial B_l}\phi_\alpha^{(l)}(y)d\sigma(y)=\sum_{l=1}^{m}\int_{\partial B_l}\phi^{(l)}(y)d\sigma(y)=0.$$

It then follows from (3.8) that

$$u(x)=H(x)+\sum_{|\alpha|=1}^{+\infty}\sum_{|\beta|=1}^{+\infty}\frac{(-1)^{|\beta|}}{\alpha!\beta!}\partial^\alpha H(0)\partial^\beta\Gamma(x)M_{\alpha\beta}, \quad |x|\to\infty, \tag{3.9}$$

where

$$M_{\alpha\beta} := \sum_{l=1}^{m} \int_{\partial B_l} y^\beta \phi_\alpha^{(l)}(y) d\sigma(y), \quad \alpha, \beta \in \mathbb{N}^d.$$

The asymptotic expansion formula (3.9) shows that the perturbations of the electric potential in $\mathbb{R}^d$ due to the presence of the set of inclusions $\cup_{l=1}^m B_l$ are completely described by $M_{\alpha\beta}$.

DEFINITION 3.1. *Suppose that $B = \cup_{l=1}^m B_l \subset \mathbb{R}^d$ where $\overline{B_l}$'s are mutually disjoint, and the conductivity of B_l is k_l. Suppose that the center of B in the sense of (3.2) is $\bar{z}$. The generalized polarization tensor associated with the inclusions $B = \cup_{l=1}^m B_l$, $M_{\alpha\beta}$, for $\alpha, \beta \in \mathbb{N}^d$, is defined by*

$$M_{\alpha\beta} := \sum_{l=1}^{m} \int_{\partial B_l - \bar{z}} y^\beta \phi_\alpha^{(l)}(y) d\sigma(y),$$

where $\phi_\alpha^{(l)}$ is the solution of (3.5) with B_l replaced with $B_l - \bar{z}$. If $|\alpha| = |\beta| = 1$, we denote $M_{\alpha\beta}$ by M_{pq}, $p, q = 1, \ldots, d$, and call $M = (M_{pq})_{p,q=1}^d$ the polarization tensor of Pólya–Szegö or the first-order polarization tensor.

It should be observed that $M_{\alpha\beta}$ depends on the conductivities k_l as well as the domains B_l. Thus it would be more precise to say that the GPT is associated with the conductivity distribution $\chi(\Omega \setminus \bigcup_{l=1}^m \overline{B_l}) + \sum_{l=1}^m k_l \chi(B_l)$. We also note that since $\int_{\partial B_l} \phi_\alpha^{(l)} d\sigma = 0$ if $|\alpha| = 1$, the first-order polarization tensor is invariant under translation of the inclusion.

If there is a single inclusion B whose centroid is the origin, then

$$\phi_\alpha(y) := (\lambda I - \mathcal{K}_B^*)^{-1}\big(\nu_x \cdot \nabla x^\alpha\big)(y), \quad y \in \partial B,$$

and hence we can rephrase the definition in the following way:

$$M_{\alpha\beta} := \int_{\partial B} y^\beta (\lambda I - \mathcal{K}_B^*)^{-1}\big(\nu_x \cdot \nabla x^\alpha\big)(y)\, d\sigma(y).$$

We can represent the GPT's in terms of solutions to transmission problems [**18**].

LEMMA 3.2. *For all $\alpha, \beta \in \mathbb{N}^d$, $M_{\alpha\beta}$ associated with the single inclusion B can be rewritten in the following form:*

$$M_{\alpha\beta} = (k-1) \int_{\partial B} x^\beta \frac{\partial x^\alpha}{\partial \nu}\, d\sigma(x) + (k-1)^2 \int_{\partial B} x^\beta \frac{\partial \psi_\alpha}{\partial \nu}\bigg|_-(x)\, d\sigma(x), \tag{3.10}$$

where ψ_α is the unique solution of the transmission problem

$$\begin{cases} \Delta \psi_\alpha(x) = 0, \quad x \in B \cup (\mathbb{R}^d \setminus \overline{B}), \\ \psi_\alpha\big|_+(x) - \psi_\alpha\big|_-(x) = 0 \quad x \in \partial B, \\ \dfrac{\partial \psi_\alpha}{\partial \nu}\bigg|_+(x) - k \dfrac{\partial \psi_\alpha}{\partial \nu}\bigg|_-(x) = \nu \cdot \nabla x^\alpha \quad x \in \partial B, \\ \psi_\alpha(x) \to 0 \text{ as } |x| \to \infty \quad \text{if } d = 3, \\ \psi_\alpha(x) - \dfrac{1}{2\pi} \ln |x| \displaystyle\int_{\partial B} \nu \cdot \nabla y^\alpha \, d\sigma(y) \to 0 \text{ as } |x| \to \infty \quad \text{if } d = 2. \end{cases} \tag{3.11}$$

Definition 3.1 contains all the higher-order tensors. One significant advantage of using boundary integrals for defining GPT's is that all the computation can be carried out on ∂B without going to unbounded spaces.

The following simple observation is from [**35**].

LEMMA 3.3. *If $|\alpha| + |\beta|$ is odd and B is symmetric about its center then $M_{\alpha\beta}$ is zero.*

The following lemma is also of importance to us.

LEMMA 3.4. *Let B' be a domain and $B = \mathcal{R}B'$ where $\mathcal{R}$ is a unitary transformation, and let M and M' be the first-order polarization tensor associated with B and B', respectively. Then*

$$M = \mathcal{R}M'\mathcal{R}^T,$$

where T denotes the transpose.

The classical Pólya–Szegö polarization tensors were introduced by Pólya, Szegö, and Schiffer in relation to certain problems arising in hydrodynamics and in electrostatics [**124, 128**] in the form given in Lemma 3.2. If the conductivity k is zero, namely, if B is insulated, the polarization tensor of Pólya–Szegö is called the virtual mass.

It is worth noticing that the definition 3.1 of GPT's is valid even when $k = 0$ or ∞. If $k = 0$, namely, if B is insulated, then

$$M_{\alpha\beta}(0, B) := \int_{\partial B} y^\beta \left(-\frac{1}{2}I - \mathcal{K}_B^*\right)^{-1} (\nu_y \cdot \nabla y^\alpha)(y)\, d\sigma(y),$$

while if $k = \infty$, namely, if B is perfectly conducting and the constants $a_\alpha, \alpha \in I$, where I is a finite index set, are such that $\sum_{\alpha\in I} a_\alpha y^\alpha$ is a harmonic polynomial, then

$$\sum_{\alpha\in I} a_\alpha M_{\alpha\beta}(+\infty, B) := \int_{\partial B} y^\beta \left(\frac{1}{2}I - \mathcal{K}_B^*\right)^{-1} (\nu_y \cdot \nabla \sum_{\alpha\in I} a_\alpha y^\alpha)(y)\, d\sigma(y).$$

The following lemma is easy to prove.

LEMMA 3.5. *Let I be a finite index set. The following convergences hold:*

(i)
$$M_{\alpha\beta}(k, B) \to M_{\alpha\beta}(0, B) \quad \text{as } k \to 0, \quad \forall\, \alpha, \beta \in \mathbb{N}^d.$$

(ii) *Let I be a finite index set and let $a_\alpha, \alpha \in I$, be such that $\sum_{\alpha\in I} a_\alpha y^\alpha$ is a harmonic polynomial. Then,*
$$\sum_{\alpha\in I} a_\alpha M_{\alpha\beta}(k, B) \to \sum_{\alpha\in I} a_\alpha M_{\alpha\beta}(+\infty, B) \quad \text{as } k \to +\infty.$$

The polarization tensor M of Pólya–Szegö can be explicitly computed for disks and ellipses in the plane and balls and ellipsoids in three-dimensional space [**98**]. If, for example, B is an ellipse whose semi-axes are on the x_1- and the x_2-axis and of length a and b, respectively, then its polarization tensor of Pólya–Szegö M takes the form

$$M = (k-1)|B| \begin{pmatrix} \dfrac{a+b}{a+kb} & 0 \\ 0 & \dfrac{a+b}{b+ka} \end{pmatrix}, \tag{3.12}$$

where $|B|$ denotes the volume of B. For an arbitrary ellipse whose semi-axes are not aligned with the coordinate axes, one can use Lemma 3.4 to compute its Pólya–Szegö polarization tensor.

All the higher-order tensors for disks and balls were computed in [**109**]. The GPT's can be explicitly computed for disks in the plane and balls in three-dimensional space. From [**109**] the following results hold.

LEMMA 3.6. (i) *Let B be the disk of radius r and center 0. Suppose that $a_\alpha, \alpha \in I$, and $b_\beta, \beta \in J$, where I and J are finite index sets, are constants such that $f = \sum a_\alpha y^\alpha, g = \sum b_\beta y^\beta$ are harmonic polynomials of homogeneous degrees n and m, respectively. Then*

$$\sum_{\alpha\in I,\beta\in J} a_\alpha b_\beta M_{\alpha\beta}(B,k) = \begin{cases} \dfrac{n\pi r^{2n}}{\lambda} & \text{if } f = g, \\ 0 & \text{otherwise,} \end{cases}$$

up to a multiplicative constant that is independent of k and B, where δ_{nm} denotes the Kronecker symbol.

(ii) *Let B be the ball of radius r and center 0. Then*

$$\sum_{\alpha\in I,\beta\in J} a_\alpha b_\beta M_{\alpha\beta}(B,k) = \frac{(k-1)n(2n+1)}{nk+n+1} r^{2n+1}\delta_{nm}\delta_{ll'},$$

up to a multiplicative constant that is independent of k and B, where $\sum_{\alpha\in I} a_\alpha y^\alpha = |y|^n Y_{n,l}(\frac{y}{|y|})$ and $\sum_{\beta\in J} b_\beta y^\beta = |y|^m Y_{m,l'}(\frac{y}{|y|})$.

Here $\{Y_{n,1}, \ldots, Y_{n,2n+1}\}$ is a set of orthonormal harmonics of degree n.

The reader is referred to [**109**] for (similar) explicit calculations of the GPT's in the case of ellipses.

The GPT's seem to carry important geometric and potential theoretic properties of the domain B. Let us see one example illustrating what kind of information the first-order polarization tensor carries, leaving other important properties to later sections.

Let us look at Figures 1 and 2 from [**22, 18**]. We consider two inclusions of disk shape. We compute the first-order polarization tensor associated with two inclusions following Definition 3.1 and find the ellipse whose first-order polarization tensor is the computed one. We call such ellipse the equivalent ellipse. Figures 1 and 2 show how the equivalent ellipse changes as the conductivities and the sizes of the inclusions B_s vary. The solid line represents the actual inclusions and the dashed lines are the equivalent ellipses. The equivalent ellipse represents the overall property of the multiple inclusions as a conductor immersed in a material of conductivity 1.

If the inclusions are far apart from each other so that the interaction between inclusions are negligible, then we get from (2.20) that

$$\phi_j^{(s)} = (\lambda_l I - \mathcal{K}_{D_s}^*)^{-1}(\nu_j) + O(\delta^{-d}) \quad \text{on } \partial D_s, \quad j = 1, \ldots d,$$

and hence

$$M = \sum_{s=1}^{m} M^{(s)} + O(\delta^{-d}),$$

where $M^{(s)}$ is the first-order tensor associated with B_s.

3.2. NtD map, symmetry and positivity of GPT's. We now explain some important properties of GPT's obtained in [**16, 22, 19**]. We first state the following uniqueness result from [**16**].

THEOREM 3.7. *Let Ω be a domain with smooth boundary such that $\cup_{l=1}^m \overline{B_l} \subset \Omega$. Then $M_{\alpha\beta}, \alpha, \beta \in \mathbb{N}^d$, uniquely determines the Neumann-to-Dirichlet map on Ω, and hence $\cup_{l=1}^m B_l$ and $k_1, \ldots, k_m$.*

Theorem 3.7 shows that all the GPT's completely characterize the domain and its conductivity. However, it seems to be difficult to characterize the geometric

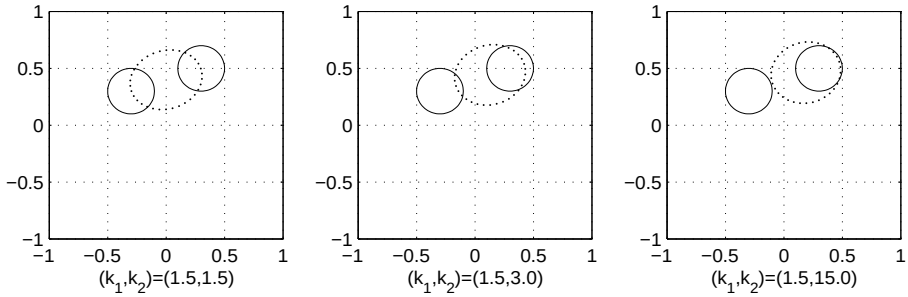

$a_0^i, a_1^i, a_2^i, b_0^i, b_1^i, b_2^i$	k_i	$\bar{k}$	a	b	θ	$\bar{z}$
-0.3,0.2,0, 0.3,0.2,0 0.3,0.2,0, 0.5,0.2,0	1.5 1.5	1.5	0.313	0.256	0.322	(-0.000, 0.400)
	1.5 3	2.077	0.307	0.261	0.322	(0.129, 0.443)
	1.5 15	3.324	0.301	0.266	0.322	(0.188, 0.463)

FIGURE 1. When the two disks have the same radius and the conductivity of the one on the right-hand side is increasing, the equivalent ellipse moves toward the right inclusion. In the table $\bar{k}$ and $\bar{z}$ are the overall conductivity and center defined by (3.1) and (3.2) and a, b, θ are the semi-axes lengths and angle of orientation measured in radians of the equivalent ellipse.

information of the domain carried by individual $M_{\alpha\beta}$. We will see that the first-order tensor carries information on the volume and orientation of the inclusion, and higher-order ones carry information on the weighted volume.

THEOREM 3.8 (Symmetry). (i) *The first-order polarization tensor M is symmetric.*

(ii) *Let I and J be finite index sets. Suppose that $a_\alpha, \alpha \in I$, and $b_\beta, \beta \in J$, are constants such that $\sum_{\alpha\in I} a_\alpha y^\alpha$ and $\sum_{\beta\in J} b_\beta y^\beta$ are harmonic polynomials, then*

$$\sum_{\alpha\in I,\beta\in J} a_\alpha b_\beta M_{\alpha\beta} = \sum_{\alpha\in I,\beta\in J} a_\alpha b_\beta M_{\beta\alpha},$$

or in other words, the GPT's are symmetric on the set of harmonic polynomials.

We also have a theorem on the positivity of the GPT's.

THEOREM 3.9 (Positivity). *Suppose that either $k_l - 1 > 0$ or $k_l - 1 < 0$ for all $l = 1, \dots, m$. Let*

$$\kappa := \max_{1\le l\le m} \left|1 - \frac{1}{k_l}\right|.$$

Let I be a finite index set. For any $(a_\alpha)_{\alpha\in I}$ such that $\sum_{\alpha\in I} a_\alpha y^\alpha$ is harmonic,

$$\left|\sum_{\alpha,\beta\in I} a_\alpha a_\beta M_{\alpha\beta}\right| \ge \frac{|\kappa-1|}{m+1} \sum_{l=1}^{m} |k_l - 1| \int_{B_l} \left|\nabla\Big(\sum_{\alpha\in I} a_\alpha y^\alpha\Big)\right|^2 dy. \tag{3.13}$$

In particular, if $k_l - 1 > 0$ (resp. < 0) for all $l = 1, \dots, m$, then M is positive (resp. negative) definite.

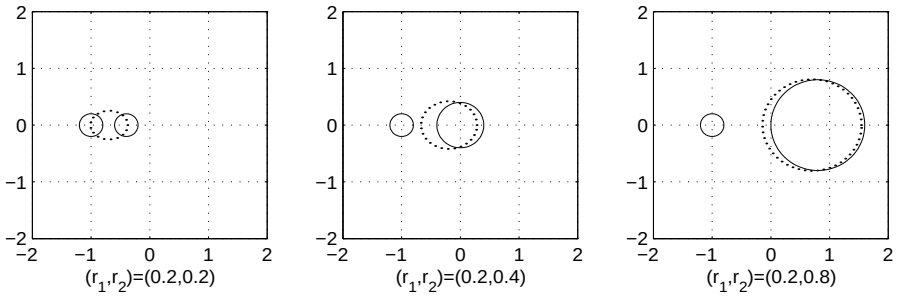

k_i	$a_0^i, a_1^i, a_2^i, b_0^i, b_1^i, b_2^i$	$\bar{k}$	a	b	θ	$\bar{z}$
1.5	-1,0.2,0, 0,0.2,0	1.5	0.317	0.254	0	(-0.700 , 0.000)
1.5	-0.4,0.2,0, 0,0.2,0					
1.5	-1,0.2,0, 0,0.2,0	1.5	0.478	0.420	0	(-0.200, 0.000)
1.5	0,0.2,0, 0,0.2,0					
1.5	-1,0.2,0, 0,0.2,0	1.5	0.844	0.806	0	(0.694, 0.000)
1.5	0.8,0.2,0, 0,0.2,0					

FIGURE 2. When the conductivities of the two disks are the same and the radius of the disk on the right-hand side is increasing, the equivalent ellipse moves toward the right inclusion.

3.3. Optimal bounds. We now explain refined estimates of the eigenvalues of the polarization tensors associated with a single inclusion.

THEOREM 3.10. *Let I be a finite index set. Suppose that B is a single inclusion and $\sum_{\alpha\in I} a_\alpha x^\alpha$ is a harmonic polynomial. Then we get the following inequalities:*

(3.14)
$$(1-\frac{1}{k})\int_B |\nabla(\sum_{\alpha\in I} a_\alpha x^\alpha)|^2\,dx \le \sum_{\alpha,\beta\in J} a_\alpha a_\beta M_{\alpha\beta} \le (k-1)\int_B |\nabla(\sum_{\alpha\in I} a_\alpha x^\alpha)|^2\,dx.$$

In particular, if κ is an eigenvalue of $M=(M_{\alpha\beta})_{|\alpha|=|\beta|=1}$, then

$$\frac{1}{k}(k-1)|B| \le \kappa \le (k-1)|B|. \tag{3.15}$$

The proof of Theorem 3.10 is given in [**27**]. The estimates (3.15) are optimal as estimates for eigenvalues. This can be seen from Figure 3. We do not know whether (3.14) is also optimal. Estimates (3.15) can be improved in the following way.

THEOREM 3.11. *Let M be the first-order polarization tensor associated with the domain B whose volume $|B|=1$. Then,*

$$\frac{1}{k-1}\,Trace(M) \le (d-1+\frac{1}{k}), \tag{3.16}$$

and

$$(k-1)\,Trace(M^{-1}) \le (d-1+k). \tag{3.17}$$

In particular, if $d=2$ and λ_1 and λ_2 are two eigenvalues of M, then

$$\lambda_1+\lambda_2 \le \frac{(k-1)(k+1)}{k}, \tag{3.18}$$

and

$$\frac{1}{\lambda_1}+\frac{1}{\lambda_2} \le \frac{k+1}{k-1}. \tag{3.19}$$

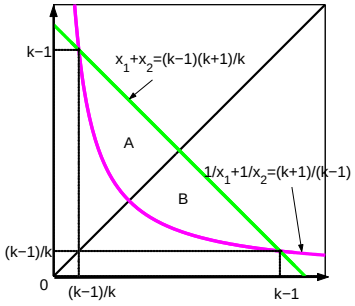

FIGURE 3. The optimal bounds for the polarization tensor in $\mathbb{R}^2$.

Figure 3 shows these bounds graphically. The square box $[1-1/k, k-1]\times[1-1/k, k-1]$ in Figure 3 represents the estimates (3.15). This box is called a Wiener box in the community of composite materials.

The bounds in (3.16) and (3.17) are called the Hashin-Shtrikman bounds since these authors first derived, using variational methods, similar kind of geometry independent bounds for composite materials. The estimates (3.16) and (3.17) for first-order polarization tensors were obtained by Capdeboscq and Vogelius [**53**]. They also showed that the bounds are optimal in two dimensions in the sense that each point inside the bounds is a pair of eigenvalues of the first-order polarization tensor associated with a domain. They showed that each point inside the bounds is attained as a first-order polarization tensor associated with a coated ellipse, or a washer of elliptic shape [**54**]. In fact, every point on the lower bound $1/\lambda_1+1/\lambda_2 = (k+1)/(k-1)$ corresponds to an ellipse as one can see from (3.12), and as ellipses get thinner, corresponding points on the lower bound move to the upper or lower corner. If we start from an ellipse corresponding to a point on the lower bound, and make confocal washers of elliptic shape, then corresponding points move toward the upper bound following a certain curve as the washers get thinner and larger. These curves make foliations and cover all regions inside the bounds except the upper bound. This result is exact and the first-order polarization tensor for the elliptic washer can be computed using elliptic coordinates. These optimal estimates were efficiently used to estimate the size of unknown inclusions [**53**].

On the other hand, it is shown numerically (and asymptotically) that each point inside the bounds is attained by a simply connected domain [**9**]. It turns out that if we start from a disk and vary the domain to make a thin and long cross as in Figure 4, the corresponding eigenvalues move from the intersection point of the lower hyperbola and the line $\lambda_1 = \lambda_2$ toward the intersection point of the upper bound and the line $\lambda_1 = \lambda_2$ following the line $\lambda_1 = \lambda_2$. Note that the intersection point of the lower hyperbola and the line $\lambda_1 = \lambda_2$ is the pair of eigenvalues of the first-order polarization tensor associated with the disk. We also note that the cross-shaped domain in Figure 4 is invariant under rotation by $\pi/2$, and hence the corresponding first-order polarization tensor is of the form λI for some λ where I is the 2×2 identity matrix. Thus by interpolating a cross-shape domain and an ellipse, we can obtain foliation of the region inside the bounds (3.18) and (3.19). It should be noted that the result of [**9**] is numerical and proven asymptotically; exact computation of first-order polarization tensors associated with cross shape domains seems unlikely.

Finally, we briefly discuss about a conjecture of Pólya-Szegö. Observe that among the points in HS-bounds, the intersection point of the lower bound and the line $\lambda_1 = \lambda_2$, $(2(k-1)/(k+1), 2(k-1)/(k+1))$, has the minimal trace, and this is the eigenvalue of the first-order polarization tensor associated with the disk of

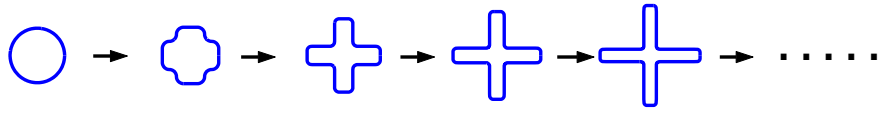

FIGURE 4. The variation of cross-domains starting from disk.

unit area. Pólya and Szegö [**124**] conjectured that the disk (or the sphere for three dimensions) is a unique domain with minimal trace. This conjecture has not yet been proved.

3.4. Anisotropic polarization tensors. Let B be a bounded Lipschitz domain in $\mathbb{R}^d$, $d = 2, 3$. Suppose that the conductivity of B is $\widetilde{A}$ and that of $\mathbb{R}^d \setminus \overline{B}$ is A, where A and $\widetilde{A}$ are constant $d \times d$ positive-definite symmetric matrices with $A \neq \widetilde{A}$. The matrix $\widetilde{A} - A$ is assumed to be either positive-definite or negative-definite. The conductivity profile of B is

$$\gamma_B := \chi_{\mathbb{R}^d \setminus \overline{B}} A + \chi_B \widetilde{A},$$

where χ_B is the characteristic function corresponding to B.

We now define the anisotropic polarization tensors (APT).

DEFINITION 3.12. *For a multi-index $\alpha \in \mathbb{N}^d$ with $|\alpha| \geq 1$, let $(f_\alpha, g_\alpha) \in L^2(\partial B) \times L^2(\partial B)$ be the unique solution to*

$$\begin{cases} \mathcal{S}_B^{\widetilde{A}} f_\alpha - \mathcal{S}_B^A g_\alpha = x^\alpha \\ \nu \cdot \widetilde{A} \nabla \mathcal{S}_B^{\widetilde{A}} f_\alpha|_- - \nu \cdot A \nabla \mathcal{S}_B^A g_\alpha|_+ = \nu \cdot A \nabla x^\alpha \end{cases} \quad \text{on } \partial B. \tag{3.20}$$

For a pair of multi-indices α, β, define the generalized anisotropic polarization tensors associated with the domain B and anisotropic conductivities $\widetilde{A}$ and A, or the conductivity profile γ_B, by

$$M_{\alpha\beta} = \int_{\partial B} x^\beta g_\alpha(x) d\sigma(x).$$

When $\alpha = \mathsf{e}_p$ and $\beta = \mathsf{e}_q$ for $p, q = 1, \cdots, d$, where $(\mathsf{e}_1, \ldots, texttte_d)$ is the standard basis for $\mathbb{R}^d$, denote $M_{\alpha\beta}$ by M_{pq}, i.e.,

$$M_{pq} = \int_{\partial B} x_q g_p(x) d\sigma(x),$$

with $g_p = g_\alpha$.

We note that the first-order APT was first introduced in [**84**] and it is proved there that M_{pq} is symmetric and positive (negative, resp.) definite if $\widetilde{A} - A$ is positive (negative, resp.) definite. The generalized APT's enjoy the same properties.

We first demonstrate that the APT's are a natural extension of the generalized polarization tensors for the isotropic case.

For a multi-index α with $|\alpha| \geq 1$, let

$$\theta_\alpha := (\mathcal{S}_B^{\widetilde{A}} f_\alpha) \chi_B + (\mathcal{S}_B^A g_\alpha) \chi_{\mathbb{R}^d \setminus \overline{B}}.$$

Then θ_α is the solution to the following transmission problem:

(3.21)
$$\begin{cases} \nabla\cdot(A\nabla\theta_\alpha)=0 \quad \text{in } \mathbb{R}^d\setminus\overline{B},\\ \nabla\cdot(\widetilde{A}\nabla\theta_\alpha)=0 \quad \text{in } B,\\ \theta_\alpha|_- - \theta_\alpha|_+ = x^\alpha \quad \text{on } \partial B,\\ \nu\cdot\widetilde{A}\nabla\theta_\alpha|_- - \nu\cdot A\nabla\theta_\alpha|_+ = \nu\cdot A\nabla x^\alpha \quad \text{on } \partial B,\\ \theta_\alpha(x)\to 0 \quad \text{as } |x|\to\infty \quad \text{if } d=3,\\ \theta_\alpha(x) - \dfrac{1}{2\pi\sqrt{|A|}}\ln||A_*x||\displaystyle\int_{\partial B}\theta_\alpha(y)d\sigma(y)\to 0 \quad \text{as } |x|\to\infty \quad \text{if } d=2. \end{cases}$$

It then follows from (2.30) and (3.20) that for any pair of multi-indices α,β,

$$\begin{aligned} M_{\alpha\beta} &= \int_{\partial B} x^\beta g_\alpha d\sigma\\ &= \int_{\partial B} x^\beta(\nu\cdot A\nabla\mathcal{S}_B^A g_\alpha|_+ - \nu\cdot A\nabla\mathcal{S}_B^A g_\alpha|_-)d\sigma\\ &= \int_{\partial B} x^\beta(\nu\cdot\widetilde{A}\nabla\mathcal{S}_B^{\widetilde{A}} f_\alpha|_- - \nu\cdot A\nabla x^\alpha)d\sigma - \int_{\partial B}\nu\cdot A\nabla x^\beta(\mathcal{S}_B^{\widetilde{A}} f_\alpha - x^\alpha)d\sigma\\ &= \int_{\partial B}\big(\nu\cdot(\widetilde{A}-A)\nabla x^\beta\big)\theta_\alpha|_- d\sigma. \end{aligned}$$

In particular, if A and $\widetilde{A}$ are isotropic, or $A=I_d$ and $\widetilde{A}=kI_d$, where I_d is the $d\times d$ identity matrix, then

$$M_{\alpha\beta} = (k-1)\int_{\partial B}\frac{\partial x^\beta}{\partial\nu}\theta_\alpha d\sigma = (k-1)\left[\int_{\partial B} x^\beta\frac{\partial x^\alpha}{\partial\nu} + \int_{\partial B} x^\beta\frac{\partial\theta_\alpha}{\partial\nu}\Big|_+ d\sigma\right],$$

which is exactly (up to a multiplicative constant) the isotropic generalized polarization tensor as defined in (3.10), since

$$\theta_\alpha = \begin{cases} (k-1)\psi_\alpha \quad \text{in } \mathbb{R}^d\setminus\overline{B},\\ (k-1)\psi_\alpha + x^\alpha \quad \text{in } B, \end{cases}$$

where ψ_α is the solution of (3.11).

The perturbation of electrical potential due to the presence of the inclusion is completely described by APT, which naturally illustrates usefulness of the notion of APT.

THEOREM 3.13. *Let H^A be a solution of $\nabla\cdot(A\nabla u)=0$ in $\mathbb{R}^d$, and let u be the solution to the following problem:*

$$\begin{cases} \nabla\cdot(\gamma_B\nabla u) &= 0 \quad \text{in } \mathbb{R}^d,\\ u(x) - H^A(x) &= O(|x|^{1-d}) \quad \text{as } |x|\to\infty. \end{cases}$$

Then we have

$$u(x) = H^A(x) + \sum_{|\alpha|,|\beta|=1}^{+\infty}\frac{1}{\alpha!\beta!}\partial^\beta\Gamma^A(x)\partial^\alpha H^A(0)M_{\alpha\beta}, \quad |x|\to\infty.$$

We write a transformation formula for the first-order APT. We denote the first-order APT $M=(M_{pq})_{1\le p,q\le d}$ associated with the conductivity distribution γ_B by $M(A,\widetilde{A};B)$. Then the following lemma can be proved by a simple change of variables.

LEMMA 3.14. *For any unitary transform R the following holds*

$$M(A,\widetilde{A};B) = RM(R^TAR, R^T\widetilde{A}R; R^{-1}(B))R^T,$$

where T denotes the transpose.

The following explicit formula is from [**85**].

LEMMA 3.15. *If B is an ellipse whose semi-axes are on the x_1- and x_2-axes and of length a and b, respectively, then its first-order APT $M(I_2, \widetilde{A}; B)$ takes the form*

$$M(I_2, \widetilde{A}; B) = |B| \left(I_2 + (\widetilde{A} - I_2)(\frac{1}{2} I_2 - C) \right)^{-1} (\widetilde{A} - I_2),$$

where the matrix

$$C = \frac{a-b}{2(a+b)} \begin{pmatrix} 1 & 0 \\ 0 & -1 \end{pmatrix},$$

and I_2 is the 2×2 identity matrix.

In particular, if B is a disk, then $M(I, \widetilde{A}; B) = 2|B|(\widetilde{A} + I)^{-1}(\widetilde{A} - I)$.

For an arbitrary ellipse whose semi-axes are not aligned with the coordinate axes, one can use Lemma 3.14 to compute its first-order APT.

We now collect some important properties of the APT such as symmetry and positivity. For the first-order APT these properties were obtained in [**84**]. The estimates for positivity of general APT give better results than the one in [**84**] and are derived in [**23**].

DEFINITION 3.16. *The function H is called A-harmonic in an open set D if H is the solution to*

$$\nabla \cdot (A \nabla H) = 0 \quad \text{in } D. \tag{3.22}$$

THEOREM 3.17 (Symmetry). *Let I_1 and I_2 be finite sets of multi-indices and let $\{a_\alpha | \alpha \in I_1\}$ and $\{b_\beta | \beta \in I_2\}$ be such that $\sum_{\alpha \in I_1} a_\alpha x^\alpha$ and $\sum_{\beta \in I_2} b_\beta x^\beta$ are A-harmonic. Then*

$$\sum_{\alpha \in I_1} \sum_{\beta \in I_2} a_\alpha b_\beta M_{\alpha\beta} = \sum_{\alpha \in I_1} \sum_{\beta \in I_2} a_\alpha b_\beta M_{\beta\alpha}.$$

In particular, $M_{pq} = M_{qp}$, $p, q = 1, \cdots, d$.

Optimal estimates for the generalized anisotropic polarization tensors were obtained in [**23**]; see also [**94**].

THEOREM 3.18. *Let I be a finite index set. Let $\{a_\alpha | \alpha \in I\}$ be a set of coefficients such that $v(x) = \sum_{\alpha \in I} a_\alpha x^\alpha$ is A-harmonic. Then we obtain the following bounds:*

$$\int_B (\widetilde{A} - A) \nabla v \cdot \widetilde{A}^{-1} A \nabla v \leq \sum_{\alpha, \beta \in I} a_\alpha a_\beta M_{\alpha\beta} \leq \int_B (\widetilde{A} - A) \nabla v \cdot \nabla v. \tag{3.23}$$

By taking $v(x) = \xi \cdot x$ for $\xi \in \mathbb{R}^d$, we get the following corollary for the first-order APT.

COROLLARY 3.19. *Let $M = (M_{\alpha\beta})_{|\alpha|=|\beta|=1}$ be the matrix of the first-order APT. Then*

$$|B|(\widetilde{A} - A)\xi \cdot \widetilde{A}^{-1} A \xi \leq M\xi \cdot \xi \leq |B|(\widetilde{A} - A)\xi \cdot \xi, \quad \xi \in \mathbb{R}^d.$$

In particular, M is positive (negative, resp.) definite if $\widetilde{A} - A$ is positive (negative, resp.) definite.

As an immediate consequence of (3.23) we obtain the following estimates for the isotropic case [**23**]. We note that these estimates are improvements over those in [**18**].

COROLLARY 3.20. *Let $A = \gamma I_d$ and $\widetilde{A} = \widetilde{\gamma} I_d$ for positive constants γ and $\widetilde{\gamma}$ with $\gamma \neq \widetilde{\gamma}$ and let $\{a_\alpha | \alpha \in I\}$ be the set of coefficients such that $v = \sum_{\alpha \in I} a_\alpha x^\alpha$ is harmonic, where I_d is the $d \times d$ identity matrix and I is a set of multi-indices. Then we get the following inequalities:*

$$\frac{\gamma}{\widetilde{\gamma}}(\widetilde{\gamma} - \gamma) \int_B |\nabla v|^2 \leq \sum_{\alpha,\beta \in I} a_\alpha a_\beta M_{\alpha\beta} \leq (\widetilde{\gamma} - \gamma) \int_B |\nabla v|^2.$$

In particular, if κ is an eigenvalue of $M = (M_{\alpha\beta})_{|\alpha|=|\beta|=1}$, then

$$\frac{\gamma}{\widetilde{\gamma}}(\widetilde{\gamma} - \gamma)|B| \leq \kappa \leq (\widetilde{\gamma} - \gamma)|B|.$$

3.5. Further results. There is a concept of polarization tensor for the isotropic linear elasticity, which is called the Elastic Moment Tensor (EMT). It is a 4-tensor, not a matrix (2-tensor), and enjoys properties of symmetry and positivity. See [**116, 28**]. EMT has been effectively used in detection of small elastic inclusions [**83**].

4. Reconstruction of small inclusions

We now describe promising techniques for the reconstruction of diametrically small inclusions via boundary measurements. We review some of the numerical methods in [**6, 15, 22, 32, 33, 49, 52, 53, 55, 73, 86, 103**] for the isotropic conductivity problem and in [**84**], for the anisotropic conductivity problem.

The first method that has been designed to detect conductivity inclusions is an iterative least-square algorithm of Cedio-Fenya *et al.* [**55**]. In all methods based on least-square algorithms and iteration schemes, one must make a good initial guess. Without a good initial guess, one needs tremendous computational cost and time to get a close image to true solution.

Here we only explain some direct (non-iterative) methods. These methods are very effective and easy to implement. Combining them with the size estimations obtained in the papers [**91, 2, 102**], we get a good initial guess for the inverse conductivity problems for piecewise constant conductivity distributions. The size estimations are upper and lower bounds of the size of the conductivity inclusion (not necessary of small volume) derived by comparing the boundary voltage potential with the background solution for given appropriate Neumann data. These estimates reduce to those obtained from Theorem 3.11 by Capdeboscq and Vogelius in [**53, 54**] when the conductivity inclusion is of small volume. See Step 2 in the quadratic algorithm, described below.

Let us begin with the description of the configuration of the medium.

Configuration of the Medium. The conductor Ω, which is a bounded domain in $\mathbb{R}^d$, $d = 2$ or 3, contains collections of multiple inclusions $D = \cup_{s=1}^m D_s$ which satisfy the following conditions:

(H1): Each D_s is well-separated from that others and the boundary of Ω, *i.e.*, there exists $d_0 > 0$ such that $dist(D_s, D_t) > d_0$, $s \neq t$, and $dist(D, \partial\Omega) > d_0$.

(H2): Each D_s consists of multiple closely spaced inclusions:

$$D_s = \cup_{l=1}^{m_s} D_s^l = \epsilon_s \cup_{l=1}^{m_s} B_s^l + z_s,$$

where ϵ_s is a small number representing the common order of magnitude of D_s, and z_s denotes the location of D_s. Here B_s^l is a bounded Lipschitz domain in $\mathbb{R}^d$ such that there exist positive constants C_1 and C_2 such that

$$C_1 \leq \operatorname{diam} B_s^l \leq C_2, \quad \text{and} \quad C_1 \leq \operatorname{dist}(B_s^l, B_s^{l'}) \leq C_2, \quad l \neq l',$$

for each $s = 1, \ldots, m$.

So the inclusion D consists of several collections of closely spaced multiple inclusions and takes the form

$$D = \cup_{s=1}^{m} D_s = \cup_{s=1}^{m} \big(\cup_{l=1}^{m_s} D_s^l \big) = \cup_{s=1}^{m} \big(\epsilon_s \cup_{l=1}^{m_s} B_s^l + z_s \big).$$

See Figure 5. Detection of such inclusions has some practical significance since some anomalies inside a body may be located very closely to each other.

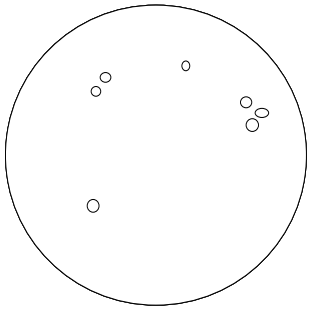

FIGURE 5. Configuration of the medium.

Suppose that the conductivity of D_s^l is $k_s^l > 0$ ($k_s^l \neq 1$). The conductivity profile of Ω is then

$$\gamma(x) = \begin{cases} k_s^l, & x \in D_s^l, \quad l = 1, \dots, m_s, \ s = 1, \dots, m, \\ 1, & x \in \Omega \setminus \overline{D}. \end{cases}$$

We consider the following Neumann problem:

$$\begin{cases} \nabla \cdot (\gamma(x) \nabla u) = 0 \quad \text{in } \Omega, \\ \dfrac{\partial u}{\partial \nu}\Big|_{\partial\Omega} = g. \end{cases} \tag{4.1}$$

The problem is then to detect the inclusion D by means of finitely many boundary measurements, g and $u|_{\partial\Omega}$ where u is the solution to (4.1).

We note that we do not consider here those inclusions which are very close to the boundary. In such cases, interaction between the boundary and the inclusions is not negligible, and to describe the interaction a somewhat different idea is required. For this we refer to Section 6.

4.1. Asymptotic expansions. Let u be the solution of (4.1). According to Theorem 2.10, u on $\partial\Omega$ or $\Lambda_D(g)$ can be represented as

$$\Lambda_D(g)(x) = \Lambda_0(g)(x) - (-\frac{1}{2} I + \mathcal{K}_\Omega)^{-1} \left(\sum_{s=1}^{m} \sum_{l=1}^{m_s} \mathcal{S}_{D_s^l} \psi_l^{(s)} |_{\partial\Omega} \right)(x), \quad x \in \partial\Omega, \tag{4.2}$$

where $\psi_l^{(s)}$ is the solution of

$$(\lambda_s^l I - \mathcal{K}_{D_s^l}^*) \psi_l^{(s)} - \sum_{(t,k) \neq (s,l)} \frac{\partial (\mathcal{S}_{D_t^k} \psi_k^{(t)})}{\partial \nu_l^{(s)}}\Big|_{\partial D_s^l} = \frac{\partial H}{\partial \nu_l^{(s)}}\Big|_{\partial D_s^l} \quad \text{on } \partial D_s^l, \tag{4.3}$$

and

$$H(x) = -\mathcal{S}_\Omega(g)(x) + \mathcal{D}_\Omega(\Lambda(g))(x), \quad x \in \Omega. \tag{4.4}$$

Recalling that $D_s^l = \epsilon_s B_s^l + z_s$, we make a change of variables $x = \epsilon_s x' + z_s$ for a fixed s. Observe that for $x = \epsilon_s x' + z_s \in \partial D_s^l$

$$\frac{\partial (\mathcal{S}_{D_t^k} \psi_k^{(t)})}{\partial \nu_l^{(s)}} (\epsilon_s x' + z_s) = \frac{1}{\omega_d} \int_{\partial D_t^k} \frac{\langle \epsilon_s x' + z_s - y, \nu_l^{(s)}(x') \rangle}{|\epsilon_s x' + z_s - y|^d} \psi_k^{(t)}(y) d\sigma(y),$$

where $\nu_l^{(s)}(x')$ denotes the unit normal to ∂B_s^l.

If $t = s$, by making the change of variables $y = \epsilon_s y' + z_s$, we can see that

$$\frac{\partial(\mathcal{S}_{D_s^k}\psi_k^{(s)})}{\partial\nu_l^{(s)}}(\epsilon_s x' + z_s) = \frac{\partial(\mathcal{S}_{B_s^k}\widetilde{\psi}_k^{(s)})}{\partial\nu_l^{(s)}}(x'), \quad x' \in \partial B_s^k, \quad k = 1, \dots, m_s,$$

where

$$\widetilde{\psi}_k^{(s)}(x') := \psi_k^{(s)}(\epsilon_s x' + z_s), \quad x' \in \partial B_s^k.$$

On the other hand, if $t \neq s$, then we have

$$\begin{aligned}
&\frac{\partial(\mathcal{S}_{D_t^k}\psi_k^{(t)})}{\partial\nu_l^{(s)}}(\epsilon_s x' + z_s) \\
&= \frac{1}{\omega_d}\int_{\partial D_t^k}\left[\frac{\langle \epsilon_s x' + z_s - y, \nu_l^{(s)}(x')\rangle}{|\epsilon_s x' + z_s - y|^d} - \frac{\langle \epsilon_s x' + z_s - y_0, \nu_l^{(s)}(x')\rangle}{|\epsilon_s x' + z_s - y_0|^d}\right]\psi_k^{(t)}(y)d\sigma(y),
\end{aligned}$$

for some $y_0 \in \partial D_t^k$ since $\int_{\partial D_t^k}\psi_k^{(t)}d\sigma = 0$. Since D_t^k and D_s^l are well-separated, in other words, $|z_s - y| > d_0$ for all $y \in \partial D_t^k$, it follows from the mean value theorem that

$$\left|\frac{\partial(\mathcal{S}_{D_t^k}\psi_k^{(t)})}{\partial\nu_l^{(s)}}(\epsilon_s x' + z_s)\right| \leq C\int_{\partial D_t^k}|y - y_0||\psi_k^{(t)}(y)|d\sigma(y) \leq C\epsilon_s^d\|\widetilde{\psi}_k^{(t)}\|_{L^2(\partial B_t^k)}.$$

It means that the impact of D_t^k observed at D_s^l is $O(\epsilon_s^d)$ which is negligible provided that they are far apart. We now rephrase the integral equation (4.3) as follows

$$(\lambda_s^l I - \mathcal{K}_{B_s^l}^*)\widetilde{\psi}_l^{(s)}(x') - \sum_{k\neq l}\frac{\partial(\mathcal{S}_{B_s^k}\widetilde{\psi}_k^{(s)})}{\partial\nu_l^{(s)}}(x') = \frac{\partial H}{\partial\nu_l^{(s)}}(\epsilon_s x' + z_s) + O(\epsilon^d), \quad x' \in \partial B_s^l,$$

where $\epsilon = \max\epsilon_s$. For each multi-index α, let $\phi_{l\alpha}^{(s)}$, $l = 1, \dots, m_s$, be the solution to

$$(\lambda_s^l I - \mathcal{K}_{B_s^l}^*)\phi_{l\alpha}^{(s)}(x') - \sum_{k\neq l}\frac{\partial(\mathcal{S}_{B_s^k}\phi_k^{(s)})}{\partial\nu_{l\alpha}^{(s)}}(x') = \frac{\partial x^\alpha}{\partial\nu_l^{(s)}}(x'), \quad x' \in \partial B_s^l,$$

as before. Since

$$\frac{\partial H}{\partial\nu_l^{(s)}}(\epsilon_s x' + z_s) = \sum_{|\alpha|\geq 1}\epsilon_s^{|\alpha|-1}\partial^\alpha H(z_s)\frac{\partial x^\alpha}{\partial\nu_l^{(s)}}(x'), \quad x' \in \partial B_s^l,$$

we have from the linearity of the equation that

$$\widetilde{\psi}_l^{(s)} = \sum_{|\alpha|\geq 1}\epsilon_s^{|\alpha|-1}\partial^\alpha H(z_s)\phi_{l\alpha}^{(s)} + O(\epsilon^d).$$

In a similar way to the derivation of (3.4) we can show that for $x \in \partial\Omega$

$$\begin{aligned}
\sum_{l=1}^{m_s}\mathcal{S}_{D_s^l}\psi_l^{(s)}(x) &= \epsilon_s^{d-1}\sum_{l=1}^{m_s}\int_{\partial B_s^l}\Gamma(x - \epsilon y' - z_s)\widetilde{\psi}_l^{(s)}(y')d\sigma(y') \\
&= \sum_{|\alpha|=1}^{\infty}\sum_{|\beta|=1}^{\infty}\frac{\epsilon_s^{|\alpha|+|\beta|+d-2}}{\alpha!\beta!}(\partial^\alpha H)(z_s)\partial_z^\beta\Gamma(x - z_s)M_{\alpha\beta}^{(s)} + O(\epsilon^{2d}),
\end{aligned}$$

where $M_{\alpha\beta}^{(s)}$, $s = 1, \dots, m$, is the polarization tensor associated with $B_s = \cup_{l=1}^{m_s}B_s^l$. Observe that the error term is $O(\epsilon^{2d})$, not $O(\epsilon^{2d-1})$. This is because $\int_{\partial B_s^l}\widetilde{\psi}_l^{(s)}d\sigma = 0$.

Since $(-\frac{1}{2}I + \mathcal{K}_\Omega)(N(\cdot - z))(x) = \Gamma(x - z)$ for $z \in \Omega$ and $x \in \mathbb{R}^d \setminus \overline{\Omega}$ by (2.10), it follows from (4.2) that

$$\Lambda_D(g) = \Lambda_0(g) - \sum_{s=1}^{m} \sum_{|\alpha|=1}^{\infty} \sum_{|\beta|=1}^{\infty} \frac{\epsilon_s^{|\alpha|+|\beta|+d-2}}{\alpha!\beta!} (\partial^\alpha H)(z_s) \partial_z^\beta N(x, z_s) M_{\alpha\beta}^{(s)} + O(\epsilon^{2d}).$$

Since the formula is written in terms of H and H is dependent upon ϵ, we now want to remove this dependence. Observe from (4.4) and Green's representation, $U(x) = -\mathcal{S}_\Omega(g)(x) + \mathcal{D}_\Omega(\Lambda_0(g))(x)$, $x \in \Omega$, that

$$\begin{aligned} H(x) - U(x) &= \mathcal{D}_\Omega(\Lambda(g) - \Lambda_0(g))(x) \\ &= \mathcal{D}_\Omega(-\frac{1}{2}I + \mathcal{K}_\Omega)^{-1} \left(\sum_{s=1}^{m} \sum_{l=1}^{m_s} \mathcal{S}_{D_s^l} \psi_l^{(s)}|_{\partial\Omega} \right)(x), \quad x \in \Omega. \end{aligned}$$

Since $\sum_{s=1}^{m} \sum_{l=1}^{m_s} \mathcal{S}_{D_s^l} \psi_l^{(s)}(x) = O(\epsilon^d)$ for $x \in \partial\Omega$, we get

$$\|H - U\|_{C^n(K)} = O(\epsilon^d)$$

for any integer n and a compact subset K of Ω. Thus we obtain the following asymptotic expansion formula.

THEOREM 4.1. *Suppose that the inclusion D is of the form $D = \cup_{s=1}^{m} D_s$, and each D_s consists of multiple closely spaced inclusions, i.e., $D_s = \cup_{l=1}^{m_s} \epsilon_s B_s^l + z_s$. Then, the following asymptotic expansion holds uniformly on $\partial\Omega$:*

(4.5)

$$\begin{aligned} &\Lambda_D(g)(x) - \Lambda_0(g)(x) \\ &= -\sum_{s=1}^{m} \sum_{|\alpha|=1}^{d} \sum_{|\beta|=1}^{d} \frac{\epsilon_s^{|\alpha|+|\beta|+d-2}}{\alpha!\beta!} (\partial^\alpha U)(z_s) \partial_z^\beta N(x, z_s) M_{\alpha\beta}^{(s)} + O(\epsilon^{2d}), \quad x \in \partial\Omega. \end{aligned}$$

We remark that in order to find terms higher than ϵ^{2d}, the interaction between inclusions and $\partial\Omega$ should be considered. If we only look at the leading order terms, the formula (4.5) takes the following simpler form:

$$\Lambda_D(g)(x) - \Lambda_0(g)(x) = -\sum_{s=1}^{m} \epsilon_s^d \nabla U(z_s) M^{(s)} \nabla_z N(x, z_s) + O(\epsilon^{d+1}), \quad x \in \partial\Omega, \tag{4.6}$$

where $M^{(s)}$ is the polarization tensor of Pólya–Szegö associated with B_s.

The proof of our asymptotic expansion (4.5) is radically different from the ones in [**73**], [**55**], and [**133**]. What makes it particularly original and elegant is that the rigorous derivation of high-order terms follows almost immediately. The extension of the techniques used in [**73**], [**55**], and [**133**] to construct higher-order terms in the expansion of $\Lambda_D(g)$ as $\epsilon \to 0$ is laborious. Our method based on layer techniques also enables us to extend the asymptotic expansions to the cases of inhomogeneities with Lipschitz boundaries. Previously, the leading order term was derived under the assumption that inhomogeneities are smooth [**73**], [**55**]. We also note that thanks to Lemma 3.5 our method works as well even when the inhomogeneities have extreme conductivities ($k = 0$ or $k = \infty$).

Asymptotic expansions of the perturbation due to the presence of inclusions are the basic ingredient in designing algorithms to detect unknown inclusions. Several asymptotic expansion formulae for various equations have been obtained [**15, 20, 28, 32, 34, 55, 133, 52, 41, 42**].

Note that we have $\Lambda_D(g)$ as our data collected from the measurements on $\partial\Omega$. Neglecting the small term $O(\epsilon^{d+1})$ in (4.6), we have

$$\sum_{s=1}^{m} \epsilon_s^d \nabla U(z_s) M^{(s)} \nabla_z N(x, z_s), \quad x \in \partial\Omega,$$

in our hand. Now the task is to find the locations z_s, the polarization tensors $M^{(s)}$ from this data.

For a given Neumann data (or current) $g \in L^2_0(\partial\Omega)$, define the harmonic function $H[g](x)$, $x \in \mathbb{R}^d \setminus \overline{\Omega}$, by

$$H[g](x) := -\mathcal{S}_\Omega(g)(x) + \mathcal{D}_\Omega(\Lambda_D(g))(x), \quad x \in \mathbb{R}^d \setminus \bar{\Omega}. \tag{4.7}$$

By Green's theorem $-\mathcal{S}_\Omega(g)(x) + \mathcal{D}_\Omega(\Lambda_0(g))(x) = 0$ for all $x \in \mathbb{R}^d \setminus \bar{\Omega}$, and

$$\mathcal{D}_\Omega(N(\cdot - z))(x) = \Gamma(x - z)$$

for $z \in \Omega$ and $x \in \mathbb{R}^d \setminus \overline{\Omega}$ by (2.10). Therefore, we obtain by substituting (4.6) into (4.7)

$$\begin{aligned} H[g](x) &= \mathcal{D}_\Omega\big(\Lambda_D(g) - \Lambda_0(g)\big)(x) \\ &= -\sum_{s=1}^{m} \epsilon_s^d \nabla U(z_s) M^{(s)} \nabla_z \Gamma(x - z_s) + O(\epsilon^{d+1}), \quad x \in \mathbb{R}^d \setminus \overline{\Omega}. \end{aligned} \tag{4.8}$$

We now illustrate the above expansion. Let $d = 2$ and consider a single inclusion $D = \epsilon B + z$ in $\Omega \subset \mathbb{R}^2$. We plot

$$\max_{x \in S} \ln \|H[g](x) + \epsilon^2 \nabla U(z) M \nabla_z \Gamma(x - z)\|,$$

where S is a $\mathcal{C}^2$-closed surface enclosing the domain Ω [**35**].

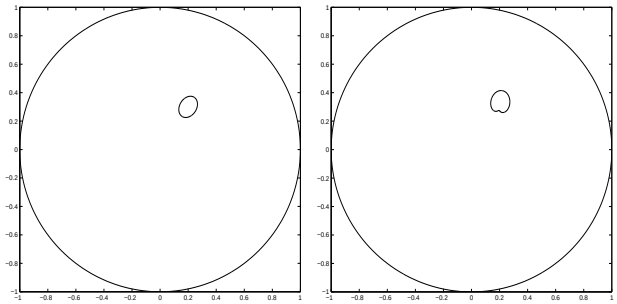

(a) (b)

FIGURE 6. Symmetric inclusion (a); non-symmetric inclusion (b).

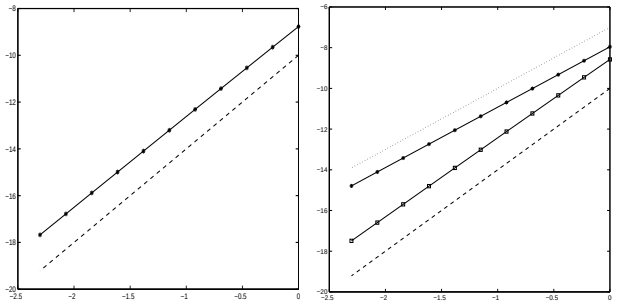

(a) (b)

FIGURE 7. Remainder of order $O(\epsilon^4)$ for (a); remainder of order $O(\epsilon^3)$ for (b).

The graphics in Figure 7 demonstrate that the expression in (4.8) (with $d = 2$) is of order $O(\epsilon^4)$ for symmetric inclusions and of order $O(\epsilon^3)$ for nonsymmetric inclusions. This is because the correction of order three is zero, as a consequence of Lemma 3.3.

We now turn to the reconstruction of $M^{(s)}$ and z_s from the data $H[g](x)$, $x \in \mathbb{R}^d \setminus \overline{\Omega}$.

4.2. Detection of a single inclusion. Here by "single" we mean a single collection of multiple closely spaced inclusions. Suppose that there is a single collection of inclusions, *i.e.*, $m = 1$. So, D takes the form $D = \epsilon \cup_{l=1}^{k} B^l + z$. Then $H[g](x)$ becomes, in its first-order term,

$$H[g](x) = -\epsilon^d \nabla U(z) M \nabla_z \Gamma(x - z) + O(\epsilon^{d+1}), \tag{4.9}$$

where $M = (M_{pq})$ is the first-order polarization tensor associated with $\cup_{l=1}^{k} B^l$. Observe that $\nabla_z \Gamma(x - z)$ behaves like $-x/(\omega_d |x|^d)$ as $|x| \to \infty$. Therefore by applying linear harmonic functions for U, we can recover M. Moreover, by applying quadratic harmonic functions for U, we can recover z. Assume for the sake of simplicity that $d = 2$. The reconstruction procedure is the following.

Quadratic algorithm:

Step 1: For $g_p = \partial x_p / \partial \nu$, $p = 1, 2$, measure $u|_{\partial\Omega}$.

Step 2: Compute the first-order polarization tensor $\epsilon^2 M = \epsilon^2 (M_{pq})_{p,q=1}^2$ for D by

$$\epsilon^2 M_{pq} = \lim_{t \to \infty} 2\pi t H[g_p](te_q).$$

The optimal estimates in Theorem 3.11 yield a very accurate estimate for $\epsilon^2 |B| = |D|$. We have

$$\frac{k}{(k-1)(k+1)} \epsilon^2 \ \mathrm{Trace}(M) \leq (1 + O(\epsilon))|D| \leq \frac{k+1}{k-1} \epsilon^2 (\mathrm{Trace}(M^{-1}))^{-1}.$$

See [**53, 54**].

Step 3: Compute $h_p = \lim_{t \to \infty} 2\pi t H[g_3](te_p)$ for $g_3 = \frac{\partial (x_1 x_2)}{\partial \nu}, p = 1, 2$. Then the center is estimated by solving

$$z = (h_1, h_2)(\epsilon^2 M)^{-1}.$$

Step 4: Let the overall conductivity $\bar{k} = \infty$ if the polarization tensor M is positive definite. Otherwise assume $\bar{k} = 0$. Use (3.12) to obtain the shape of the equivalent ellipse.

Observe that we only use 3 measurements. By visualizing the detected polarization tensor M by an ellipse, we can find a geometric figure representing $D = \epsilon \cup_{l=1}^{k} B^l + z$.

Figure 8 shows a result of numerical experiments. We note that the detected ellipse and location are in very good agreement with the equivalent ellipse and the center of $D = \cup_{l=1}^{k} D^l := \epsilon \cup_{l=1}^{k} B^l + z$ as defined in (3.1) and (3.2). For complete results, we refer to [**22, 18**]. Note that there is a method using only linear currents. See [**103, 33**].

We conclude this subsection with a comment on stability. In general, the measured voltage potential contains unavoidable observation noise, so that we have to answer the stability question. Fortunately, our algorithms are totally based on the observation of the pattern of $H[g]$; thus if

$$H^{meas}[g](x) := -\mathcal{S}_\Omega(g)(x) + \mathcal{D}_\Omega(u^{meas}) \quad \text{for } x \in \mathbb{R}^d \setminus \overline{\Omega},$$

where u^{meas} is the measured voltage on the boundary, then we have the following stability estimate

$$\begin{aligned} |H^{meas}[g](x) - H[g](x)| &\leq \left| \int_{\partial\Omega} \frac{\partial \Gamma}{\partial \nu_y}(x - y) \left(u^{meas} - u \right)(y) \, d\sigma(y) \right| \\ &\leq C \, ||u^{meas} - u||_{L^2(\partial\Omega)}, \end{aligned}$$

where C is a constant depending only on the distance of x from $\partial\Omega$. Thus we conclude that our direct algorithms are not sensitive to the observation noise.

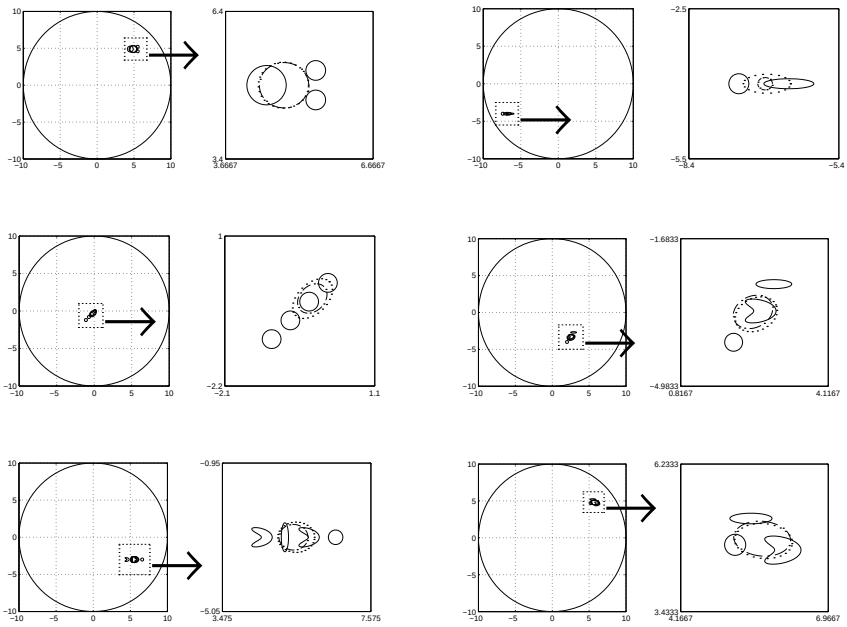

FIGURE 8. Reconstruction of closely spaced small inclusions. The dashed line is the equivalent ellipse and the dash-dot line is the detected ellipse. The numerical values are given in Table 1.

4.3. Detection of multiple inclusions. Detection of a single inclusion using (4.9) was a rather simple matter. However detection of multiple inclusions is dramatically different. We can expect this by looking at the formula (4.8). The summation in (4.8) is a mixture of information coming from all the inclusions and we need to extract individual information from it.

Linear Sampling Method. We first describe the interesting approach proposed by Brühl *et al.* in their recent paper [**49**]. This approach is related to the linear sampling method of Colton and Kirsch [**61**] (see also [**96**] and [**48**]) and allows us to reconstruct small inclusions by taking measurements only on some portion of $\partial\Omega$. It has also some similarities to a MUltiple Signal Classification (MUSIC)-type algorithm developed by Devaney [**64, 104**] for estimating the locations of a number of pointlike scatterers. We refer to Cheney [**56**] and Kirsch [**97**] for detailed discussions of the connection between MUSIC algorithm and the linear sampling method. Even if the method in [**49**] works with partial measurement, or partial NtD map, we describe the method with full NtD map for simplicity. The partial NtD map on $\partial\omega \subset \partial\Omega$ is defined to be $\Lambda_D(g) = u|_{\partial\omega}$ for g with support in $\partial\omega$.

Suppose that $\epsilon_s = \epsilon$ for all s. Then (4.6) reads

$$\Lambda_D(g) - \Lambda_0(g) = -\epsilon^d T(g) + O(\epsilon^{d+1}), \quad g \in L^2_0(\partial\Omega), \tag{4.10}$$

where

$$T(g)(x) = \sum_{s=1}^{m} \nabla U(z_s) M^{(s)} \nabla_z N(x, z_s), \quad x \in \partial\Omega.$$

The NtD maps Λ_D and Λ_0 are self-adjoint and by Theorem 2.10 $\Lambda_D - \Lambda_0$ is compact as a map on $L^2_0(\partial\Omega)$. It is also not hard to see that T is a self-adjoint compact operator on $L^2_0(\partial\Omega)$.

k_i	$a_0^i, a_1^i, a_2^i, b_0^i, b_1^i, b_2^i$	$\bar{k}$	$\bar{a}$	$\bar{b}$	$\bar{\theta}$	$\bar{z}$
		k	a	b	θ	z
100	5.5, 0.2, 0, 5.2, 0.2, 0	60.079	0.511	0.468	0.000	(4.838, 4.900)
100	5.5, 0.2, 0, 4.6, 0.2, 0	∞	0.502	0.461	0.000	(4.856, 4.899)
50	4.5, 0.4, 0, 4.9, 0.4, 0					
1.5	-7.4, 0.2, 0, -4, 0.2, 0	1.5	0.474	0.190	0.000	(-6.844, -4.000)
1.5	-6.4, 0.5, 0, -4, 0.1, 0	∞	0.146	0.123	0.000	(-6.875, -4.000)
100	0.1, 0.2, 0, 0, 0.2, 0					
100	-0.3, 0.2, 0, -0.4, 0.2, 0	3.88	0.511	0.315	0.785	(-0.236, -0.336)
1.5	-0.7, 0.2, 0, -0.8, 0.2, 0	∞	0.355	0.267	0.785	(-0.233, -0.333)
1.5	-1.1, 0.2, 0,-1.2, 0.2, 0					
5	2.9, 0.4, 0, -2.7, 0.1, 0	18.655	0.491	0.365	0.443	(2.494, -3.375)
100	2.5, 0.25, 0.2, -3.3, 0.25, 0.05	∞	0.458	0.351	0.443	(2.434, -3.321)
50	2.0, 0.2, 0, -4.0, 0.2, 0					
5	4.5, 0.15, 0.2, -3, 0.25, 0.05					
5	5.2, 0.1, 0, -3, 0.4, 0	5	0.507	0.419	-0.000	(5.502, -3.000)
5	5.8, 0.15, 0.2, -3, 0.25,0.05	∞	0.401	0.353	-0.000	(5.436, -3.000)
5	6.6, 0.2, 0, -3, 0.2, 0					
100	6.0, 0.25, 0.2, 4.6, 0.25, 0.05	100	0.549	0.331	-0.089	(5.728, 4.772)
100	5.5, 0.4, 0, 5.2, 0.1, 0	∞	0.540	0.329	-0.089	(5.712, 4.817)
100	5.2, 0.2, 0, 4.7, 0.2, 0					

TABLE 1. Table for Fig. 8. Here $\bar{k}, \bar{z}$ are the overall conductivity and center defined by (3.1) and (3.2). $\bar{a}$, $\bar{b}$, and $\bar{\theta}$ are semi axis lengths and the angle of orientation of the equivalent ellipse while a, b, and θ are those of detected ellipse assuming $k = \infty$. The point z is the detected center.

Introduce now the linear operator $\mathcal{G} : L_0^2(\partial\Omega) \to \mathbb{R}^{d\times m}$ defined by

$$\mathcal{G}g = (\nabla U(z_1), \dots, \nabla U(z_m)).$$

Endowing $\mathbb{R}^{d\times m}$ with the standard Euclidean inner product,

$$\langle a, b\rangle = \sum_{s=1}^{m} a_s \cdot b_s \text{ for } a = (a_1, \dots, a_m), b = (b_1, \dots, b_m), a_s, b_s \in \mathbb{R}^d,$$

we then obtain

$$\langle \mathcal{G}g, a\rangle = \sum_{s=1}^{m} a_s \cdot \nabla U(z_s) = \int_{\partial\Omega} \left(\sum_{s=1}^{m} a_s \cdot \nabla_z N(x, z_s) \right) g(x)\, d\sigma(x),$$

for arbitrary $a = (a_1, \dots, a_m) \in \mathbb{R}^{d\times m}$. Therefore, the adjoint $\mathcal{G}^* : \mathbb{R}^{d\times m} \to L_0^2(\partial\omega)$ is given by

$$\mathcal{G}^* a = \sum_{s=1}^{m} a_s \cdot \nabla N(\cdot, z_s).$$

We also introduce

$$\mathcal{M}a = \left(M^{(1)} a_1, \dots, M^{(m)} a_m \right), \quad a = (a_1, \dots, a_m) \in \mathbb{R}^{d\times m}.$$

Then we can immediately see that T can be decomposed as

$$T = \mathcal{G}^* \mathcal{M} \mathcal{G}.$$

Note that

$$\text{Range}(T) = \left\{ \sum_{s=1}^{m} a_s \cdot \nabla_z N(\cdot, z_s) : \ a_s \in \mathbb{R}^d \right\},$$

since $\text{Range}(T) = \ \text{Range}(\mathcal{G}^* \mathcal{M} \mathcal{G}) = \text{Range}(\mathcal{G}^*)$ and $\mathcal{M}$ and $\mathcal{G}$ are surjective.

The following theorem was proved in [**49**].

THEOREM 4.2. *Let $v \in \mathbb{R}^d \setminus \{0\}$. A point $z \in \Omega$ belongs to the set $\{z_s : s = 1, \ldots, m\}$ if and only if $v \cdot \nabla_z N(\cdot, z)\big|_{\partial\omega} \in$ Range (T).*

Since T is self-adjoint, injective, and of rank dm, it is an orthogonal projection, and hence Theorem 4.2 is equivalent to the following statement:

$$z \in \{z_s : s = 1, \ldots, m\} \quad \text{iff} \quad \cot\theta(z) = +\infty,$$

where the angle $\theta(z) \in [0, \pi/2)$ is defined by

$$\cot\theta(z) = \frac{||T(v \cdot \nabla_z N(\cdot, z)|_{\partial\Omega})||_{L^2(\partial\Omega)}}{||(I - T)(v \cdot \nabla_z N(\cdot, z)|_{\partial\Omega})||_{L^2(\partial\Omega)}}.$$

In view of (4.10) we can use $\Lambda_D - \Lambda_0$ instead of T in computing $\cot\theta(z)$. This method has been nicely implemented in [**49**] and its good ability to efficiently locate a high number of inclusions has been clearly demonstrated.

Assuming that all the inclusions are disks, we now present another method that only use two boundary measurements.

Simple Pole Method. This method for imaging multiple small inclusions is due to Kang and Lee [**86**]. See also [**39**]. Suppose that the inclusion is of the form $D = \cup_{s=1}^{m} D_s$ and each D_s is a disk, or $D_s = \epsilon_s B + z_0$ where B is a unit disk. In this case the polarization tensor $M^{(s)}$ associated with B is given by

$$M^{(s)} = \pi \frac{2(k_s - 1)}{k_s + 1} I,$$

where I is the identity matrix. Therefore, in this case we obtain from (4.8) that

$$H[g](x) = \sum_{s=1}^{m} \frac{\epsilon_s^2 (k_s - 1)}{k_s + 1} \frac{\nabla U(z_s) \cdot (x - z_s)}{|x - z_s|^2} + O(\epsilon^3), \quad x \in \mathbb{R}^2 \setminus \overline{\Omega}.$$

Thus, we get

$$H[\nu_1](x) + iH[\nu_2](x) = \sum_{s=1}^{m} \frac{\beta_s}{z - \alpha_s} + O(\epsilon^3), \quad z \in \mathbb{C} \setminus \overline{\Omega},$$

where $\beta_s := \epsilon_s^2 (k_s - 1)/(k_s + 1)$ and $\alpha_s = (z_s)_1 + i(z_s)_2$. Therefore our inclusion detection problem is reduced to the problem of finding the simple poles α_s and the residues β_s from the knowledge of a meromorphic function $f(z) = \sum_{s=1}^{m} \beta_s/(z - \alpha_s)$ on a circle $|z| = R$ enclosing all the poles.

It turns out that there is a nice way to locate the simple poles. By the Cauchy integral formula, we have

$$\frac{1}{2\pi i} \int_{|z|=R} z^n f(z) dz = \sum_{j=1}^{m} \beta_j \alpha_j^n.$$

The method of identification of simple poles is based on the following simple observations and was used by El Badia and Ha-Duong in [**38**] to recover pointwise sources.

LEMMA 4.3. *Suppose that the sequence* $\{c_n\}$ *takes the form* $c_n = \sum_{j=1}^{k} \beta_j \alpha_j^n$, $n = 0, 1, \ldots$. *If* $l_1, \ldots, l_k$ *satisfies the generating equation*

$$c_{n+k} + l_1 c_{n+k-1} + \cdots + l_k c_n = 0, \quad n = 0, 1, \ldots, k-1, \tag{4.11}$$

then $\alpha_1, \alpha_2, \cdots, \alpha_k$ *are solutions of*

$$z^k + l_1 z^{k-1} + \cdots + l_k = 0. \tag{4.12}$$

The converse is also true. Furthermore, if (4.11) holds, then it holds for all n.

LEMMA 4.4. *Let* c_n *be as in the Lemma 4.3 and let*

$$D_n = \det \begin{pmatrix} c_0 & c_1 & \cdots & c_{n-1} \\ c_1 & c_2 & \cdots & c_n \\ \vdots & \vdots & & \vdots \\ c_{n-1} & c_n & \cdots & c_{2n-2} \end{pmatrix}.$$

Then

$$D_n = \begin{cases} \beta_1 \beta_2 \cdots \beta_k \prod_{i<j} (\alpha_i - \alpha_j)^2 & \text{if } n = k, \\ 0 & \text{if } n > k. \end{cases} \tag{4.13}$$

Lemmas 4.3 and 4.4 suggest that if we know the number m of simple poles, then we first solve the system of equations (4.11) to find $l_1, \ldots, l_m$. We then solve the equation (4.12) to find the poles $\alpha_1, \ldots, \alpha_m$. Once we find $\alpha_1, \ldots, \alpha_m$, it is a simple matter to find $\beta_1, \ldots, \beta_k$. The most serious difficulty in finding poles comes from the fact that we do not know the number of poles aforehand. In order to determine this number, we use the formula (4.13). That is, we start with the bound N of the number and compute the determinants in (4.13) for $n = N, N-1, \ldots,$ until it becomes nonzero. The first number n where the determinant is nonzero is the number of simple poles we seek. Of course, these computations are performed within a given tolerance. A result of numerical test in a simple situation is given in [**86**].

We note that an EIT problem of reconstructing multiple thin inclusions can be reduced to a problem of finding simple poles for which the simple pole method may be applied. See a recent paper by Ammari *et al.* [**7**].

4.4. Detection of anisotropic inclusions. Efficient direct algorithms for reconstructing small anisotropic inclusions have been developed by Kang *et al.* in [**84**]. To bring out the main ideas of these algorithms we only consider the case where D has one component of the form $D = \epsilon B + z$. For a given $g \in L_0^2(\partial\Omega)$, let u be the solution to the Neumann problem

$$\begin{cases} \nabla \cdot \gamma_\Omega(x) \nabla u = 0 \quad \text{in } \Omega, \\ \nu \cdot A \nabla u \Big|_{\partial\Omega} = g, \\ \displaystyle\int_{\partial\Omega} u(x)\, d\sigma(x) = 0, \end{cases} \tag{4.14}$$

where $\gamma_\Omega = \chi_{\Omega \setminus \overline{D}} A + \chi_D \widetilde{A}$. The background potential U is the steady-state voltage potential in the absence of the conductivity inclusion, *i.e.*, the solution to

$$\begin{cases} \nabla \cdot A \nabla U = 0 \quad \text{in } \Omega, \\ \nu \cdot A \nabla U \Big|_{\partial\Omega} = g, \\ \displaystyle\int_{\partial\Omega} U(x)\, d\sigma(x) = 0. \end{cases} \tag{4.15}$$

Let $N^A(x,y)$, $x \in \partial\Omega$, $y \in \Omega$, be the Neumann function for $\nabla \cdot A\nabla$ on Ω, that is,

$$\begin{cases} \nabla \cdot A\nabla N^A(x,y) = -\delta_y \quad \text{in } \Omega, \\ \nu \cdot A\nabla N^A(x,y)\Big|_{\partial\Omega} = -\dfrac{1}{|\partial\Omega|}, \\ \displaystyle\int_{\partial\Omega} N^A(x,y)\, d\sigma(x) = 0, \end{cases}$$

and $M_{\alpha\beta}$ the APT's. Following the same lines of derivation of (4.5), we can prove the following asymptotic expansion of the solution u to (4.14) on $\partial\Omega$. See [**84**].

THEOREM 4.5. *For $x \in \partial\Omega$,*

$$u(x) = U(x) - \epsilon^d \sum_{|\alpha|=1}^{d} \sum_{|\beta|=1}^{d-|\alpha|+1} \frac{\epsilon^{|\alpha|+|\beta|-2}}{\alpha!\beta!} \partial^\alpha U(z) M_{\alpha\beta} \partial_z^\beta N^A(x,z) + O(\epsilon^{2d}),$$

where the remainder $O(\epsilon^{2d})$ is dominated by $C\epsilon^{2d}$ for some C independent of $x \in \partial\Omega$ and z.

We now define a function $H^A[g]$ for $g \in L_0^2(\partial\Omega)$ by

$$H^A[g](x) = -\mathcal{S}_\Omega^A(g)(x) + \mathcal{D}_\Omega^A(u|_{\partial\Omega})(x), \quad x \in \mathbb{R}^d \setminus \overline{\Omega}. \tag{4.16}$$

The following asymptotic expansion of $H^A[g]$ outside Ω holds. See [**84**].

THEOREM 4.6. *For $x \in \mathbb{R}^d \setminus \overline{\Omega}$,*

$$H^A[g](x) = -\epsilon^d \sum_{|\alpha|=1}^{d} \sum_{|\beta|=1}^{d-|\alpha|+1} \frac{\epsilon^{|\alpha|+|\beta|-2}}{\alpha!\beta!} \partial^\alpha U(z) M_{\alpha\beta} \partial_z^\beta \Gamma^A(x,z) + O(\frac{\epsilon^{2d}}{|x|^{d-1}}). \tag{4.17}$$

Suppose now that $g = \nu \cdot Aa$ for a constant vector $a \in \mathbb{R}^d$. Then $U(x) = a \cdot x$ and the formula (4.17) takes the form

$$H^A[g](x) = -\epsilon^d \sum_{|\alpha|=1} \sum_{|\beta|=1}^{d} \frac{\epsilon^{|\beta|-1}}{\beta!} \partial^\alpha U(z) M_{\alpha\beta} \partial_z^\beta \Gamma^A(x,z) + O(\frac{\epsilon^{2d}}{|x|^{d-1}}). \tag{4.18}$$

Then by explicitly computing $\partial_z^\beta \Gamma^A(x,z)$, we can show that

$$H^A[g](x) = \frac{1}{\omega_d} \langle a, \epsilon^d M A_* \frac{A_*(x-z)}{|A_*(x-z)|^d} \rangle + O(\frac{\epsilon^d}{|x|^d}) + O(\frac{\epsilon^{2d}}{|x|^{d-1}}), \tag{4.19}$$

where $\omega_d = 2\pi$ if $d = 2$, and $\omega_d = 4\pi$ if $d = 3$, and M is the first-order APT.

For a general Neumann data g, we have

$$H^A[g](x) = \frac{1}{\omega_d} \langle \nabla U(z), \epsilon^d M A_* \frac{A_*(x-z)}{|A_*(x-z)|^d} \rangle + O(\frac{\epsilon^d}{|x|^d}) + O(\frac{\epsilon^{d+1}}{|x|^{d-1}}), \tag{4.20}$$

Since

$$\frac{A_*(x-z)}{|A_*(x-z)|^d} = \frac{A_* x}{|A_* x|^d} + O(|x|^{-d}),$$

we obtain from (4.19) and (4.20) the following far-field relations [**84**].

THEOREM 4.7. *For $g \in L_0^2(\partial\Omega)$, let U be the solution of (4.15). Then, for $|x| = O(\epsilon^{-1})$,*

$$\omega_d |A_* x|^{d-1} H^A[g](x) = \langle \nabla U(z), \epsilon^d M A_* \frac{A_* x}{|A_* x|} \rangle + O(\epsilon^{d+1}). \tag{4.21}$$

If $g = \nu \cdot Aa$, then for $|x| = O(\epsilon^{-d})$

$$\omega_d |A_* x|^{d-1} H^A[g](x) = \langle a, \epsilon^d M A_* \frac{A_* x}{|A_* x|} \rangle + O(\epsilon^{2d}). \tag{4.22}$$

We note that (4.21) is a general far-field relation while (4.22) is a formula with better precision.

Using (4.19), (4.21), and (4.22), we can detect APT, the order of magnitude of D, and z.

Detection of APT: Now let $a = e_p$, or equivalently, $g = \nu \cdot Ae_p$, and choose $b_q = O(\epsilon^{-d})$ so that

$$A_* \frac{A_* b_q}{|A_* b_q|} = e_q, \quad p, q = 1, \cdots, d. \tag{4.23}$$

It then follows from (4.22) that

$$\epsilon^d M_{pq} = \omega_d |A_* b_q|^{d-1} H^A[g](b_q) \quad \text{modulo } O(\epsilon^{2d}). \tag{4.24}$$

Since ϵ is not known *a priori*, in actual computations we find unit vectors b_q satisfying (4.23) and then compute $\omega_d |tA_* b_q|^{d-1} H^A[g](tb_q)$ as $t \to \infty$. Since the first-order APT is invariant under translation as we can easily check, $\epsilon^d M$ is the first-order APT for the domain D.

Detection of Order of Magnitude: Having found $\epsilon^d M$, we proceed to find the order of magnitude ϵ and the center z. Using Corollary 3.20, we can determine the order of magnitude of D. Let μ be the smallest (in absolute value) eigenvalue of $\epsilon^d M$. Then, $\epsilon^d |B| \approx |\mu|$.

Detection of Center-Method 1: Let v_q, $q = 1, \cdots, d$, be orthonormal eigenvectors of the symmetric matrix $A_*(\epsilon^d M)A_*$ with the corresponding eigenvalue λ_q, and $a_q := A_* v_q$ and $g_q := \nu \cdot Aa_q$. Let $x(t) := ta_q + O(\epsilon^{-1})a_q^\perp$ where $a_q^\perp$ is a vector perpendicular to a_q. Then $|x(t)| = O(\epsilon^{-1})$ and hence, by (4.19), we get

$$H^A[g_q](x(t)) = \frac{\lambda_q}{\omega_d} \frac{|a_q|^2 t - a_q \cdot z}{|A_*(x(t) - z)|^d} \quad \text{modulo } O(\epsilon^{2d}). \tag{4.25}$$

Find the unique zero, call it t_q, of $H^A[g_q](x(t))$ as a function of t for $q = 1, \ldots, d$. Let $\bar{z} = t_1 a_1 + \ldots + t_d a_d$. This $\bar{z}$ is the center. In fact, by the same argument as in [**33**], we can prove that

$$|\bar{z} - z| = O(\epsilon^d).$$

Detection of Center-Method 2: Let b_q, $q = 1, \cdots, d$, be the unit vector defined by (4.23). Then, from (4.21), we get

$$\omega_d |tA_* b_q|^{d-1} H^A[g](tb_q) = \langle \nabla U(z), \epsilon^d M e_q \rangle \quad \text{modulo } O(\epsilon^{d+1}). \tag{4.26}$$

Let $g = \nu \cdot A\nabla U$ where U is a second-order homogeneous harmonic polynomial. By computing $\omega_d |tA_* b_q|^{d-1} H^A[g](tb_q)$ as $t \to \infty$, we recover $\langle \nabla U(z), \epsilon^d M e_q \rangle$, $q = 1, \cdots, d$. From this we now recover $\nabla U(z)$, and hence the center z modulo $O(\epsilon)$.

The precision of this method is $O(\epsilon)$ which is worse than Method 1. However, numerical experiments in the next section show that this method performs better when there is noise in the data.

Computational Experiments: We now present results of numerical experiments from [**84**]. In the following, Ω is assumed to be the disk centered at $(0, 0)$ and with radius $r = 2$, and the background conductivity $A = I$. We also assume that $D = \epsilon B + z$ where B is the unit disk centered at $(0, 0)$. We note that in the anisotropic case, D being a disk does not provide a special advantage. Moreover, in the process of solving the inverse problem, we don't use any *a priori* knowledge of D being a disk.

Let u be the solution of (4.14). In order to collect the data $u|_{\partial\Omega}$, we solve the direct problem (4.14) as follows: u is represented by

$$u(x) = \begin{cases} \mathcal{D}_\Omega^A u(x) - \mathcal{S}_\Omega^A g(x) + \mathcal{S}_D^A \phi(x) & \text{in } \Omega \setminus D, \\ \mathcal{S}_D^{\widetilde{A}} \psi(x) & \text{in } D, \end{cases}$$

where $u|_{\partial\Omega}$, ϕ, and ψ satisfy the following relations:

$$\begin{aligned} & u = \mathcal{D}_\Omega^A u\big|_- - \mathcal{S}_\Omega^A g\big|_- + \mathcal{S}_D^A \phi \qquad \text{on } \partial\Omega, \\ & \mathcal{D}_\Omega^A u - \mathcal{S}_\Omega^A g + \mathcal{S}_D^A \phi\big|_+ = \mathcal{S}_D^{\widetilde{A}} \phi\big|_- \qquad \text{on } \partial D, \\ & \frac{\partial}{\partial\nu}\mathcal{D}_\Omega^A u - \frac{\partial}{\partial\nu}\mathcal{S}_\Omega^A g + \frac{\partial}{\partial\nu}\mathcal{S}_D^A \phi\big|_+ = \frac{\partial}{\partial\widetilde{\nu}}\mathcal{S}_D^{\widetilde{A}} \phi\big|_- \qquad \text{on } \partial D. \end{aligned}$$

We solve this integral equation using the collocation method [**99**] and obtain $u|_{\partial\Omega}$ on $\partial\Omega$ for given data g. We also add some noise to the computed data. Adding $p\%$ noise means that we have

$$u(1 + \frac{p}{100} \cdot \text{rand}(1))$$

as the measured Dirichlet data. Here rand(1) is the random number in $(-1, 1)$.

Reconstruction Algorithm 1:

Step 1: Obtain Dirichlet data u on $\partial\Omega$ for a given Neumann data $g_q = \nu \cdot Ae_q$, $q = 1, 2$.

Step 2: For $p, q = 1, 2$, calculate $\lim_{t\to\infty} \omega_2 t H^A[g_p](te_q)$ to obtain the matrix $\epsilon^2 M$.

Step 3: Find orthonormal eigenvectors v_1, v_2 and corresponding eigenvalues μ_1, μ_2 of $\epsilon^2 M$. Let μ be the minimum of $|\mu_1|, |\mu_2|$. Order of magnitude of D is $\epsilon = \sqrt{\mu|B|^{-1}}$.

Step 4: Let $g_j' = \nu \cdot Av_j$ and $x_q(t) = tv_q + \frac{1}{\epsilon} v_q^\perp$, $q = 1, 2$. Find the zero, say t_q, of $H^A[g_q'](x_q(t)) = v_q \cdot e_1 H^A[g](x_q(t)) + v_q \cdot e_2 H^A[g_2](x_q(t))$ as a function of t. We obtain the center $\bar{z} = t_1 v_1 + t_2 v_2$.

Reconstruction Algorithm 2: Step 4 in the above algorithm is replaced with

Step 4′: For $g = \nu \cdot A\nabla(x_1 x_2)$, compute $h_q = \lim_{t\to\infty} \omega_2 t H^A[g](te_q)$, $q = 1, 2$. Then $(z_1, z_2) = (h_1, h_2) \begin{pmatrix} \epsilon^2 M_{12} & \epsilon^2 M_{22} \\ \epsilon^2 M_{11} & \epsilon^2 M_{12} \end{pmatrix}^{-1}$. We add the same amount of random noise in this step as well.

The following computational experiments from [**84**] clearly demonstrate the viability of the reconstruction algorithms. The first experiment is when $\widetilde{A} - A$ is positive definite; the second one is when $\widetilde{A} - A$ is not positive-definite; the third one is to investigate the role of the condition number of $\widetilde{A} - A$ in the reconstruction process.

Experiment 1: Let $\widetilde{A} = \begin{pmatrix} 10 & 2 \\ 2 & 5 \end{pmatrix}$ and the actual inclusion, $D = (-1, -1) + 0.2B$. Note that $\widetilde{A} - A$ is positive-definite. Figure 9 shows the results when there are 0%, 2%, and 5% random noise. Figure 10 is the result when $\widetilde{A} = \begin{pmatrix} 10 & 1 \\ 1 & 2 \end{pmatrix}$ and $D = (0, 1) + 0.2B$.

These results show that both Algorithms 1 and 2 detect the order of magnitude of the inclusion fairly well even with the presence of noise. However, Algorithm 2 performs better than Algorithm 1 in detecting the center when there is noise. A probable cause for this is that the zeros of functions in (4.25), which is already small, are sensitive to the noise.

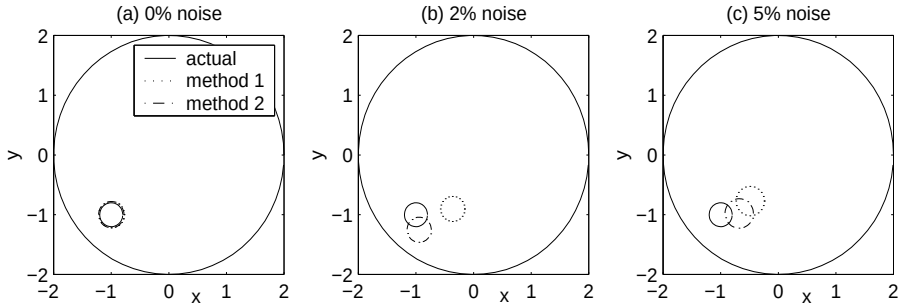

FIGURE 9. First example.

z	r	noise(%)	$\bar{r}$	$\bar{z_1}$	$\lvert z-\bar{z_1}\rvert$
				$\bar{z_2}$	$\lvert z-\bar{z_2}\rvert$
$(-1,-1)$	0.2	0	0.2204	$(-0.9994,-0.9994)$	8.1154e-004
				$(-0.9994,-0.9994)$	8.4362e-004
		2	0.2101	$(-0.3681,-0.9038)$	0.6391
				$(-0.9445,-1.2519)$	0.2580
		5	0.2463	$(-0.4936,-0.7715)$	0.5556
				$(-0.6787,-0.9790)$	0.3220

TABLE 2. Results of the first example. Here r and $\bar{r}$ are the actual and computed radii, and z, $\bar{z}_1$ and $\bar{z}_2$ are the actual and the computed centers by Algorithms 1 and 2, respectively.

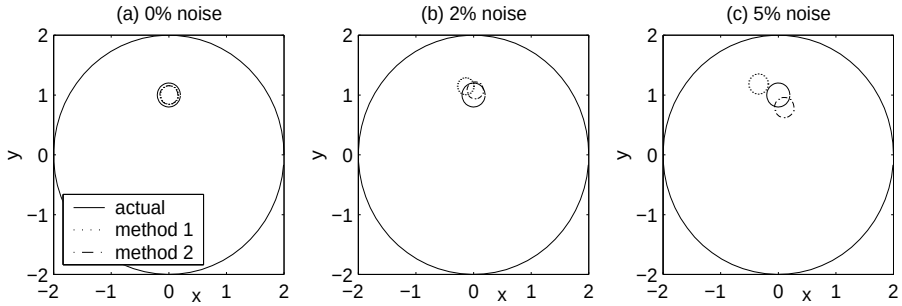

FIGURE 10. Second example.

z	r	noise(%)	$\bar{r}$	$\bar{z_1}$	$\lvert z-\bar{z_1}\rvert$
				$\bar{z_2}$	$\lvert z-\bar{z_2}\rvert$
$(0,1)$	0.2	0	0.1557	$(-0.0000,0.9999)$	1.2316e-004
				$(-0.0000,0.9998)$	1.6690e-004
		2	0.1417	$(-0.1421,1.1468)$	0.2043
				$(0.0288,1.0771)$	0.0823
		5	0.1689	$(-0.3499,1.1841)$	0.3954
				$(0.1036,0.7906)$	0.2336

TABLE 3. Results of the second example.

Figure 11 shows that the location of the unknown inclusions does not affect the performance of the algorithms as long as they are away from $\partial\Omega$.

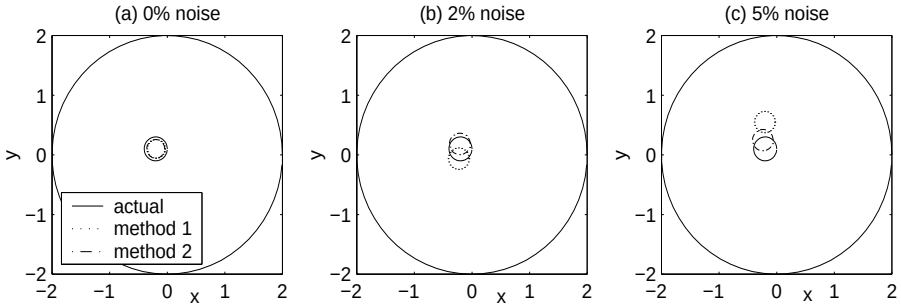

FIGURE 11. Third example.

z	r	noise(%)	$\bar{r}$	$\bar{z_1}$	$\lvert z-\bar{z_1}\rvert$
				$\bar{z_2}$	$\lvert z-\bar{z_2}\rvert$
$(-0.2, 0.1)$	0.2	0	0.1559	$(-0.2000, 0.1000)$	1.2081e-005
				$(-0.2000, 0.1000)$	1.6354e-005
		2	0.1798	$(-0.2342, -0.0643)$	0.1678
				$(-0.2108, 0.1830)$	0.0837
		5	0.1785	$(-0.2120, 0.5493)$	0.4495
				$(-0.2405, 0.2464)$	0.1519

TABLE 4. Results of the third example.

Experiment 2: This experiment is to see whether the algorithms work in the case when $\widetilde{A} - A$ is not positive or negative-definite. Let $\widetilde{A} = \begin{pmatrix} 2 & 0 \\ 0 & \frac{1}{2} \end{pmatrix}$ and $D = (1,0) + 0.2B$. Figure 12 shows the result. The algorithm seems to be working equally well for this case. It would be interesting to prove that the reconstruction formulae hold even when $\widetilde{A} - A$ is not positive or negative-definite. In this example as well, Algorithm 2 performs better in detection of the center.

Experiment 3: This experiment is to see how the condition number of $\widetilde{A} - A$ affects the precision of the algorithm. Suppose $A = I$. We first take $\widetilde{A} = \begin{pmatrix} \lambda & 0 \\ 0 & 2 \end{pmatrix}$ and observe how the relative error $|z - \bar{z}|/\epsilon^2$ changes as λ increases. We then take $\widetilde{A} = \begin{pmatrix} \lambda+1 & 0 \\ 0 & \lambda \end{pmatrix}$ and make the same observations. Figure 13 compares changes of relative errors of these two cases when $\lambda = 10, 10^2, 10^4, 10^5, 10^6$. It exhibits clear difference: In the first case when the condition number of $\widetilde{A} - A$ increases as λ increases, the relative error is increasing, while in the second case when the condition number does not change, the error is stabilized. The second case is somewhat similar to the isotropic case and this kind of result is expected; see [**88**] or [**16**]. It is known that long and thin inclusions, or crack-like inclusions (inclusions of high Lipschitz character) are hard to detect. See, for example, [**33**]. This experiment suggests that in addition to this geometric obstruction, in the anisotropic case there is another obstruction of high condition number of $\widetilde{A} - A$.

Numerical results show that the second reconstruction algorithm performs better in the presence of noise. They also show that the reconstruction procedure works well even when $A - \widetilde{A}$ is not positive or negative definite, and that the error of reconstruction increases as the condition number of $A - \widetilde{A}$ increases. It would be interesting to investigate these points in a mathematically rigorous way.

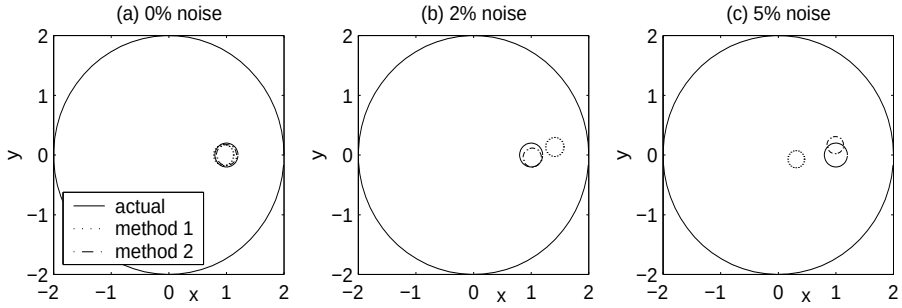

FIGURE 12. Fourth example.

z	r	noise(%)	$\bar{r}$	$\bar{z_1}$	$\lvert z-\bar{z_1}\rvert$
				$\bar{z_2}$	$\lvert z-\bar{z_2}\rvert$
$(1,0)$	0.2	0	0.1739	$(0.9447,-0.0000)$	0.0553
				$(1.0002,-0.0000)$	1.8443e-004
		2	0.1586	$(1.4031,0.1347)$	0.4250
				$(1.0186,-0.0427)$	0.0465
		5	0.1436	$(0.3048,-0.0702)$	0.6987
				$(0.9891,0.1656)$	0.1660

TABLE 5. Results of the fourth example.

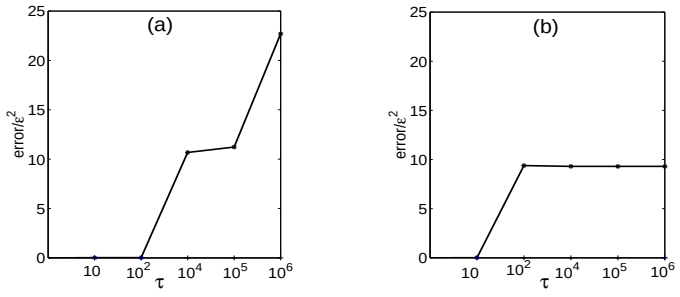

FIGURE 13. The graphs show how the quantities $|z-\bar{z}|/\epsilon^2$ change as λ goes to ∞. (a) The condition number of $\widetilde{A}-A$ is λ and the relative error increases. (b) The condition number of $\widetilde{A}-A$ is 1 and the relative error does not increase.

4.5. Further results and concluding remarks. The algorithms presented in this section detect the locations and the GPT's from boundary measurements. It is the detected first-order polarization tensor which yields an information on the size and orientation of the inclusion. However, the information from the first-order polarization tensor is a mixture of the conductivity and the volume. It is impossible to extract the conductivity from the first-order polarization tensor. A small inclusion with high conductivity and larger inclusion with lower conductivity can have the same-first order polarization tensor. Similarly, the material property of the inclusion, namely, anisotropic conductivity, can not be distinguished by means of the first-order polarization tensor. It would be interesting and important to extract information on the material property, such as conductivity and anisotropy, of the inclusion from boundary measurements. It is likely that higher-order polarization tensors yield such information. We refer to [**85**] for a complete characterization

of pairs of anisotropies and ellipses which yield the same first-order polarization tensor.

When comparing the different methods that have been designed for imaging small inclusions, it is fair to point out that the methods that rely on "single measurements" are more limited in their abilities to effectively locate a high number of small inclusions than those that use "many boundary measurements".

In connection with the algorithms described in this section, we should mention that there have been interesting works on asymptotic expansions of the perturbation due to the presence of small well-separated inclusions and to reconstruct them from boundary measurements in many other contexts: for the Helmholtz equation [**12, 13, 14, 20**], for the full Maxwell equations [**17, 34, 35, 133, 134**], for thin inclusions [**7, 8, 44, 45, 46**], and for linear elasticity [**4, 28, 83**]. Recently layer potential techniques have been used to derive asymptotic expansion of the voltage potential due to the presence of internal corrosion [**31**].

5. Effective properties of composites

Let us begin by defining the concept of effective property in a rigorous way. Set Ω to be a bounded domain in $\mathbb{R}^d$, with a connected Lipschitz boundary $\partial\Omega$. Consider a periodic dilute composite filling Ω. The material consists of a matrix of constant isotropic conductivity $\sigma_0 > 0$ containing a periodic array of small conductivity inclusions centered in those period cells that fall inside Ω. The periodic array has period ϵ, and each period contains an inclusion of constant isotropic conductivity $\sigma > 0$ which is of the form $\epsilon^{1+\beta}B$ for some $\beta > 0$. Here B is a bounded Lipschitz domain in $\mathbb{R}^d$ containing the origin, $|B|$ is 1. As $\epsilon \to 0$ the volume fraction of the inhomogeneities is $f = \epsilon^{d\beta}$.

Let $Y =]-1/2, 1/2[^d$ denote the unit cell and denote $\rho = \epsilon^\beta$. We set the periodic function

$$\gamma = \sigma_0 \chi(Y \setminus D) + \sigma\chi(D),$$

where $D = \rho B$.

For a small parameter ϵ, $\gamma_\epsilon(x) := \gamma(x/\epsilon)$ makes a highly oscillating conductivity and represents the material property of the composite. Figure 14 shows a geometry of a composite in $\mathbb{R}^2$.

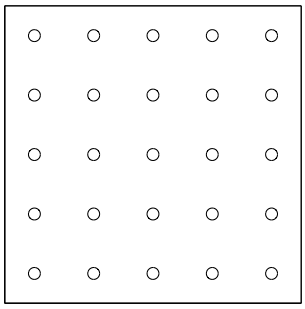

FIGURE 14. Periodic composite material in $\mathbb{R}^2$. Inclusion $D = \rho B$, distance between inclusions ϵ, the volume fraction $f = \rho^2$. Conductivity of inclusion equals σ, conductivity of background equals σ_0.

Consider the conductivity problem

$$\nabla \cdot \gamma_\epsilon \nabla u_\epsilon = 0 \quad \text{in } \Omega \tag{5.1}$$

with an appropriate boundary condition on $\partial\Omega$. The theory of homogenization tells us that the solution u_ϵ converges weakly to a function u_0 in $W^{1,2}(\Omega)$ and there

exists a constant (anisotropic) conductivity, γ^*, such that

$$\nabla \cdot \gamma^* \nabla u_0 = 0 \quad \text{in } \Omega. \tag{5.2}$$

The replacement of the original equation (5.1) by (5.2) is a valid approximation in a certain limit [**43**].

The coefficient γ^* is called an effective conductivity or a homogenized coefficient. It represents the overall macroscopic material property of the periodic composite material; see [**82**]. For a more intuitive approach, see [**115**]. See also [**58**] and [**3**] for applications to structural optimization.

In general, effective conductivities can not be computed exactly except for a few configurations. We consider the problem of determining the effective property of the composite when the volume fraction $f = |D|$ goes to zero. In other words, the inclusions have much less volume than the matrix. This kind of material is called a dilute material. Many approximations for the effective properties of composites are based on the solution for dilute materials.

When the inclusion D is a disk or sphere, then the effective electrical conductivity, γ^*, of the composite medium is given by the well-known Maxwell-Garnett formula[1] [**126**]:

$$\gamma^* = \sigma_0 \Big[1 + f \frac{d(\sigma - \sigma_0)}{(\sigma - \sigma_0) + d\sigma_0} + df^2 \frac{(\sigma - \sigma_0)^2}{((\sigma - \sigma_0) + d\sigma_0)^2}\Big] I + o(f^2), \tag{5.3}$$

where $d = 2, 3$ is the space dimension.

This formula has been generalized in many directions: to include higher power terms of the volume fraction f for spherical inclusions, [**81, 126, 138**]; to include other shapes of the inclusion such as ellipses, [**137, 66, 74, 111, 65, 82, 76, 116, 52, 125, 105**]; to include the case when $f = O(1)$; see the book of Milton [**115**] and the one of Torquato [**130**] and the references therein.

We begin with the derivation of an asymptotic expansion of the effective electrical conductivity of an isotropic composite medium for arbitrary shaped inclusions. The approach is valid for inclusions with Lipschitz boundaries and high contrast mixtures, and allows us to compute higher-order terms in the asymptotic expansion of the effective conductivity. After that, we extend this derivation to anisotropic composites.

Our asymptotic expansions have important implications for imaging composites. They show what information can be reconstructed from boundary measurements and how well. It is not surprising that the volume fractions and the GPT's form the only microstructural information that can be reconstructed from boundary measurements. The volume fraction is the simplest but most important piece of microstructural information. The GPT's involve microstructural information beyond that contained in the volume fractions (material contrast, inclusion shape and orientation). Indeed, if arbitrary shaped inclusions orient according to a certain probability distribution then our expansions show that only the moments of the orientational distribution functions of the inclusions can be recovered from (experimental) measurements of the effective conductivity of the composite. We refer to Hashin and Monteiro [**78**] and Torquato [**131**] for related interesting problems in imaging composites.

5.1. Computation of effective conductivity. We shall explain a scheme for deriving an asymptotic expansion of the effective property of the dilute composite material. This result is from [**29**]. Our approach can be viewed as a generalization of an elegant method which was first used for problems of the present form by Hasimoto [**79, 118**]. Hasimoto's method was designed to construct higher-order

[1] Several different pairs of names are attached to this formula; see [**115**].

terms in (5.3) when the inclusion is a sphere. It has been implemented numerically yielding results that are valid for fairly large volume fraction f [**127**].

Suppose for the sake of simplicity that $d = 2$. The effective conductivity matrix $\gamma^* = (\gamma^*_{ij})_{i,j=1,2}$ of Ω is defined by (see for instance [**82, 115**])

$$\gamma^*_{ij} := \int_Y (\sigma_0 \chi(Y \setminus D) + \sigma \chi(D)) \nabla u_i \cdot \nabla u_j,$$

where u_i, for $i = 1, 2$, is the unique solution to

$$\begin{cases} \nabla \cdot (\sigma_0 \chi(Y \setminus D) + \sigma \chi(D)) \nabla u_i = 0 \quad \text{in } Y, \\ \\ u_i - y_i \text{ periodic with period 1 (in each direction)}, \\ \\ \displaystyle\int_Y u_i = 0. \end{cases} \tag{5.4}$$

Using Green's formula we can rewrite γ^* in the following form:

$$\gamma^*_{ij} = \sigma_0 \int_{\partial Y} u_j \frac{\partial u_i}{\partial \nu}. \tag{5.5}$$

The matrix γ^* depends on ϵ as a parameter, and cannot be written explicitly.

According to Theorem 2.14, the solution to (5.4) can be written as

$$u_i(x) = x_i + C_i + \mathcal{G}_D(\lambda I - \mathcal{B}^*_D)^{-1}(\nu_i)(x) \quad \text{in } Y, \quad i = 1, 2,$$

where λ is given by

$$\lambda = \frac{\sigma + \sigma_0}{2(\sigma - \sigma_0)}. \tag{5.6}$$

For simplicity, we set for $i = 1, 2$

$$\phi_i(y) = (\lambda I - \mathcal{B}^*_D)^{-1}(\nu_i)(y) \quad \text{for } y \in \partial D. \tag{5.7}$$

Thus we get from (5.5)

$$\gamma^*_{ij} = \sigma_0 \int_{\partial Y} (y_j + C + \mathcal{G}_D \phi_j(y)) \frac{\partial}{\partial \nu}(y_i + \mathcal{G}_D \phi_i(y)) d\sigma.$$

Because of periodicity of $\mathcal{G}_D \phi_j$, we get

$$\int_{\partial Y} \frac{\partial}{\partial \nu} \mathcal{G}_D \phi_j d\sigma = \int_{\partial Y} \nu_j \mathcal{G}_D \phi_i d\sigma = \int_{\partial Y} \mathcal{G}_D \phi_j(y) \frac{\partial}{\partial \nu} \mathcal{G}_D \phi_i(y) d\sigma = 0,$$

and hence we have

$$\gamma^*_{ij} = \sigma_0 \Big[\delta_{ij} + \int_{\partial Y} y_j \frac{\partial}{\partial \nu} \mathcal{G}_D \phi_i(y)\, d\sigma(y) \Big]. \tag{5.8}$$

Periodicity of $\mathcal{G}_D \phi_i$ and the divergence theorem applied on $Y \setminus \overline{D}$ yield

$$\begin{aligned} \int_{\partial Y} y_j \frac{\partial}{\partial \nu} \mathcal{G}_D \phi_i(y)\, d\sigma &= \int_{\partial D} y_j \frac{\partial}{\partial \nu} \mathcal{G}_D \phi_i \big|_+(y)\, d\sigma - \int_{\partial D} \nu_j \mathcal{G}_D \phi_i(y)\, d\sigma \\ &= \int_{\partial D} y_j \phi_i(y)\, d\sigma + \int_{\partial D} y_j \frac{\partial}{\partial \nu} \mathcal{G}_D \phi_i \big|_-(y)\, d\sigma - \int_{\partial D} \nu_j \mathcal{G}_D \phi_i(y)\, d\sigma \\ &= \int_{\partial D} y_j \phi_i(y)\, d\sigma. \end{aligned}$$

Let

$$\psi_i(y) = \phi_i(\rho y) \quad \text{for } y \in \partial B.$$

Then by (5.8), we obtain

$$\gamma^* = \sigma_0 [I + fP], \tag{5.9}$$

where $f = \rho^2$ is the volume fraction of D and $P := (P_{ij})$ is given by

$$P_{ij} := \int_{\partial B} y_j \psi_i(y)\, d\sigma(y), \quad i, j = 1, 2. \tag{5.10}$$

In order to derive an asymptotic expansion of γ^* we now expand P in terms of ρ. In view of (2.27), the integral equation (5.7) can be rewritten as

$$(\lambda I - \mathcal{K}_D^*)\phi_i(x) - \int_{\partial D} \frac{\partial}{\partial \nu_x} R(x-y)\phi_i(y)\, d\sigma(y) = \nu_i(x), \quad x \in \partial D,$$

which, by an obvious change of variables, yields

$$(\lambda I - \mathcal{K}_B^*)\psi_i(x) - \rho \int_{\partial B} \frac{\partial}{\partial \nu_x} R(\rho(x-y))\psi_i(y)\, d\sigma(y) = \nu_i(x), \quad x \in \partial B.$$

Because of (2.28) we get

$$\nu \cdot \nabla R(\rho(x-y)) = -\frac{\rho}{2}\nu \cdot (x-y) + O(\rho^{3\beta})$$

uniformly in $x, y \in \partial B$. Since $\int_{\partial B} \psi_i(y)\, d\sigma(y) = 0$, we now have

$$(\lambda I - \mathcal{K}_B^*)\psi_i(x) - \frac{\rho^2}{2}\nu_x \cdot \int_{\partial B} y\psi_i(y)\, d\sigma(y) + O(\rho^4) = \nu_i(x), \quad x \in \partial B.$$

Therefore, we obtain

$$\psi_i = (\lambda I - \mathcal{K}_B^*)^{-1}(\nu_i) + \frac{\rho^2}{2}\sum_{k=1}^{2}(\lambda I - \mathcal{K}_B^*)^{-1}(\nu_k) \cdot \int_{\partial B} y_k \psi_i(y)\, d\sigma(y) + O(\rho^4). \tag{5.11}$$

Let $\widetilde{\psi}_i := (\lambda I - \mathcal{K}_B^*)^{-1}(\nu_i)$, $i = 1, 2$. Then $M_{ij} = \int_{\partial B} y_j \widetilde{\psi}_i(y) d\sigma(y)$, etc. By iterating the formula (5.11), we get

$$\psi_i = \widetilde{\psi}_i + \frac{\rho^2}{2}\sum_{k=1}^{2}\widetilde{\psi}_k \int_{\partial B} y_k \widetilde{\psi}_i(y)\, d\sigma(y) + O(\rho^4) \quad \text{on } \partial B.$$

It then follows from the definition (5.10) of P that

$$P_{ij} = M_{ij} + \frac{\rho^2}{2}\sum_{k=1}^{2} M_{kj}M_{ik} + O(\rho^4),$$

and then we obtain from (5.9) the following theorem.

THEOREM 5.1. *We have*

$$\gamma^* = \sigma_0\Big[I + fM(I - \frac{f}{2}M)^{-1}] + O(f^3), \tag{5.12}$$

where M is the Pólya-Szegö polarization tensor associated to the scaled inclusion B and the conductivity $k = \sigma_0(2\lambda+1)/(2\lambda-1)$. Here λ is given by (5.6).

Formula (5.12) relates Theorem 3.11 with the theory of bounds in homogenization. See Milton [**115**] and Torquato [**130**] for detailed derivations of bounds in homogenization.

In the case of circular inclusions the Pólya-Szegö polarization tensor M is known exactly:

$$M = mI, \quad m = \frac{2(\sigma - \sigma_0)}{\sigma + \sigma_0}|B|,$$

and therefore, (5.12) yields the well-known Maxwell-Garnett formula (5.3):

$$\gamma^* = \sigma_0\Big[1 + f\frac{2(\sigma-\sigma_0)}{\sigma+\sigma_0} + 2f^2\frac{(\sigma-\sigma_0)^2}{(\sigma+\sigma_0)^2}\Big]I + o(f^2).$$

Let $\mathcal{E}$ be an ellipse whose semi-axes are on the x_1- and x_2-axes and of length a and b, respectively. If $B = \frac{1}{|\mathcal{E}|}\mathcal{R}(\theta)\mathcal{E}$ where $\mathcal{R}(\theta) = \begin{pmatrix}\cos\theta & -\sin\theta \\ \sin\theta & \cos\theta\end{pmatrix}$, $\theta \in [0, \pi]$,

and $|\mathcal{E}| = \pi ab$ is the volume of $\mathcal{E}$, then using Lemma 3.4 and Theorem 5.1, we obtain that the effective conductivity of the composite is given by

$$\gamma^* = \sigma_0 \Bigg[I + (\frac{\sigma}{\sigma_0} - 1)\frac{f}{\pi ab} \times \mathcal{R}(\theta) \begin{pmatrix} \frac{a+b}{(a+\frac{\sigma}{\sigma_0}b) - \frac{f}{2}(\frac{\sigma}{\sigma_0}-1)(a+b)} & 0 \\ 0 & \frac{a+b}{(\frac{\sigma}{\sigma_0}a+b) - \frac{f}{2}(\frac{\sigma}{\sigma_0}-1)(a+b)} \end{pmatrix} \mathcal{R}^T(\theta) \Bigg] + O(f^3),$$

where $\mathcal{R}^T$ denotes the transpose of $\mathcal{R}$.

This formula can be used to solve the inverse problem of determining the volume fraction f, the conductivity contrast σ/σ_0, the semi-lengths a and b, or the orientation θ of the inclusions from measurements of the effective conductivity of the composite. Indeed, if the elliptical inclusions orient according to a probability distribution $\Psi(\theta)$ then the effective conductivity

$$\gamma^* = \sigma_0 \Bigg[I + (\frac{\sigma}{\sigma_0} - 1)\frac{f}{\pi ab} \times \int_0^{2\pi} \mathcal{R}(\theta) \times \begin{pmatrix} \frac{a+b}{(a+\frac{\sigma}{\sigma_0}b) - \frac{f}{2}(\frac{\sigma}{\sigma_0}-1)(a+b)} & 0 \\ 0 & \frac{a+b}{(\frac{\sigma}{\sigma_0}a+b) - \frac{f}{2}(\frac{\sigma}{\sigma_0}-1)(a+b)} \end{pmatrix} \mathcal{R}^T(\theta)\, \Psi(\theta)\, d\theta \Bigg] + O(f^3),$$

which shows that only the second moments of the orientational distribution functions of the inclusions $\Psi(\theta)$ can be recovered. See [**135**]. Using Lemma 3.4 and Theorem 5.1, this result can be trivially extended to arbitrary shaped inclusions.

The method presented above basically enables us to derive all the higher-order terms of the asymptotic expansion of the effective conductivity. The construction of these terms depends only on the ability to continue the Taylor expansion (2.28). For example, by the (higher-order) Taylor expansion

$$R(x) = R(0) - \frac{1}{4}(x_1^2 + x_2^2) + R_4(x) + O(|x|^6),$$

we get

$$\nu \cdot \nabla R(\rho(x-y)) = -\frac{\rho}{2}\nu \cdot (x-y) + \rho^3 \nu \cdot \nabla_x R_4(x-y) + O(\rho^{5\beta})$$

uniformly in $x, y \in \partial B$. Write

$$R_4(x-y) = \sum_{|l|+|l'|=4} c_{l,l'} x^l y^{l'}.$$

Then for each fixed l', $\sum_l c_{l,l'} x^l$ is harmonic since

$$\sum_l c_{l,l'} x^l = \frac{1}{l'!} \partial_y^{l'} (R_4(x-y))\big|_{y=0}.$$

In the same way we can derive the following theorem:

THEOREM 5.2. *The effective conductivity γ^* has an asymptotic expansion as $\rho \to 0$:*

$$\gamma^* = \sigma_0 \Big[I + fM(I - \frac{f}{2}M)^{-1} + f^3 A \Big] + O(f^4), \tag{5.13}$$

where M is the (first-order) polarization tensor and A is given by

$$A_{ij} = \sum_{\substack{|l|+|l'|=4 \\ |l|>0,\, |l'|>0}} c_{l,l'} M_{lj} M_{il'}, \quad i,j = 1,2.$$

5.2. Anisotropic composites. The asymptotic expansion formula (5.13) has been generalized in [**23**] to include anisotropic materials. Let the periodic anisotropic conductivity in the unit cell Y be defined by

$$\gamma = A\chi(Y \setminus D) + \widetilde{A}\chi(D),$$

where A and $\widetilde{A}$ are constant $d \times d$ positive-definite symmetric matrices with $A \neq \widetilde{A}$. Here Y and D are defined similarly to the isotropic case.

For a small parameter ϵ, we consider the problem of determining the effective anisotropic properties of the composite with the anisotropic conductivity $\gamma(x/\epsilon)$ as $\epsilon \to 0$.

Write

$$A = \begin{pmatrix} a & b \\ b & c \end{pmatrix}, \quad a, c > 0 \text{ and } ac - b^2 > 0,$$

and introduce

$$\alpha := -\frac{b}{c} + i\frac{\sqrt{|A|}}{c} \quad \text{and} \quad \beta := -\frac{b}{a} + i\frac{\sqrt{|A|}}{a},$$

where $|A|$ is the determinant of A. We also define real-valued functions θ and η by

$$\theta(z) + i\eta(z) := \sum_{n=1}^{\infty} \frac{n}{1 - e^{-2\pi i n z}}, \quad \Im z > 0.$$

Let K be given by

$$\begin{aligned} K = {} & \frac{1}{4}\begin{pmatrix} \frac{1}{a} & 0 \\ 0 & \frac{1}{c} \end{pmatrix} + \frac{\pi}{\sqrt{|A|}}\left(\frac{1}{24} + \theta(\alpha)\right)\begin{pmatrix} 1 & -\frac{b}{c} \\ -\frac{b}{c} & \frac{2b^2 - ac}{c^2} \end{pmatrix} \\ & + \frac{\pi}{\sqrt{|A|}}\left(\frac{1}{24} + \theta(\beta)\right)\begin{pmatrix} \frac{2b^2 - ac}{a^2} & -\frac{b}{a} \\ -\frac{b}{a} & 1 \end{pmatrix} \\ & + \frac{\pi\eta(\alpha)}{c}\begin{pmatrix} 0 & -1 \\ -1 & \frac{2b}{c} \end{pmatrix} + \frac{\pi\eta(\beta)}{a}\begin{pmatrix} \frac{2b}{a} & -1 \\ -1 & 0 \end{pmatrix}. \end{aligned} \tag{5.14}$$

The following result is proved in [**23**].

THEOREM 5.3. *Let K be the matrix defined by (5.14). Then we have an asymptotic formula for the effective conductivity*

$$\gamma^* = A + fM\Big(I - 2fKM\Big)^{-1} + O(f^3), \tag{5.15}$$

where $M = (M_{ij})_{1 \le i,j \le 2}$ is the first-order APT corresponding to γ_B.

Note that if A is diagonal, then we obtain

$$\gamma^* = A + fM\Big(I - \frac{f}{2}A^{-1}(I + c(A)E)M\Big)^{-1} + O(f^3),$$

where $c(A)$ is the number defined by

$$c(A) := \frac{4\pi}{\sqrt{|A|}}\left(\frac{a}{24} + a\theta\left(i\sqrt{\frac{a}{c}}\right) - \frac{c}{24} - c\theta\left(i\sqrt{\frac{c}{a}}\right)\right),$$

and $E = \begin{pmatrix} 1 & 0 \\ 0 & -1 \end{pmatrix}$. If A is isotropic, or $A = \sigma_0 I$, then $c(A) = 0$ and the above formula becomes

$$\gamma^* = \sigma_0 I + fM\Big(I - \frac{f}{2\sigma_0}M\Big)^{-1} + O(f^3),$$

and coincides with (5.12) since the first-order anisotropic polarization tensor is equal to $\sigma_0 \times$ the first-order isotropic one.

5.3. Further results. The formulae (5.13) and (5.15) have been extended to elastic composites. A general scheme to derive accurate asymptotic expansions of the elastic effective properties of dilute composite materials in terms of the elastic moment tensor and the volume fraction occupied by the elastic inclusions has been presented in [**26**]. Our formula is valid for general shaped Lipschitz inclusions with arbitrary phase moduli. Moreover, it exhibits an interesting feature of the effective elasticity tensor of composite materials: the presence of a distortion factor. The derivation of this formula is much more difficult than the one presented here for the effective conductivity because of the tensorial nature of the periodic Green's functions of the Lamé system.

Our approach is expected to have a great potential for rigorously deriving very accurate approximations for the effective viscosity of a suspension of general shaped obstacles suspended in a viscous fluid. We refer to Einstein [**67**] and Batchelor and Green [**40**] for approximations corresponding to a suspension of hard spheres in a viscous fluid. See also Lévy and Sánchez-Palencia [**105**].

6. Near-boundary conductivity inclusions

The dipole-type approximation is only valid when the field within the inclusion is nearly constant and the inclusion is not too close to the boundary. On decreasing the inclusion-boundary separation, the assumption that the field within the inclusion is nearly constant begins to fail because the inclusion-boundary interaction becomes significant.

The purpose of this section is to have a clearer picture of the inclusion-boundary interaction to making a reasonable extrapolation from the dipole approximation of a small inclusion inside a conductor to its signature when it is brought close to the boundary of the conductor.

This problem is of practical interest in many areas such as surface defect detection in the semiconductor industry and optical particle sizing. Many theoretical models have been developed and many experimental measurements have been carried out in recent years, see [**139**].

We shall provide an approximation which is valid when the inclusion is small and at a distance comparable to its diameter apart from the boundary of the conductor. Since the formula carries information on the location, the conductivity and the volume of the inclusion, it can be efficiently exploited for imaging inclusions close to the boundary of the background conductor. In fact, since the boundary perturbation amplitude has a relative peak near the inclusion, the peak clearly manifests the presence of the inclusion. However, it is not trivial how this peaks depends on the inclusion shape and its depth. See formula (6.11).

Before deriving an asymptotic expansion of the voltage potentials in the presence of a conductivity inclusion of small volume that is close to the boundary, we first set out optimal gradient estimates for solutions to the isotropic conductivity problem in the following two situations: when two circular conductivity inclusions are very close but not touching and when a circular inclusion is very close to the boundary of the domain where the inclusion is contained. These estimates imply that the gradient of the voltage potential stays bounded and an asymptotic expansion of the solution can be derived when a small inclusion is brought close to the boundary of the conductor.

6.1. Estimates of the stress. Suppose that Ω, which is a disk of radius ρ, contains an inclusion B, which is a disk of radius r. Suppose, as before, that the conductivity of Ω is 1 and that of B is $k \neq 1$. For a given $g \in \mathcal{C}^\alpha(\partial\Omega)$, $\alpha > 0$, let u be the solution to the transmission problem (2.12).

The first question we consider is whether ∇u can be arbitrarily large as the inclusion B get closer to the boundary $\partial\Omega$. We are especially interested in the

case of extreme conductivities $k = \infty$ (a perfect conductor) or $k = 0$ (an insulated inclusion). This difficult question arises not only in imaging but also in the study of composite media, see [**37**].

If $0 < C_1 < k < C_2 < +\infty$ for some constants C_1 and C_2, a uniform upper bound on the gradient of u in much more general setting has been derived by Li and Vogelius in [**107**]. Here we provide very precise estimates for $\|\nabla u\|_{L^\infty(\Omega)}$ for arbitrary conductivities.

According to Theorem 2.8, the solution u to (2.12) for a given Neumann data g can be represented as

$$u(x) = \mathcal{D}_\Omega(f)(x) - \mathcal{S}_\Omega(g)(x) + \mathcal{S}_B(\phi)(x), \quad x \in \Omega, \quad f := u\big|_{\partial\Omega}, \tag{6.1}$$

where $\phi \in L^2_0(\partial B)$ satisfies the integral equation

$$(\lambda I - \mathcal{K}_B^*)\phi = \frac{\partial}{\partial \nu}\big(\mathcal{D}_\Omega(f) - \mathcal{S}_\Omega(g)\big) \quad \text{on } \partial B,$$

with λ given by (2.16). Since B is a disk, it follows from (2.5) that $\mathcal{K}_B^*\phi = 0$ on ∂B and hence

$$\lambda\phi = \frac{\partial}{\partial \nu}\big(\mathcal{D}_\Omega(f) - \mathcal{S}_\Omega(g)\big) \quad \text{on } \partial B. \tag{6.2}$$

On the other hand, since $f = u|_{\partial\Omega}$, $\mathcal{D}_\Omega(f)|_- = (\frac{1}{2}I + \mathcal{K}_\Omega)f$ and Ω is a disk, we have

$$\frac{1}{2}f = -\mathcal{S}_\Omega(g) + \mathcal{S}_B(\phi) \quad \text{on } \partial\Omega. \tag{6.3}$$

It then follows from (6.2) and (6.3) that f and ϕ are the solutions of the following system of integral equations

$$\begin{cases} \dfrac{1}{2}f - \mathcal{S}_B\phi &= \mathcal{S}_\Omega g \quad \text{on } \partial\Omega, \\ \lambda\phi + \dfrac{\partial(\mathcal{D}_\Omega f)}{\partial \nu_B} &= -\dfrac{\partial(\mathcal{S}_\Omega g)}{\partial \nu_B} \quad \text{on } \partial B. \end{cases}$$

Let x_1 be the point on ∂B closest to $\partial\Omega$ and x_2 be the point on $\partial\Omega$ closest to ∂B, and let R_B and R_Ω be the reflections with respect to ∂B and $\partial\Omega$, respectively. Let p_1 and p_2 be fixed points of $R_B R_\Omega$ and $R_\Omega R_B$, respectively, and let J_1 be the line segment between p_1 and x_1 and J_2 that between p_2 and x_2.

The functions f and ϕ are given by explicit series which converge absolutely and uniformly. Precise estimates of these explicit series lead us to the following theorem [**24**].

THEOREM 6.1. *Let*

$$\epsilon := dist(B, \partial\Omega), \quad r^* := \sqrt{\frac{\rho - r}{\rho r}}, \quad \sigma := \frac{k-1}{k+1} (= \frac{1}{2\lambda}),$$

where λ is given by (2.16), and let u be the solution to (2.12).

(i) *If $k < 1$, then there exists a constant C_1 independent of k, r, ϵ, and g such that for ϵ small enough,*

$$\frac{C_1 \inf\limits_{x \in J_1} |\langle \nabla \mathcal{S}_\Omega(g)(x), T_B(x_1)\rangle|}{1 + \sigma + 4r^*\sqrt{\epsilon}} \leq |\nabla u|_+(x_1)|,$$

and

$$\frac{C_1 \inf\limits_{x \in J_2} |\langle \nabla \mathcal{S}_\Omega(g)(x), T_\Omega(x_2)\rangle|}{1 + \sigma + 4r^*\sqrt{\epsilon}} \leq |\nabla u|_-(x_2)|.$$

Here T_B and T_Ω denote the positively oriented unit tangent vector field on ∂B and $\partial\Omega$, respectively.

(ii) *For any $k \neq 1$, there exists a constant C_2 independent of k, r, and ϵ such that for ϵ small enough,*

$$\|\nabla u\|_{L^\infty(\Omega)} \leq \frac{C_2 \|g\|_{\mathcal{C}^\alpha(\partial\Omega)}}{1 - |\sigma| + r^*\sqrt{\epsilon}}.$$

If z is the center of Ω and if $g(x) := a \cdot \nu_x$ on $\partial\Omega$ for some constant vector a, then $\mathcal{S}_\Omega(g) = -\frac{1}{2} a \cdot x + \text{constant}$, and hence we can achieve

$$\langle \nabla \mathcal{S}_\Omega(g)(x), T_B(x_1) \rangle \neq 0 \text{ and } \langle \nabla \mathcal{S}_\Omega(f)(x), T_\Omega(x_2) \rangle \neq 0 \quad \text{for any } x,$$

by choosing a appropriately.

Theorem 6.1 shows that in the case of the Neumann problem, if the inclusion is insulated ($k = 0$ and hence $\sigma = -1$), then

$$\frac{C_1'}{r^*\sqrt{\epsilon}} \leq \|\nabla u\|_{L^\infty(\Omega)} \leq \frac{C_2'}{r^*\sqrt{\epsilon}},$$

for some constants C_1' and C_2'. Thus ∇u blows up at the rate of $1/\sqrt{\epsilon}$ as long as the magnitude of r is much larger than that of ϵ. It also shows that the gradient blows up at the points x_1 and x_2. If r is the same order as ϵ, then $r^* \approx 1/\sqrt{\epsilon}$ and hence ∇u does not blow up. In fact, it stays bounded and an asymptotic expansion of the solution as $\epsilon \to 0$ can be derived.

Note that for the Dirichlet problem the situation is reversed: ∇u blows up for a perfect conductor ($k = +\infty$), see [**24**].

Another interesting situation is when two circular conductivity inclusions are very close but not touching. To describe this second situation, let B_1 and B_2 be two circular inclusions contained in a matrix which we assume to be the free space $\mathbb{R}^2$. For $i = 1, 2$, we suppose that the conductivity k_i of the inclusion B_i is a constant different from the constant conductivity of the matrix, which is assumed to be 1 for convenience. The conductivity k_i of the inclusion may be 0 or ∞. The conductivity problem considered in this case is the following transmission problem for a given entire harmonic function H:

$$\begin{cases} \nabla \cdot \Big(1 + \displaystyle\sum_{i=1,2} (k_i - 1)\chi(B_i)\Big) \nabla u = 0 \quad \text{in } \mathbb{R}^2, \\ u(x) - H(x) = O(|x|^{-1}) \quad \text{as } |x| \to \infty. \end{cases} \tag{6.4}$$

The gradient ∇u of the solution u to (6.4) represents the perturbation of the field ∇H in the presence of inclusions B_1 and B_2. We are interested in the behavior of the gradient of the solution to the equation (6.4) as the distance between B_1 and B_2 goes to zero. Optimal bounds on ∇u can be proved. To state them, let us fix some notations. For $i = 1, 2$, let $B_i = B(z_i, r_i)$, the disk centered at z_i and of radius r_i. Let R_i, $i = 1, 2$, be the reflection with respect to ∂B_i, *i.e.*,

$$R_i(x) := \frac{r_i^2 (x - z_i)}{|x - z_i|^2} + z_i, \quad i = 1, 2.$$

It is easy to see that the combined reflections $R_1 R_2$ and $R_2 R_1$ have unique fixed points. Let I be the line segment between two fixed points. Let x_j, $j = 1, 2$, be the point on ∂B_j closest to the other disk. We also let

$$r_{\min} := \min(r_1, r_2), \quad r_{\max} := \max(r_1, r_2), \quad r_* := \sqrt{(2r_1 r_2)/(r_1 + r_2)}.$$

Finally let

$$\lambda_i := \frac{k_i + 1}{2(k_i - 1)}, \quad i = 1, 2 \quad \text{and} \quad \tau := \frac{1}{4\lambda_1 \lambda_2}.$$

The following result for the behavior of the gradient is obtained in [**25, 24**].

THEOREM 6.2. *Let $\epsilon := dist(B_1, B_2)$ and let $\nu^{(j)}$ and $T^{(j)}$, $j = 1, 2$, be the unit normal and tangential vector fields to ∂B_j, respectively. Let u be the solution of (6.4).*

(i) *If ϵ is sufficiently small, there is a constant C_1 independent of k_1, k_2, r_1, r_2, and ϵ such that*

$$\frac{C_1 \inf_{x\in I} |\langle \nabla H(x), \nu^{(j)}(x_j)\rangle|}{1 - \tau + (r_*/r_{\min})\sqrt{\epsilon}} \leq |\nabla u|_+(x_j)|, \quad j = 1, 2, \tag{6.5}$$

provided that $k_1,\ k_2 > 1$, and

$$\frac{C_1 \inf_{x\in I} |\langle \nabla H(x), T^{(j)}(x_j)\rangle|}{1 - \tau + (r_*/r_{\min})\sqrt{\epsilon}} \leq |\nabla u|_+(x_j)|, \quad j = 1, 2, \tag{6.6}$$

provided that $k_1,\ k_2 < 1$.

(ii) *Let Ω be a bounded set containing B_1 and B_2. Then there is a constant C_2 independent of k_1, k_2, r_1, r_2, ϵ, and Ω such that*

$$\|\nabla u\|_{L^\infty(\Omega)} \leq \frac{C_2 \|\nabla H\|_{L^\infty(\Omega)}}{1 - |\tau| + (r_*/r_{\max})\sqrt{\epsilon}}. \tag{6.7}$$

Note that if $H(x) = a\cdot x$ for some constant vector a, which is the most interesting case, then

$$\langle \nabla H(x), \nu^{(j)}(x_j)\rangle = \langle a, \nu^{(j)}(x_j)\rangle,$$

and hence does not vanish if we choose a appropriately.

Theorem 6.2 quantifies the behavior of ∇u in terms of the conductivities of the inclusions, their radii, and the distance between them. For example, if k_1 and k_2 degenerate to $+\infty$ or zero, then $\tau = 1$ and hence (6.5) and (6.7) read

$$\frac{C_1'}{(r_*/r_{\min})\sqrt{\epsilon}} \leq |\nabla u(x_j)|, \quad j = 1, 2, \quad \|\nabla u\|_{L^\infty(\Omega)} \leq \frac{C_2'}{(r_*/r_{\max})\sqrt{\epsilon}}, \tag{6.8}$$

for some constants C_1' and C_2', which shows that ∇u blows up at the rate of $1/\sqrt{\epsilon}$ as the inclusions get closer. It further shows that the gradient blows up at x_j which is the point on ∂B_j closest to the other disk.

The proof of the above optimal estimates makes use of quite explicit but non-trivial expansion formulae, originally derived in [**22**]. It is achieved by using a significantly different method from [**47**], [**107**], and [**50**].

6.2. Asymptotic expansions. Suppose that $D = \epsilon B + z$, where $z \in \Omega$ is such that $\text{dist}(z, \partial\Omega) = \delta\epsilon$. Here B is a bounded domain in $\mathbb{R}^2$ containing the origin with a connected $\mathcal{C}^2$-boundary and the constant $\delta > \max_{x\in\partial B} |x|$. Let u denote the voltage potential in the presence of the conductivity inclusion D, that is, the solution to (2.12) . Recall that the background voltage potential, U, is the unique solution to (2.21).

In this case, a more complicated asymptotic formula established in [**6**] should be used instead of (4.5). The dipole-type expansion (4.5) is valid only when the potential u within the inclusion D is nearly constant. On decreasing $\text{dist}(D, \partial\Omega)$ this assumption begins to fail because higher-order multi-poles become significant due to the interaction between D and $\partial\Omega$. Our approximation in [**6**] which is valid when the inclusion is at a distance comparable to its diameter apart from the boundary provides some essential insight for understanding this interaction. Moreover, since it carries information on the location, the conductivity and the volume of the inclusion, it can be efficiently exploited for imaging near-boundary inclusions.

To mathematically set our expansion, let z_0 be the normal projection of z onto $\partial\Omega$. Define

$$w(x) := \frac{\epsilon}{2(z_0 - x)\cdot \nu_{z_0}}, \quad x \in \partial D,$$

where ν_{z_0} is the outward normal to $\partial\Omega$ at z_0, and introduce

$$W(x) := \nu_{z_0} \cdot \int_{\partial D} \frac{N(x,y) - N(x,z)}{\epsilon} (\lambda I - \mathcal{K}_D^*)^{-1}(w\nu)(y)\, d\sigma(y), \quad x \in \partial\Omega. \tag{6.9}$$

It is not difficult to see that

$$W(x) = \begin{cases} O(1) & \text{if } |x - z_0| = O(\epsilon), \\ O(\epsilon) & \text{if } |x - z_0| \gg O(\epsilon). \end{cases} \tag{6.10}$$

The following asymptotic formula from [**6**] holds.

THEOREM 6.3. *Suppose that $g \in \mathcal{C}^1(\partial\Omega)$ and Ω is of class $\mathcal{C}^2$. We also assume that $W(z_0) \neq 1$. Then the following asymptotic expansion holds uniformly on $\partial\Omega$:*

$$\begin{aligned}(u - U)(x) = &-\epsilon \nabla U(z_0)\cdot \Big(\int_{\partial B} N(x, z + \epsilon y)(\lambda I - \mathcal{K}_B^*)^{-1}(\nu)\, d\sigma(y)\Big) \\ &- \epsilon \frac{W(x)}{1 - W(z_0)} \nabla U(z_0)\cdot \Big(\int_{\partial B} N(z_0, z + \epsilon y)(\lambda I - \mathcal{K}_B^*)^{-1}(\nu)\, d\sigma(y)\Big) \\ &+ O(\epsilon^{3/2}).\end{aligned}$$

Moreover, if $|x - z_0| \gg O(\epsilon)$ then

$$\begin{aligned}(u - U)(x) = &-\epsilon^2 \nabla U(z_0) M \nabla N(x, z_0) \\ &- \epsilon \frac{W(x)}{1 - W(z_0)} \nabla U(z_0)\cdot \Big(\int_{\partial B} N(z_0, z + \epsilon y)(\lambda I - \mathcal{K}_B^*)^{-1}(\nu)\, d\sigma(y)\Big) \\ &+ O(\epsilon^{5/2}),\end{aligned}$$

where $M = \int_{\partial B} y(\lambda I - \mathcal{K}_B^*)^{-1}(\nu)\, d\sigma(y)$ is the first-order polarization tensor and N is the Neumann function defined in (2.8).

Since $\int_{\partial B} N(x, z + \epsilon y)(\lambda I - \mathcal{K}_B^*)^{-1}(\nu)\, d\sigma(y) = O(1)$ for x near z_0, Theorem 6.3 and (6.10) show that $(u - U)(x) = O(\epsilon)$ near z_0, while $(u - U)(x) = O(\epsilon^2)$ for x far away from z_0. Thus $u - U$ has a relative peak near z_0.

Some words are in order for the condition $W(z_0) \neq 1$. Since

$$|W(z_0)| \leq C\|w\|_{L^\infty(\partial D)},$$

where the constant C is independent of δ, the condition is fulfilled (at least) if δ is large enough.

When the boundary is planar, a simpler approximation formula has been derived in [**30**]. One of the feature of that formula is that it is expressed in terms of the half-space polarization tensors.

Let us now document the viability of our results in Theorem 6.3 by numerical examples. Consider a unit disk in $\mathbb{R}^2$ with background conductivity 1 containing a single disk-shaped imperfection of small radius ϵ and conductivity k. The imperfection is centered at $z = (1 - \delta\epsilon, 0)$ on the axis $y = 0$ at a distance $(\delta - 1)\epsilon$ from the boundary where the constant $\delta > 1$. Let $z_0 = (1, 0)$.

Since

$$\int_{\partial D} \nu_y\, d\sigma(y) = 0 \text{ and } \int_{\partial\Omega} N(x, y) d\sigma(x) = 0, \text{ for } y \in \Omega,$$

then using property (2.5) we have

$$(\lambda I - \mathcal{K}_D^*)^{-1}(\nu)(y) = \frac{1}{\lambda}\nu_y, \forall\, y \in \partial\Omega,$$

and

$$N(x,y) = -2\Gamma(x-y) \text{ modulo constants}, \forall\, x \in \partial\Omega, y \in \Omega.$$

From Theorem 6.3 it then follows that

(i) for $x \in \partial\Omega$,

$$\begin{aligned}(u-U)(x) \quad \simeq \quad & -\frac{\epsilon}{\pi\lambda}\nabla U(z_0)\cdot\Big(\int_{\partial B}\ln|x-z-\epsilon y|\nu_y\,d\sigma(y)\Big)\\ & -\frac{\epsilon W(x)}{\pi\lambda(1-W(z_0))}\nabla U(z_0)\cdot\Big(\int_{\partial B}\ln|z_0-z-\epsilon y|\nu_y\,d\sigma(y)\Big).\end{aligned}$$

(ii) if $|x-z_0| \gg O(\epsilon)$,

$$\begin{aligned}(u-U)(x) \quad \simeq \quad & -\frac{4\epsilon^2}{\lambda}\nabla U(z_0)\cdot\frac{x-z_0}{|x-z_0|^2}\\ & -\frac{\epsilon W(x)}{\pi\lambda(1-W(z_0))}\nabla U(z_0)\cdot\Big(\int_{\partial B}\ln|\delta\nu_{z_0}-y|\nu_y\,d\sigma(y)\Big).\end{aligned}$$

(iii)

$$(u-U)(z_0) \simeq -\frac{\epsilon}{\pi\lambda(1-W(z_0))}\nabla U(z_0)\cdot\Big(\int_{\partial B}\ln|\delta\nu_{z_0}-y|\nu_y\,d\sigma(y)\Big).$$

We now present numerical simulations from [**6**] using these asymptotic expansions. In these experiments, we examine numerically the transmission problem (2.12) in cylindrical coordinates (r,θ) with Neumann boundary data $g(1,\theta) = \cos\theta + \sin\theta$. The analytical solution of the homogeneous problem (2.21) is then given by $U(r,\theta) = r(\cos\theta + \sin\theta)$. Therefore, $(u-U)(z_0)$ can be approximated as follows:

(6.11)

$$(u-U)(z_0) \simeq -\frac{\epsilon(k-1)}{\pi(k+1)(1-W(z_0))}\int_0^{2\pi}\ln\left((\delta-\cos\theta)^2+\sin^2\theta\right)(\cos\theta+\sin\theta)\,d\theta,$$

where

$$W(z_0) = \frac{1-k}{2\pi(k+1)}\int_0^{2\pi}\ln\left(\frac{(\delta-\cos\theta)^2+\sin^2\theta}{\delta^2}\right)\frac{\cos\theta}{\delta-\cos\theta}\,d\theta.$$

Formula (6.11) can be used to solve the inverse problem of finding δ, ϵ, or k from the maximum value of the boundary perturbations.

The first set of computations (see Figure 15) show the dependence of the perturbation of the boundary conductivity $(u-U)|_{\partial\Omega}$ as a function of the distance variable δ for different values of ϵ and for a fixed imperfection conductivity of $k = 2$. The next three figures (Figure 16) show the results for a larger value of the conductivity, $k = 10$.

We observe that the minimal value (near $\theta = 0$) is constant and this is clearer as the distance δ decreases. We can conclude that the perturbation amplitude is asymptotically first-order in ϵ.

We can also plot these same results for $k = 10$ fixed as a function of δ with $\epsilon = 0.1$ - see Figure 17 (a). We clearly observe the dependence of the amplitude and sharpness of the peak as a function of the distance.

The results of the above computations are resumed in Table 6 and Table 7 where the maximal value of $|u-U|$ on the boundary $\partial\Omega$ is given as a function of the three parameters k, δ and ϵ.

To check the influence of the angular position of the perturbation, a computation with $z = (0.5, 0.5)$ was performed. In Figure 18 we observe that the perturbation is indeed centered at $\theta = \pi/4$. We conclude that the angular position of the imperfection corresponds to the position of the perturbation peak.

Next, we compare in Table 8 the values of $(u-U)(z_0)$ computed from the asymptotic formula (6.11) with those computed by a direct simulation as in Tables 6 and 7.

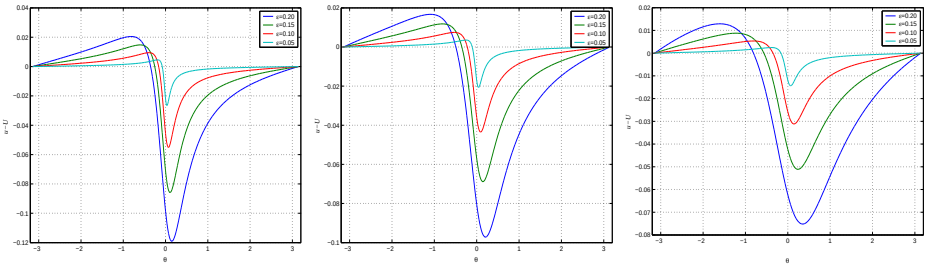

(a) (b) (c)

FIGURE 15. $k = 2$ and ϵ varying with (a) $\delta = 1.5$, (b) $\delta = 2$ and (c) $\delta = 3$. Colors: blue $\epsilon = 0.2$; green $\epsilon = 0.15$; red $\epsilon = 0.1$ and cyan $\epsilon = 0.05$.

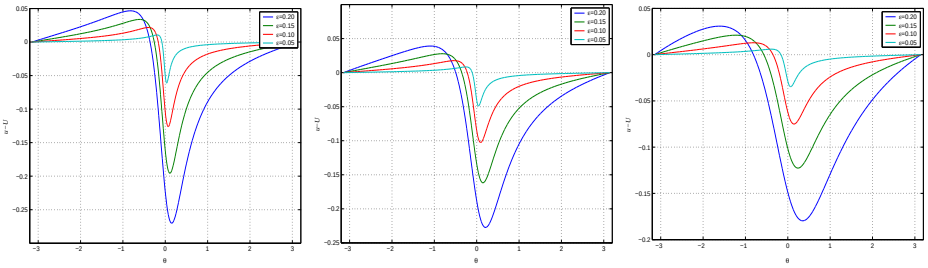

(a) (b) (c)

FIGURE 16. $k = 10$ and ϵ varying with (a) $\delta = 1.5$, (b) $\delta = 2$ and (c) $\delta = 3$. Colors: blue $\epsilon = 0.2$; green $\epsilon = 0.15$; red $\epsilon = 0.1$ and cyan $\epsilon = 0.05$.

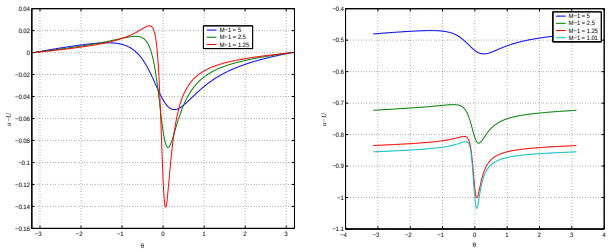

(a) (b)

FIGURE 17. $\epsilon = 0.1$ and varying distance δ with (a) $k = 10$, (b) $k = +\infty$. Colors: blue $\delta - 1 = 5$; green $\delta - 1 = 2.5$; red $\delta - 1 = 1.25$ and cyan $\delta - 1 = 1.01$.

Finally, we consider a homogeneous disk with a perfectly conducting circular imperfection. The boundary condition on the perimeter of the imperfection is homogeneous Dirichlet, $u = 0$. The results as a function of δ are shown in Figure 17 (b). As in the cases above,

(i) the peak of the perturbation corresponds to the angular position of the imperfection;
(ii) as the imperfection approaches the boundary, the peak amplitude tends to a finite limit.

	$\delta = 1.5$	$\delta = 2.0$	$\delta = 3.0$
$\epsilon = 0.20$	0.119 (**0.60**)	0.097 (**0.49**)	0.075 (**0.38**)
$\epsilon = 0.15$	0.086 (**0.57**)	0.069 (**0.46**)	0.051 (**0.34**)
$\epsilon = 0.10$	0.055 (**0.55**)	0.044 (**0.44**)	0.031 (**0.31**)
$\epsilon = 0.05$	0.027 (**0.54**)	0.021 (**0.42**)	0.014 (**0.28**)

TABLE 6. $\max_{\partial\Omega} |u - U|$ and $\max_{\partial\Omega} |u - U| / \epsilon$ (in bold) for $k = 2$.

	$\delta = 1.5$	$\delta = 2.0$	$\delta = 3.0$
$\epsilon = 0.20$	0.270 (**1.35**)	0.227 (**1.14**)	0.180 (**0.90**)
$\epsilon = 0.15$	0.196 (**1.30**)	0.162 (**1.07**)	0.123 (**0.82**)
$\epsilon = 0.10$	0.126 (**1.26**)	0.103 (**1.03**)	0.075 (**0.75**)
$\epsilon = 0.05$	0.061 (**1.22**)	0.049 (**1.00**)	0.035 (**0.69**)

TABLE 7. $\max_{\partial\Omega} |u - U|$ and $\max_{\partial\Omega} |u - U| / \epsilon$ (in bold) for $k = 10$.

	$\delta = 3.0$	$\delta = 4.0$	$\delta = 5.0$
$\epsilon = 0.05$	0.0118 (**0.236**)	0.0093 (**0.185**)	0.0076 (**0.152**)
	0.0116 (**0.232**)	0.0085 (**0.171**)	0.0068 (**0.135**)
$\epsilon = 0.02$	0.0046 (**0.228**)	0.0035 (**0.173**)	0.0028 (**0.140**)
	0.0046 (**0.232**)	0.0034 (**0.171**)	0.0027 (**0.135**)
$\epsilon = 0.01$	0.0023 (**0.230**)	0.0017 (**0.170**)	0.0014 (**0.135**)
	0.0023 (**0.232**)	0.0017 (**0.171**)	0.0014 (**0.135**)

TABLE 8. Comparison of $(u-U)(z_0)$ computed numerically (upper lines) and $(u-U)(z_0)$ computed from the asymptotic formula (6.11) (lower lines) for $k = 2$. Bold values are $(u - U)(z_0)/\epsilon$.

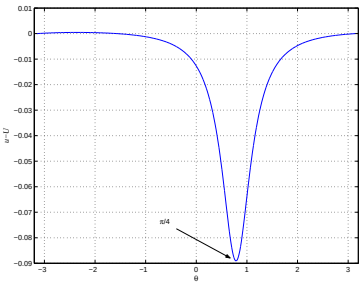

FIGURE 18. Boundary perturbations for $z = (0.5, 0.5)$.

6.3. Further results. Li and Nirenberg proved that the stress for linear elasticity stays bounded if the Lamé parameters are bounded [**106**]. It would be very interesting to characterize the blow-up rate of the stress when the inclusions are either hard ones or holes, *i.e.*, when the Young's modulus is either ∞ or zero. Another interesting problem is to extend the optimal gradient estimates to the three-dimensional case. We think that the blow-rate of the gradient of the voltage potential when two spheres of not necessary equal radii approaching one another can be computed using a bispherical coordinate system that fits the given geometry.

Acknowledgement

The authors are grateful to Martin Hanke for his careful reading of a first version of this paper.

References

[1] G. Alessandrini, Examples of instability in inverse boundary value problems, Inverse Problems, 13 (1997), 887–897.

[2] G. Alessandrini, E. Rosset, and J.K. Seo, Optimal size estimates for the inverse conductivity problem with one measurement, Proc. Amer. Math. Soc., 128 (2000), 53–64.

[3] G. Allaire, *Shape Optimization by the Homogenization Method*, Springer-Verlag, New York, 2002.

[4] C. Alves and H. Ammari, Boundary integral formulae for the reconstruction of imperfections of small diameter in an elastic medium, SIAM J. Appl. Math., 62 (2002), 94–106.

[5] H. Ammari, An inverse initial boundary value problem for the wave equation in the presence of imperfections of small volume, SIAM J. Control Optim., 41 (2002), 1194–1211.

[6] H. Ammari, M. Asch, and H. Kang, Boundary voltage perturbations caused by small conductivity inhomogeneities nearly touching the boundary, Adv. Appl. Math., 35 (2005), 368–391.

[7] H. Ammari, E. Beretta, and E. Francini, Reconstruction of thin conductivity imperfections, Applicable Anal., 83 (2004), 63–78.

[8] ————————-, Reconstruction of thin conductivity imperfections II: The case of multiple segments, Applicable Anal., 85 (2006), 87–105.

[9] H. Ammari, Y. Capdeboscq, H. Kang, E. Kim, and M. Lim, Attainability by simply connected domains of optimal bounds for the polarization tensor, to appear in European J. Appl. Math.

[10] H. Ammari, E. Iakovleva, and H. Kang, Reconstruction of a small inclusion in a 2-D open waveguide, SIAM J. Appl. Math., 65 (2005), 2107–2127.

[11] H. Ammari, E. Iakovleva, H. Kang, and K. Kim, Direct algorithms for thermal imaging of small inclusions, Multiscale Modeling and Simulation: A SIAM Interdisciplinary Journal, 4 (2005), 1116–1136.

[12] H. Ammari, E. Iakovleva, and D. Lesselier, A MUSIC algorithm for locating small inclusions buried in a half-space from the scattering amplitude at a fixed frequency, Multiscale Modeling and Simulation: A SIAM Interdisciplinary Journal, 3 (2005), 597–628.

[13] ————————-, Two numerical methods for recovering small inclusions from the scattering amplitude at a fixed frequency, SIAM J. Sci. Comput., 27 (2005), 130–158.

[14] H. Ammari, E. Iakovleva, and S. Moskow, Recovery of small inhomogeneities from the scattering amplitude at a fixed frequency, SIAM J. Math. Anal., 34 (2003), 882–900.

[15] H. Ammari and H. Kang, High-order terms in the asymptotic expansions of the steady-state voltage potentials in the presence of conductivity inhomogeneities of small diameter, SIAM J. Math. Anal., 34 (2003), 1152–1166.

[16] ————————, Properties of generalized polarization tensors, Multiscale Modeling and Simulation: A SIAM Interdisciplinary Journal, 1 (2003), 335–348.

[17] ————————, A new method for reconstructing electromagnetic inhomogeneities of small volume, Inverse Problems, 19 (2003), 63–71.

[18] ————————, *Reconstruction of Small Inhomogeneities from Boundary Measurements*, Lecture Notes in Mathematics, Volume 1846, Springer-Verlag, Berlin, 2004.

[19] ————————, Reconstruction of conductivity inhomogeneities of small diameter via boundary measurements, Contemporary Math. 348 (2004), 23–32.

[20] ————————, Boundary layer techniques for solving the Helmholtz equation in the presence of small inhomogeneities, J. Math. Anal. Appl., 296 (2004), 190–208.

[21] ————————, Reconstruction of elastic inclusions of small volume via dynamic measurements, submitted to Appl. Math. Optimization.

[22] H. Ammari, H. Kang, E. Kim, and M. Lim, Reconstruction of closely spaced small inclusions, SIAM J. Numer. Anal., 42 (2005), 2408–2428.

[23] H. Ammari, H. Kang, and K. Kim, Polarization tensors and effective properties of anisotropic composite materials, J. Differ. Equat., 215 (2005), 401–428.

[24] H. Ammari, H. Kang, H. Lee, J. Lee, and M. Lim, Optimal bounds on the gradient of solutions to conductivity problems, submitted to Trans. Amer. Math. Soc.

[25] H. Ammari, H. Kang, and M. Lim, Gradient estimates for solutions to the conductivity problem, Math. Ann., 332 (2005), 277–286.

[26] ————————, Effective parameters of elastic composites, to appear in Indiana Univ. J. Math.

[27] ————————, Polarization tensors and their applications, Proc. Second International Conference on Inverse Problems: recent developments and numerical approaches, Shanghai, 2004, Journal of Physics: Conference Series, 12 (2005), 13–22.

[28] H. Ammari, H. Kang, G. Nakamura, and K. Tanuma, Complete asymptotic expansions of solutions of the system of elastostatics in the presence of an inclusion of small diameter and detection of an inclusion, J. Elasticity, 67 (2002), 97–129.

[29] H. Ammari, H. Kang, and K. Touibi, Boundary layer techniques for deriving the effective properties of composite materials, Asymp. Anal., 41 (2005), 119–140.

[30] ————————, An asymptotic formula for the voltage potential in the case of a near-surface conductivity inclusion, to appear in Z. Angew. Math. Phys.
[31] H. Ammari, H. Kang, and M. Vogelius, Detection of internal corrosion from steady state voltage boundary perturbations, preprint.
[32] H. Ammari, S. Moskow, and M.S. Vogelius, Boundary integral formulas for the reconstruction of electromagnetic imperfections of small diameter, ESAIM: Cont. Opt. Calc. Var., 9 (2003), 49–66.
[33] H. Ammari and J.K. Seo, An accurate formula for the reconstruction of conductivity inhomogeneities, Adv. Appl. Math., 30 (2003), 679–705.
[34] H. Ammari, M.S. Vogelius, and D. Volkov, Asymptotic formulas for perturbations in the electromagnetic fields due to the presence of imperfections of small diameter II. The full Maxwell equations, J. Math. Pures Appl. 80 (2001), 769–814.
[35] H. Ammari and D. Volkov, Correction of order three for the expansion of two dimensional electromagnetic fields perturbed by the presence of inhomogeneities of small diameter, J. Comput. Phys., 189 (2003), 371–389.
[36] K. Astala and L. Päivärinta, Calderon's inverse conductivity problem in the plane, preprint 2003.
[37] I. Babuška, B. Andersson, P. Smith, and K. Levin, Damage analysis of fiber composites. I. Statistical analysis on fiber scale, Comput. Methods Appl. Mech. Engrg. 172 (1999), 27–77.
[38] A. El Badia and T. Ha-Duong, An inverse source problem in potential analysis, Inverse Problems, 16 (2000), 651–663.
[39] L. Baratchart, A. Ben Abda, F. Ben Hassen, and J. Leblond, Recovery of pointwise sources or small inclusions in 2D domains and rational approximation, Inverse Problems, 21 (2005), 51–74.
[40] G.K. Batchelor and J.T. Green, The determination of the bulk stress is suspension of spherical particles to order c^2, J. Fluid. Mech. 56 (1972), 401–427.
[41] F. Ben Hassen and E. Bonnetier, Asymptotic formulas for the voltage potential in a composite medium containing close or touching disks of small diameter, Multiscale Modeling and Simulation: A SIAM Interdisciplinary Journal, 4 (2005), 250–277.
[42] ————————–, Asymptotics of the voltage potential in a composite medium that contains misplaced inclusions, preprint, 2005.
[43] A. Bensoussan, J.L. Lions, and G. Papanicolaou, *Asymptotic Analysis of Periodic Structures*, North Holland, 1978.
[44] E. Beretta and E. Francini, Asymptotic formulas for perturbations in the electromagnetic fields due to the presence of thin inhomogeneities in *Inverse Problems: Theory and Applications*, 49–63, Contemp. Math., 333, Amer. Math. Soc., Providence, RI, 2003.
[45] E. Beretta, E. Francini, and M.S. Vogelius, Asymptotic formulas for steady state voltage potentials in the presence of thin inhomogeneities. A rigorous error analysis, J. Math. Pures Appl., 82 (2003), 1277–1301.
[46] E. Beretta, A. Mukherjee, and M.S. Vogelius, Asymptotic formuli for steady state voltage potentials in the presence of conductivity imperfections of small area, Z. Angew. Math. Phys., 52 (2001), 543–572.
[47] E. Bonnetier and M. Vogelius, An elliptic regurality result for a composite medium with touching fibers of circular cross-section, SIAM J. Math. Anal. 31 (2000), 651–677.
[48] M. Brühl, Explicit characterization of inclusions in electrical impedance tomography, SIAM J. Math. Anal., 32 (2001), 1327–1341.
[49] M. Brühl, M. Hanke, and M.S. Vogelius, A direct impedance tomography algorithm for locating small inhomogeneities, Numer. Math., 93 (2003), 635–654.
[50] B. Budiansky and G.F. Carrier, High shear stresses in stiff fiber composites, J. Appl. Mech. 51 (1984), 733–735.
[51] A.P. Calderón, On an inverse boundary value problem, Seminar on Numerical Analysis and its Applications to Continuum Physics, Soc. Brasileira de Matemática, Rio de Janeiro, 1980, 65–73.
[52] Y. Capdeboscq and M.S. Vogelius, A general representation formula for the boundary voltage perturbations caused by internal conductivity inhomogeneities of low volume fraction, Math. Modelling Num. Anal., 37 (2003), 159–173.
[53] ————————, Optimal asymptotic estimates for the volume of internal inhomogeneities in terms of multiple boundary measurements, Math. Modelling Num. Anal., 37 (2003), 227–240.
[54] ————————, A review of some recent work on impedance imaging for inhomogeneities of low volume fraction, to appear in Proceedings of the Pan-American Advanced Studies Institute on PDEs, Inverse Problems and Nonlinear Analysis, January 2003. Contemporary Mathematics (2004).

[55] D.J. Cedio-Fengya, S. Moskow, and M.S. Vogelius, Identification of conductivity imperfections of small diameter by boundary measurements: Continuous dependence and computational reconstruction, Inverse Problems, 14 (1998), 553–595.
[56] M. Cheney, The linear sampling method and the MUSIC algorithm, Inverse Problems, 17 (2001), 591–595.
[57] H. Cheng and L. Greengard, A method of images for the evaluation of electrostatic fields in systems of closely spaced conducting cylinders, SIAM J. Appl. Math., 58 (1998), 122–141.
[58] A. Cherkaev, *Variational Methods for Structual Optimization,* Appl. Math. Sciences 140, Springer, New York, 2000.
[59] D. Cioranescu and P. Donato, *An Introduction to Homegenization*, Oxford Lecture Series in Mathematics and its Application 17, Oxford University Press, 1999.
[60] R.R. Coifman, A. McIntosh, and Y. Meyer, L'intégrale de Cauchy définit un opérateur borné sur L^2 pour les courbes lipschitziennes, Ann. Math., 116 (1982), 361–387.
[61] D. Colton and A. Kirsch, A simple method for solving inverse scattering problems in the resonance region, Inverse Problems, 12 (1996), 383–393.
[62] G. Dassios, Low-frequency moments in inverse scattering theory, J. Math. Phys., 31 (1990), 1691–1692.
[63] G. Dassios and R.E. Kleinman, On Kelvin inversion and low-frequency scattering, SIAM Rev., 31 (1989), 565–585.
[64] A.J. Devaney, Super-resolution processing of multi-static data using reversal and MUSIC, to appear in J. Acoust. Soc. Am.
[65] J.F. Douglas and A. Friedman, Coping with complex boundaries, IMA Series on Mathematics and its Applications Vol. 67, 166–185, Springer, New York, 1995.
[66] J.F. Douglas and E.J. Garboczi, Intrinsic viscosity and polarizability of particles having a wide range of shapes, Adv. Chem. Phys., 91 (1995), 85–153.
[67] A. Einstein, Eine neue Bestimmung der Moleküldimensionen, Ann. Phys. 19 (1906), 289–306.
[68] L. Escauriaza, E.B. Fabes, and G. Verchota, On a regularity theorem for weak solutions to transmission problems with internal Lipschitz boundaries, Proc. Amer. Math. Soc., 115 (1992), 1069–1076.
[69] L. Escauriaza and J.K. Seo, Regularity properties of solutions to transmission problems, Trans. Amer. Math. Soc., 338 (1993), 405–430.
[70] G.B. Folland, *Introduction to Partial Differential Equations*, Princeton University Press, Princeton, NJ, 1976.
[71] A. Friedman, Detection of mines by electric measurements, SIAM J. Appl. Math., 47 (1987), 201–212.
[72] A. Friedman and B. Gustafsson, Identification of the conductivity coefficient in an elliptic equation, SIAM J. Math. Anal., 18 (1987), 777–787.
[73] A. Friedman and M.S. Vogelius, Identification of small inhomogeneities of extreme conductivity by boundary measurements: a theorem on continuous dependence, Arch. Rat. Mech. Anal., 105 (1989), 299–326.
[74] E.J. Garboczi and J.F. Douglas, Intrinsic conductivity of objects having arbitrary shape and conductivity, Physical Review E 53 (1996), 6169–6180.
[75] D. Gilbarg and N.S. Trudinger, *Elliptic Partial Differential Equations of Second Order*, Grundlehren der Mathematischen Wissenschaften, 224, Springer-Verlag, Berlin-New York, 1977.
[76] L. Greengard and M. Moura, On the numerical evaluation of electrostatic fields in composite materials, Acta Numerica (1994), 379–410.
[77] Z. Hashin, Analysis of composite materials-A survey, J. Appl. Mech., 50 (1983), 481–505.
[78] Z. Hashin and P.J.M. Monteiro, An inverse method to determine the elastic properties of the interphase between the aggregate and the cement paste, Cement and ConcreteResearch, 32 (2002), 1291–1300.
[79] H. Hasimoto, On the periodic fundamental solutions of the Stokes equations and their application to viscous flow past a cubic array of spheres, J. Fluid Mech., 5 (1959), 317–328.
[80] V. Isakov, On uniqueness of recovery of a discontinuous conductivity coefficient, Comm. Pure Appl. Math., 41 (1988), 865–877.
[81] D.J. Jefferey, Conduction through a random suspension of spheres, Proc. R. Soc. London Ser. A, 335 (1973), 355–367.
[82] V.V. Jikov, S.M. Kozlov, and O.A. Oleinik, *Homogenization of Differential Operators and Integral Functionals*, Springer-Verlag, 1994.
[83] H. Kang, E. Kim, and J. Lee, Identification of Elastic Inclusions and Elastic Moment Tensors by Boundary Measurements, Inverse Problems, 19 (2003), 703–724.
[84] H. Kang, E. Kim, and K. Kim, Anisotropic polarization tensors and determination of an anisotropic inclusion, SIAM J. Appl. Math., 65 (2003), 1276–1291.

[85] H. Kang and K. Kim, Anisotropic polarization tensors for ellipses and ellipsoids, preprint, 2005.
[86] H. Kang and H. Lee, Identification of simple poles via boundary measurements and an application to EIT, Inverse Problems, 20 (2004), 1853–1863.
[87] H. Kang and J.K. Seo, Layer potential technique for the inverse conductivity problem, Inverse Problems, 12 (1996), 267–278.
[88] ————————, Identification of domains with near-extreme conductivity: Global stability and error estimates, Inverse Problems, 15 (1999), 851–867.
[89] ————————, Inverse conductivity problem with one measurement: Uniqueness of balls in R^3, SIAM J. Appl. Math., 59 (1999), 1533–1539.
[90] ————————, Recent progress in the inverse conductivity problem with single measurement, in Inverse Problems and Related Fields, CRC Press, Boca Raton, FL, 2000, 69–80.
[91] H. Kang, J.K. Seo, and D. Sheen, The inverse conductivity problem with one measurement: stability and estimation of size, SIAM J. Math. Anal., 28 (1997), 1389–1405.
[92] J.B. Keller, Stresses in narrow regions, Trans. ASME J. Appl. Mech. 60 (1993), 1054–1056.
[93] J.B. Keller, Removing small features from computational domains, J. Comput. Phys., 113 (1994), 148–150.
[94] K. Kim, *Anisotropic Polarization Tensors and Applications*, PhD thesis, Seoul National University, 2004.
[95] H. Kim and J.K. Seo, Identification problems in linear elasticity, J. Math. Anal. Appl., 215 (1997), 514–531.
[96] A. Kirsch, Characterization of the shape of the scattering obstacle using the spectral data of the far field operator, Inverse Problems, 14 (1998), 1489–1512.
[97] ————————————-, The MUSIC algorithm and the factorization method in inverse scattering theory for inhomogeneous media, Inverse Problems, 18 (2002), 1025–1040.
[98] R.E. Kleinman and T.B.A. Senior, Rayleigh scattering in *Low and High Frequency Asymptotics,* 1–70, edited by V.K. Varadan and V.V. Varadan, North-Holland, 1986.
[99] R. Kress, *Linear Integral Equations*, Applied Mathematical Sciences 82, Springer, 1989.
[100] R.V. Kohn and M.S. Vogelius, Determining conductivity by boundary measurements, interior results, II, Comm. Pure Appl. Math., 38 (1985), 643–667.
[101] S.M. Kozlov, On the domain of variations of added masses, polarization and effective characteristics of composites, J. Appl. Math. Mech., 56 (1992), 102–107.
[102] O. Kwon and J.K. Seo, Total size estimation and identification of multiple anomalies in the inverse electrical impedance tomography, Inverse Problems, 17 (2001), 59–75.
[103] O. Kwon, J.K. Seo, and J.R. Yoon, A real-time algorithm for the location search of discontinuous conductivities with one measurement, Comm. Pure Appl. Math., 55 (2002), 1–29.
[104] S.K. Lehman and A.J. Devaney, Transmission mode time-reversal super-resolution imaging, J. Acoust. Soc. Am., 113 (2003), 2742–2753.
[105] T. Lévy and E. Sánchez-Palencia, Einstein-like approximation for homogenization with small concentration. II. Navier-Stokes equation, Nonlinear Anal., 9 (1985), 1255–1268.
[106] Y.Y. Li and L. Nirenberg, Estimates for elliptic systems from composite material, Comm. Pure Appl. Math. LVI (2003), 892–925.
[107] Y.Y. Li and M. Vogelius, Gradient estimates for solutions to divergence form elliptic equations with discontinuous coefficients, Arch. Rational Mech. Anal. 153 (2000), 91–151.
[108] M. Lim, Symmetry of an boundary integral operator and a characterization of balls, Illinois Jour. of Math. 45 (2001), 537–543.
[109] ————, *Reconstruction of Inhomogeneities via Boundary Measurements*, Ph.D. thesis, Seoul National University, 2003.
[110] R. Lipton, Inequalities for electric and elastic polarization tensors with applications to random composites, J. Mech. Phys. Solids, 41 (1993), 809–833.
[111] M.L. Mansfield, J.F. Douglas, and E.J. Garboczi, Intrinsic viscosity and electrical polarizability of arbitrary shaped objects, Physical Review E, 64 (2001), 061401.
[112] X. Markenscoff, Stress amplification in vanishing small geometries, Computational Mechanics 19 (1996), 77–83.
[113] E. Martensen, Eine Integralgleichung für die legarithmische Gleichgewichtsbelegung und die Krümung der Randkurve eines ebenen Gebiets, Z. angew Math. Mech. 72 (1992), T596–T599.
[114] O. Mendez and W. Reichel, Electrostatic characterization of spheres, Forum Math. 12 (2000), 223–245.
[115] G.W. Milton, *The Theory of Composites*, Cambridge Monographs on Applied and Computational Mathematics, Cambridge University Press, 2001.
[116] A.B. Movchan and S.K. Serkov, The Pólya-Szegö matrices in asymptotic models of dilute composite, Euro. J. Appl. Math., 8 (1997), 595–621.
[117] A. Nachmann, Global uniqueness for a two-dimensional inverse boundary value problem, Ann. Math., 142 (1996), 71–96.

[118] G.C. Papanicolaou, Diffusion in random media, in *Surveys in Applied Mathematics, Volume 1*, 205–253, edited by J.P. Keller, D.W. McLaughlin, and G.C. Papanicolaou, Plenum Press, New York, 1995.
[119] L. Payne and G. Philippin, On some maximum principles involving harmonic functions and their derivatives, SIAM J. Math Anal. 10 (1979), 96–104.
[120] L. Payne and H. Weinberger, New bounds in harmonic and biharmonic problems, J. Math. Phys., 33 (1954), 291–307.
[121] G. Philippin, On a free boundary value problem in electrostatics, Math. Meth. Appl. Sci. 12 (1990), 387–392.
[122] W. Reichel, Radial symmetry for an electrostatic, a capillarity and some fully nonlinear overdetermined problem on exterior domains, Z. Anal. Anwendungen 15 (1996), 619–635.
[123] ————————-, Radial symmetry for elliptic boundary-value problems on exterior domains, Arch. Rational Mech. Anal., 137 (1997), 381–394.
[124] G. Pólya and G. Szegö, *Isoperimetric Inequalities in Mathematical Physics*, Annals of Mathematical Studies Number 27, Princeton University Press, Princeton, NJ, 1951.
[125] E. Sánchez-Palencia, Einstein-like approximation for homogenization with small concentration. I. Elliptic problems, Nonlinear Anal., 9 (1985), 1243–1254.
[126] A.S. Sangani, Conductivity of n-dimensional composites containing hyperspherical inclusion, SIAM J. Appl. Math., 50 (1990), 64–73.
[127] A.S. Sangani and A. Acrivos, The effective conductivity of a periodic array of spheres, Proc. Roy. Soc. London A., 386 (1983), 263.
[128] M. Schiffer and G. Szegö, Virtual mass and polarization, Trans. Amer. Math. Soc., 67 (1949), 130–205.
[129] J. Sylvester and G. Uhlmann, A global uniqueness theorem for an inverse boundary value problem, Ann. Math., 125 (1987), 153–169.
[130] S.T. Torquato, *Random Heterogeneous Materials: Microstructure and Macroscopic Properties*, Springer-Verlag, New York, 2002.
[131] ———, Modeling of physical properties of composite materials, Internal J. Solids and Struc., 37 (2000), 411–422.
[132] G.C. Verchota, Layer potentials and boundary value problems for Laplace's equation in Lipschitz domains, J. Funct. Anal., 59 (1984), 572–611.
[133] M.S. Vogelius and D. Volkov, Asymptotic formulas for perturbations in the electromagnetic fields due to the presence of inhomogeneities, Math. Model. Numer. Anal., 34 (2000), 723–748.
[134] D. Volkov, Numerical methods for locating small dielectric inhomogeneities, Wave Motion, 38 (2003), 189–206.
[135] X. Zheng, M.G. Forest, R. Lipton, R. Zhou, and Q. Wang, Exact scaling laws for electrical conductivity properties of nematic polymer nanocomposite monodomains, Adv. Funct. Mater., 15 (2005), 627–638.
[136] R.W. Zimmerman, Elastic moduli of a solid containing spherical inclusions, Mech. Materials, 12 (1991), 17–24.
[137] ————————, Effective conductivity of a low-dimensional medium containing elliptical inhomogeneities, Proc. R. Soc. Lond. A, 452 (1996), 1713–1727.
[138] M. Zuzovski and H. Brenner, Effective conductivity of composite materials composed of cubic arrangements of spherical particles embedded in an isotropic matrix, ZAMP, 28 (1977), 979–992.
[139] *Light Scattering from Microstructures*, edited by F. Moreno and F. Gonzalez, Lecture Notes in Physics, vol. 534, Springer-Verlag 2000.

Centre de Mathématiques Appliquées, Ecole Polytechnique, 91128 Palaiseau Cedex, France.
E-mail address: ammari@cmapx.polytechnique.fr

School of Mathematical Sciences, Seoul National University, Seoul 151-747, Korea.
E-mail address: hkang@math.snu.ac.kr